Long-range atomic interactions for novel quantum technologies
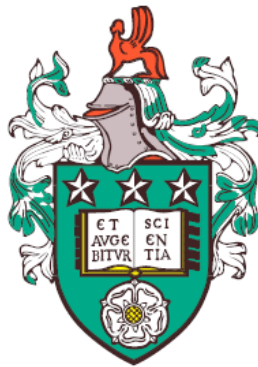
Nicholas Furtak-Wells

School of Physics and Astronomy

University of Leeds

Submitted in accordance with the requirements for the degree of

Doctor of Philosophy

June 2019

Declaration

The candidate confirms that the work submitted is his/her own, except where work which has formed part of jointly authored publications has been included. The contribution of the candidate and the other authors to this work has been explicitly indicated below. The candidate confirms that appropriate credit has been given within the thesis where reference has been made to the work of others.

Some of the work in Chapters 5 and 6 of the thesis has appeared in publication as follows:

N. Furtak-Wells, L. A. Clark, R. Purdy and A. Beige, *Quantizing the electromagnetic field near two-sided semitransparent mirrors*, Phys. Rev. A **97**, 043827 (2018).

I was the lead investigator of the research and the contribution of other authors was in discussion with me.

Some of the work in Chapter 7 of the thesis is in preparation to be published as follows:

N. Furtak-Wells et al., *Atomic long-range interactions through mirror-images*, in preparation, (2019).

I was the lead investigator of the research and the contribution of other authors was in discussion with me.

Some of the work in Chapter 8 of the thesis is in preparation to be published as follows:

N. Furtak-Wells, R. Purdy and A. Beige, *A continuous-mode model for optical cavities*, in preparation, (2019).

Acknowledgements

I would like to thank all the people who have supported me throughout my time working towards this thesis. In particular, I would like to thank my supervisor, Dr Almut Beige, for providing extensive knowledge throughout my PhD, being extremely patient and having a constant enthusiasm for science, especially photons! I would like to thank my parents for helping me with this opportunity as well as their constant support, guidance, patience and all of the visits to Leeds!

I would like to thank all my friends and co-workers who have supported me over the past three years. In particular, I would like to thank the lads; Lewis Clark, Kristian Patrick, Jake Southall, Gangcheng "Sanguine" Wang, Erick Hinds Mingo, Konstantinos Meichanetzidis, Siddharth Sinha, Richard Matthews, Richard Ross, William Harrald, Matthew Bignold and Adam Infante.

List of publications

[1] N. Furtak-Wells, L. A. Clark, R. Purdy and A. Beige *Quantising the electromagnetic field near a semi-transparent mirror*, Phys. Rev. A **97**, 043827 (2018).

[2] N. Furtak-Wells *et al.*, *Atomic long-range interactions through mirror-images*, in preparation, (2019).

[3] N. Furtak-Wells, R. Purdy and A. Beige, *A continuous-mode model for optical cavities*, in preparation, (2019).

Abstract

Atomic interactions have a wide range of potential applications in quantum technology but are, unfortunately, usually relatively short-range. In this thesis a novel approach to quantising the electromagnetic field in the presence of two-sided semi-transparent mirrors with finite transmission, reflection and absorption rates is presented. The *image-detector method* allows one to correctly reproduce the appropriate dynamics of wave packets in the presence of semi-transparent mirrors by mapping onto analogous free-space scenarios meaning photons are characterised as they are in free space. Moreover, radiating atoms in the presence of semi-transparent mirrors exhibit modified spontaneous emission rates due to boundary conditions imposed on the electromagnetic field. Through the image-detector method mirror-mediated dipole-dipole interactions are predicted which modify atomic spontaneous emission rates. The spontaneous emission rates explicitly depend on the optical properties of the semi-transparent mirror and these mirror-mediated dipole-dipole interactions are considered to be long range, as atoms placed several wavelengths from the mirror still exhibit modified spontaneous emission rates. In addition, the model readily extends to describe optical cavities. The results presented in this thesis are expected to pave the way for the modelling of more complex scenarios and for designing novel photonic devices for quantum technology applications, such as non-invasive glucose-sensing technology.

Contents

List of Figures

Chapter 1

Introduction

In this chapter some background information is presented as well as the key motivations behind this body of work. A brief introduction of modelling open quantum systems and an outline for the thesis is also included.

1.1   Background

Technology is always changing and adapting with the key objective of developing and designing new forms of technology to improve the users' daily lives. Harnessing the inherent strangeness of nature at the quantum scale, one can use these properties to design quantum technologies that are more powerful than current classical ones. These types of technologies are currently being popularised through recent efforts to design a quantum computer, in particular efforts from numerous companies; Google (Bristlecone), D-Wave as well as ongoing projects with IBM and Samsung. Kimble *et al.* [1] postulated a potential quantum internet designed with nodes (optical cavities) and fibres connecting them together, thereby demonstrating optical networks and optical systems as excellent candidates for designing novel quantum technologies.

In order to design new technologies using optical networks it is important to understand how light behaves within optical cavities. Understanding these components is essential and while it is well understood how to describe light within idealised optical cavities, it still remains challenging to model more realistic configurations e.g. two-sided optical resonators with off-resonant laser driving [2].
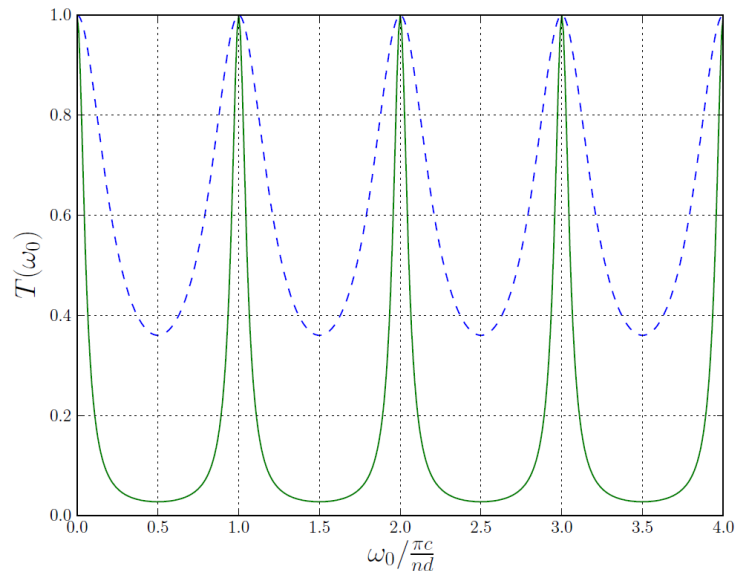
Figure 1.1: Predicted experimental transmission rate $T(\omega_0)$ for a Fabry-Pérot cavity driven by monochromatic light of frequency ω_0 where the dashed line represents a refractive index of $n = 3$ and the solid line represents a refractive index of $n = 20$.

There exists several models which allow one to describe light within a cavity. The input-output formalism provides a phenomenological approach, where the modes inside and outside of the cavity are related through a linear coupling and the mirrors impose boundary conditions on electric field amplitudes [3–5]. This formalism models light scattering through optical cavities in such a way that is consistent with Maxwell's equations (see Refs. [6, 7]). For another perspective, there exists the modes-of-the-universe description [8–13], which describe the electromagnetic field in terms of the modes of a much larger cavity - the universe. The quantisation in Refs. [8–10] results in a quasi-mode representation of the electromagnetic field, where the non-orthogonal modes allow for leakage of photons through the cavity mirrors.

Barlow *et al.* [2] proposed a master equation description for a two-sided optical cavity, where a laser-driven resonator is considered (dielectric slab of arbitrary length d and a refractive index that is larger than air, $n > 1$). This paper correctly predicts spontaneous photon emission rates for an optical cavity using a

continuous-mode description, while providing consistency with classical electro-dynamics. For an idealised cavity one would expect the transmission of light to occur at the discrete cavity frequencies, due to the strict boundary conditions imposed by the mirrors. However, experimental observation shows the transmission is not restricted to these discrete frequencies, i.e. transmission through the cavity occurs across a broad range of frequencies [14], with Ref. [2] able to predict the appropriate behaviour (see Fig. 1.1). However, this approach is unable to correctly describe the electromagnetic field in the presence of a single mirror due to non-physical terms arising in the Hamiltonian. This leaves the challenge to design a continuous-mode model that is able to describe the electromagnetic field for one- and two-mirror setups, whilst only using basic quantum optics assumptions and tools.

1.2 Motivation

The motivation behind the work outlined in this thesis can be summarised through three important questions.

1). What gaps have been identified?

Comparing the theoretically-predicted transmission rate of optical cavities with experimental observations (cf. Fig. 1.1), one can see that the traditional discrete-mode description of the electromagnetic field within an optical cavity does not tell the full story. Instead, it is more appropriate to treat the electromagnetic field using a continuous-mode model, allowing for a broader range of frequencies within the cavity.

As there are no rules regarding how to implement boundary conditions in the postulates of quantum mechanics, it has been difficult for previous authors to provide a full description of a radiating atom in the presence of a reflective interface. Nevertheless, the spontaneous emission of an atom in the presence of a perfectly-reflecting mirror is well-understood, as imposing strict boundary conditions is fairly straightforward. However, modelling a radiating atom in the

presence of a semi-transparent mirror is not as straightforward. Moreover, previous models are unable to account for the possible dissipation of light by the interface.

2). Why did you decide to work on this?

The main aim behind this project was to design a continuous-mode model to quantise the electromagnetic field in the presence of two-sided semi-transparent mirrors. This model should pave the way to understand more complex systems as well as designing novel quantum technologies such as the non-invasive glucose sensing technology discussed in Chapter 7.

3). What are the original contributions to research?

Chapter 5 outlines the so-called image-detector method to quantise the electromagnetic field in the presence of two-sided semi-transparent mirrors by mapping onto analogous free space scenarios. Applying this model to examine a radiating atom in the presence of a two-sided semi-transparent mirror in Chapter 6 allows one to determine analytical expressions for the atomic spontaneous emission rate (cf. Eq. (6.7)). Chapter 7 predicts a long-range dipole-dipole interaction mediated by the mirror, which provides insight into understand novel quantum technologies such as the non-invasive glucose sensing technology discussed later. Again, analytical expressions for the collective spontaneous emission rates (cf. Eqs. (7.20) – (7.24)) are presented, where these rates explicitly depend on the optical properties of the semi-transparent mirror. Moreover, a summary table is provided in Chapter 9 to compare the form of the various spontaneous emission rates derived in this thesis. Finally, in Chapter 8 the model is extended to present a continuous-mode model for optical cavities.

1.3 Open quantum systems

If a quantum system has no interaction with its environment, it is characterised as a closed quantum system, which evolves in time according to the Schrödinger equation. This means the state $|\psi\rangle$ evolves according to

$$\partial_t |\psi\rangle = -\frac{i}{\hbar} \hat{H} |\psi\rangle \,, \qquad (1.1)$$

where $\hat{H}$ is the Hamiltonian operator describing the system. However, when modelling quantum optical systems with spontaneous emission, it is necessary to model the dynamics differently. These types of systems must be treated as open quantum systems as they interact with their environment to produce measurable phenomena.

Consider a quantum system interacting with some external system (more commonly known as a bath) that has infinitely many degrees of freedom, then the system is no longer described in terms of pure states. Instead a statistical ensemble (or density matrix) description is used. The time evolution of the density matrix $\hat{\rho}$ is governed by a master equation. Assuming Markovianity and a weak-coupling between system and bath, the master equation is Lindbladian [15] and is of the form

$$\dot{\hat{\rho}}(t) = -\frac{i}{\hbar} \left[\hat{H}, \hat{\rho}(t) \right] + \frac{1}{2} \sum_{i,j} \Gamma_{ij} \left(2\hat{L}_j \, \hat{\rho}(t) \, \hat{L}_i^\dagger - \left[\hat{L}_i^\dagger \hat{L}_j, \hat{\rho}(t) \right]_+ \right) \,, \qquad (1.2)$$

where $\hat{L}_{i,j}$ are Lindblad operators and Γ_{ij} denotes the decay rate for the $i \rightarrow j$ transition. Chapter 3 will discuss a general derivation for the above master equation as well as considering explicit examples in later chapters.

1.4 Outline

This thesis is split into three parts. The first part consists of Chapters 2, 3 and 4, providing a theoretical background on the basics of quantum mechanics, quantum optics and modelling open quantum systems. Collectively these chapters provide the necessary background information required to understand the overall project.

The second part consists of Chapter 5 which looks at the novel theoretical model known as the image-detector method. This model correctly describes the behaviour of wave packets in the presence of two-sided semi-transparent mirrors for both classical and quantum scenarios. By mapping onto analogous free-space scenarios, one is able to obtain expressions for the electromagnetic field Hamiltonian $\hat{H}_{\text{field}}$, as well as expressions for the electromagnetic field observables $\hat{\mathbf{E}}_{\text{mirr}}(\mathbf{r})$ and $\hat{\mathbf{B}}_{\text{mirr}}(\mathbf{r})$ as functions of the mirrors optical properties.

The third section considers applications of the image-detector method and consists of Chapters 6, 7 and 8. In the following chapters applications of the outlined model are presented in order to justify its validity. Chapter 6 demonstrates the validity of the model outlined in Chapter 5 by predicting the correct spontaneous emission rates for an atom in the presence of a perfectly-reflecting mirror, as well as generating analytical expressions for the spontaneous decay rate for an atom in the presence of a two-sided semi-transparent mirrors Γ_{mirr}. Chapter 7 implements the image-detector method to predict long-range dipole-dipole interaction mediated by a two-sided semi-transparent mirror. The interaction leads to modifications in collective spontaneous emission rates, where analytical expressions for the spontaneous emission rates $\widetilde{\Gamma}_{\pm}$ are obtained. In Chapter 8 a continuous-mode model is presented to describe the electromagnetic field within optical cavities, where expressions for the electromagnetic field Hamiltonian $\hat{H}_{\text{field}}$ as well as expressions for the electromagnetic field observables $\hat{\mathbf{E}}_{\text{cav}}(\mathbf{r})$ and $\hat{\mathbf{B}}_{\text{cav}}(\mathbf{r})$ are obtained.

Finally, in Chapter 9, potential future work based on this work is discussed and a summary of the results presented in this thesis.

Part I

Theoretical Background

Chapter 2

Electrodynamics in free-space

In this chapter the classical and quantum theories of light will be reviewed. Moreover, when quantising the electromagnetic field both canonical and phenomenological approaches will be presented and consistency of the results confirmed.

2.1 Classical electrodynamics

In 1865 James Clerk Maxwell published his seminal paper - A Dynamical Theory of the Electromagnetic Field - in which he unified the theories of electricity, magnetism and light [16]. He linked these together through four elegant equations which describe the dynamics of electric and magnetic fields, as well as any constraints placed on them. Fundamentally, he proved that light is the physical manifestation of oscillating electric and magnetic fields which propagate through space at the speed of light, c.

In free space, i. e. in a medium with permittivity ε_0 and permeability μ_0 and in the absence of any charges or currents, one can write Maxwell's equations in the following way

$$
\begin{aligned}
\nabla \cdot \mathbf{E}_{\text{free}}(\mathbf{r}, t) &= 0 \ , & \nabla \times \mathbf{E}_{\text{free}}(\mathbf{r}, t) &= -\dot{\mathbf{B}}_{\text{free}}(\mathbf{r}, t) \ , \\
\nabla \cdot \mathbf{B}_{\text{free}}(\mathbf{r}, t) &= 0 \ , & \nabla \times \mathbf{B}_{\text{free}}(\mathbf{r}, t) &= \varepsilon \mu \dot{\mathbf{E}}_{\text{free}}(\mathbf{r}, t) \ , \quad (2.1)
\end{aligned}
$$

where the dot notation represents a derivative with repsect to time, $\mathbf{E}_{\text{free}}(\mathbf{r}, t)$ and $\mathbf{B}_{\text{free}}(\mathbf{r}, t)$ denote the electric and the magnetic field vectors at position $\mathbf{r}$ and at a time t, respectively.

Immediately, one can see that

$$\mathbf{k} \cdot \mathbf{E}_{\text{free}}(\mathbf{r}, t) = \mathbf{k} \cdot \mathbf{B}_{\text{free}}(\mathbf{r}, t) = 0 \,, \tag{2.2}$$

which reveals that both the electric and magnetic fields are orthogonal to the direction of propagation $\mathbf{k}$ for all times t, in a homogeneous and anisotropic medium. From Eqs. (2.1) and (2.2) one can deduce that there is an extra degree of freedom missing from the description. This degree of freedom is known as polarisation and describes the orientation of the electric field amplitude. As it shall be demonstrated later, for any given wave vector $\mathbf{k}$ there are two independent polarisations $\lambda = 1, 2$.

Now, one must solve Maxwell's equations (see Eq. (2.1)). By determining these solutions one obtains analytical expressions for the electric and magnetic field vectors, $\mathbf{E}_{\text{free}}(\mathbf{r}, t)$ and $\mathbf{B}_{\text{free}}(\mathbf{r}, t)$. To do so, one must first convert them into a slightly different form. Since an electric field is the result of a time-varying magnetic field, and vice versa, it is possible to eliminate either the electric or the magnetic field from Maxwell's equations. Applying the curl operator to each line of Eq. (2.1) and making use of the following vector identity

$$\nabla \times (\nabla \times \mathbf{v}) \;=\; \nabla (\nabla \cdot \mathbf{v}) - \nabla^2 \mathbf{v} \,, \tag{2.3}$$

allows one to reduce the set of equations. Therefore, Eq. (2.1) reduces to give the two following equations

$$
\begin{aligned}
\nabla^2 \mathbf{E}_{\text{free}}(\mathbf{r}, t) &= \frac{1}{c^2} \partial_t{}^2 \mathbf{E}_{\text{free}}(\mathbf{r}, t) \,, \\
\nabla^2 \mathbf{B}_{\text{free}}(\mathbf{r}, t) &= \frac{1}{c^2} \partial_t{}^2 \mathbf{B}_{\text{free}}(\mathbf{r}, t) \,.
\end{aligned} \tag{2.4}
$$

The expressions in Eq. (2.4) are more commonly known as wave equations, which take the general form

$$\nabla^2 f(\mathbf{r}, t) \;=\; \frac{1}{v^2} \partial_t^2 f(\mathbf{r}, t) \,, \tag{2.5}$$

where v represents the propagation velocity of the wave. In the case of free space, the velocity of the wave is equal to the speed of light, i.e. $v = c$.

One-dimensional case

First, let us consider the simplest case where the direction of propagation of the field is restricted to the x-axis. From Eq. (2.4), one can write down the following one-dimensional wave equations for the electric and magnetic field

$$
\begin{aligned}
\partial_x^2 E_{\text{free}}(x,t) &= \frac{1}{c^2} \partial_t^2 E_{\text{free}}(x,t) \,, \\
\partial_x^2 B_{\text{free}}(x,t) &= \frac{1}{c^2} \partial_t^2 B_{\text{free}}(x,t) \,,
\end{aligned}
\tag{2.6}
$$

and in analogy to Eq. (2.5), the above wave equations take the general form

$$
\partial_x^2 f(x,t) = \frac{1}{v^2} \partial_t^2 f(x,t) \,.
\tag{2.7}
$$

The above equation can be solved using Fourier transforms. The Fourier transform is a mathematical operation that allows one to decompose a wave into the different frequencies it is constructed from, thereby providing a simpler problem to solve. Here, it is necessary to transform from position-space to momentum-space through the definition of the Fourier transform. The converse is also true, this is more commonly known as the inverse Fourier transform.

The Fourier transform to move between position-space (x-space) and momentum-space (k-space) is defined as

$$
\widetilde{F}(k,t) = \frac{1}{\sqrt{2\pi}} \int_{-\infty}^{\infty} \mathrm{d}x \, f(x,t) \, \mathrm{e}^{-\mathrm{i}kx} \,,
\tag{2.8}
$$

where the factor of $1/\sqrt{2\pi}$ is a normalisation constant. Similarly, the inverse Fourier transform can be defined as

$$
f(x,t) = \frac{1}{\sqrt{2\pi}} \int_{-\infty}^{\infty} \mathrm{d}k \, \widetilde{F}(k,t) \, \mathrm{e}^{\mathrm{i}kx} \,,
\tag{2.9}
$$

which moves from momentum-space back to position-space.

Now, lets look at the electric field wave equation (first expression of Eq. (2.6)), one must first multiply both sides by $\mathrm{e}^{-\mathrm{i}kx}/\sqrt{2\pi}$ and then integrate over all space. Combining this with the definition provided in Eq. (2.8), one finds that

$$
\partial_t^2 \widetilde{E}(k,t) + (ck)^2 \, \widetilde{E}(k,t) = 0 \,.
\tag{2.10}
$$

The above equation is the familiar equation of motion for a simple harmonic oscillator, which has well-known solutions taking the form $\widetilde{E}(k,t) = \widetilde{E}(k)\mathrm{e}^{rt}$ where $r = \pm \mathrm{i}ck$. This means the general solution takes the form

$$\widetilde{E}(k,t) = \widetilde{F}(k)\,\mathrm{e}^{\mathrm{i}ckt} + \widetilde{G}(k)\,\mathrm{e}^{-\mathrm{i}ckt}, \qquad (2.11)$$

where $\widetilde{F}(k)$ and $\widetilde{G}(k)$ denote the Fourier transforms of the functions $f(x)$ and $g(x)$, respectively. Now, applying the inverse Fourier transform to the above equation, which is achieved by multiplying through by $\mathrm{e}^{\mathrm{i}kx}/\sqrt{2\pi}$ and integrating over all wavenumbers k yields

$$E(x,t) = \frac{1}{\sqrt{2\pi}} \int_{-\infty}^{\infty} \mathrm{d}k\,\widetilde{F}(k)\,\mathrm{e}^{\mathrm{i}k(x-ct)} + \frac{1}{\sqrt{2\pi}} \int_{-\infty}^{\infty} \mathrm{d}k\,\widetilde{G}(k)\,\mathrm{e}^{\mathrm{i}k(x+ct)}. \quad (2.12)$$

Using the definition of the Fourier transform from Eq. (2.8), one finds that the above equation reduces to give

$$E(x,t) = f(x - ct) + g(x + ct), \qquad (2.13)$$

where the solutions of the wave equation are left- and right-moving waves, which propagate with the speed of light c. Here, the left-travelling solution is represented by a function which depends on $(x + ct)$ and the right-travelling solution is represented by a function which depends on $(x - ct)$. Notice that both left- and right-travelling waves are valid solutions of the wave equation. Moreover, since the wave equation is a linear equation, it is also true that the sum of any two solutions is also a valid solution. This observation is commonly known as the superposition principle. From the above equations, it is evident that electromagnetic waves in a vacuum obey the following relation

$$\omega = ck, \qquad (2.14)$$

where $k = 2\pi/\lambda$ and $c = f\lambda$.

Taking this into account, it is possible to write the solution of the electric and magnetic field wave equations from Eq. (2.6) in the following way [17]

$$\begin{aligned}
E_{\mathrm{free}}(x,t) &= \frac{1}{\sqrt{2\pi}} \int_{-\infty}^{\infty} \mathrm{d}k\,\widetilde{E}(k)\,\mathrm{e}^{\mathrm{i}(kx-\omega t)} + \text{c.c.}, \\
B_{\mathrm{free}}(x,t) &= \frac{1}{\sqrt{2\pi}} \int_{-\infty}^{\infty} \mathrm{d}k\,\widetilde{B}(k)\,\mathrm{e}^{\mathrm{i}(kx-\omega t)}\,\mathrm{sign}(k) + \text{c.c.}
\end{aligned} \qquad (2.15)$$

Here, c.c. denotes the complex conjugate, which represents an equally valid solution to the wave equation. The presence of the complex conjugate term ensures that the electric and magnetic field $E_{\text{free}}(x, t)$ and $B_{\text{free}}(x, t)$ are real.

Returning to the discussion regarding polarisation, the above solutions are applicable to one polarisation, specifically $\lambda = 1$. This arises as the field is restricted to propagating along the x-axis for the one-dimensional case, i.e. only wave vectors $\mathbf{k} = (k, 0, 0)$ are considered. From Eq. (2.2) it must also be true that the electric field and magnetic field are always orthogonal to the direction of propagation, leaving two possible choices for the oscillating electric and magnetic fields. For the case with polarisation $\lambda = 1$, the coordinate system is chosen such that $\mathbf{E}_{\text{free}}(\mathbf{r}, t) = (0, E_{\text{free}}(x, t), 0)$ and $\mathbf{B}_{\text{free}}(\mathbf{r}, t) = (0, 0, B_{\text{free}}(x, t))$. For polarisation $\lambda = 2$, it is assumed that $\mathbf{E}_{\text{free}}(\mathbf{r}, t) = (0, 0, E_{\text{free}}(x, t))$ and $\mathbf{B}_{\text{free}}(\mathbf{r}, t) = (0, B_{\text{free}}(x, t), 0)$. For these field vectors, Maxwell's equations simplify to

$$
\begin{aligned}
\partial_x E_{\text{free}}(x, t) &= \mp \partial_t B_{\text{free}}(x, t)\,, \\
\partial_x B_{\text{free}}(x, t) &= \mp \varepsilon\mu\, \partial_t E_{\text{free}}(x, t)\,,
\end{aligned}
\tag{2.16}
$$

where the minus and the plus signs apply to waves with linear polarisation $\lambda = 1$ and $\lambda = 2$, respectively. As was shown earlier, one can manipulate Eq. (2.16) to eliminate either the electric or magnetic field and doing so, one obtains one of the wave equations derived in Eq. (2.6). Moreover, the convention for electric and magnetic fields outlined in Eq. (2.16) will be used throughout this thesis.

Three-dimensional case

Following a similar procedure for the three-dimensional case, one starts with the wave equations from Eq. (2.4),

$$
\begin{aligned}
\nabla^2 \mathbf{E}_{\text{free}}(\mathbf{r}, t) &= \frac{1}{c^2} \partial_t^2 \mathbf{E}_{\text{free}}(\mathbf{r}, t)\,, \\
\nabla^2 \mathbf{B}_{\text{free}}(\mathbf{r}, t) &= \frac{1}{c^2} \partial_t^2 \mathbf{B}_{\text{free}}(\mathbf{r}, t)\,.
\end{aligned}
\tag{2.17}
$$

The above equations then have the associated solutions [17]

$$
\mathbf{E}_{\text{free}}(\mathbf{r}, t) = \frac{1}{(\sqrt{2\pi})^3} \sum_{\lambda=1,2} \int_{-\infty}^{\infty} \mathrm{d}^3\mathbf{k}\, \widetilde{E}(\mathbf{k})\, \mathrm{e}^{\mathrm{i}(\mathbf{k}\cdot\mathbf{r}-\omega t)} \hat{\mathrm{e}}_{\mathbf{k}\lambda} + \text{c.c.}\,,
$$

$$
\mathbf{B}_{\text{free}}(\mathbf{r}, t) = \frac{1}{(\sqrt{2\pi})^3} \sum_{\lambda=1,2} \int_{-\infty}^{\infty} \mathrm{d}^3\mathbf{k}\, \widetilde{B}(\mathbf{k})\, \mathrm{e}^{\mathrm{i}(\mathbf{k}\cdot\mathbf{r}-\omega t)} \, (\mathbf{k} \times \hat{\mathrm{e}}_{\mathbf{k}\lambda}) + \text{c.c.} \quad (2.18)
$$

Again, one can show that the general solutions to Maxwell's equations in three dimensions are superpositions of travelling waves with wave vectors $\mathbf{k}$, polarisations $\lambda = 1, 2$ and frequencies ω which obey the following fundamental relation

$$
\omega = \|\mathbf{k}\|/\sqrt{\varepsilon\mu} = \|\mathbf{k}\|\, c\,, \quad (2.19)
$$

in analogy to Eq. (2.14) where c denotes the speed of light [17].

2.2 Quantum theory of radiation

In the late 1800s, Lord Rayleigh was following the in footsteps of James Clerk Maxwell by researching the behaviour of the electromagnetic field and through his work, provided a more solid foundation for the classical theory of electromagnetic radiation. Nowadays, it is common knowledge that all physical bodies emit electromagnetic radiation, however, predicting the spectrum of radiation emitted by an idealized black body was one of his key results [18]. It was during this period of work that he derived the famous Rayleigh-Jeans law but, more importantly, his work really drew attention to key issues within the classical theory. Ultimately, all these discrepancies within the classical theory brought about the need for a new, more accurate theory - the quantum theory.

Planck published his seminal paper in 1900 on the spectrum of black body radiation [19] which eventually led to the discovery of quantum physics. In his work he was able to correctly predict the spectral density of electromagnetic radiation emitted by a blackbody in thermal equilibrium. Planck's new approach was able to correctly model the behaviour of the spectrum in the ultraviolet range, something which the classical theory simply could not predict. As it will be shown later in this chapter, Planck resolved this problem by deriving an elegant theory where he treated a region of space as a box with sides of length L which leads to a quantised wavevector and energy quanta known as photons.

2.2.1 Basics of quantum physics

Having presented the story of the classical theory of electromagnetism so far, the next step will be to present the quantum theory of electromagnetism. To do so, let us define some of the basic rules and mathematical tools used in quantum physics to describe the behaviour of physical systems [20, 21].

Postulates of quantum physics

1. States of a physical system are represented by normalised vectors which are elements of a complex Hilbert space, $\mathcal{H}$, where one is able to define the inner product of any two basis vectors such that

$$\langle m|n\rangle = \begin{cases} 1, & \text{if } m = n\,, \\ 0, & \text{otherwise}\,. \end{cases} \tag{2.20}$$

2. The Hilbert space of composite systems are defined using the tensor product, i.e. $\mathcal{H} = \mathcal{H}_1 \otimes \mathcal{H}_2$ describes the Hilbert space for two subsystems $\mathcal{H}_1$ and $\mathcal{H}_2$.

3. Observable quantities of a physical system are represented by self-adjoint operators $\hat{A}$ which are defined on the space $\mathcal{H}$. The average result of repeated measurements of an observable $\hat{A}$ with non-degenerate eigenvalues, when the system is in the state $|\psi\rangle$, is given by the expectation value

$$\langle \hat{A} \rangle = \langle\psi|\hat{A}|\psi\rangle\,. \tag{2.21}$$

   It is equally valid to say that individual measurement outcomes are eigenvalues a_m of the observable $\hat{A}$, and the probability $p(a_m)$ of making a measurement with the outcome a_m is given by

$$p(a_m) = \langle\psi|(|a_m\rangle\langle a_m|)|\psi\rangle \equiv |\langle\psi|a_m\rangle|^2\,, \tag{2.22}$$

   where $|a_m\rangle$ denotes the eigenstate associated with the eigenvalue a_m. Here, the inner product is always defined due to Postulate 1.

4. The state of a closed system $|\psi(t)\rangle$ evolves according to the time-dependent Schrödinger equation

$$i\hbar\,\partial_t|\psi(t)\rangle = \hat{H}|\psi(t)\rangle\,. \tag{2.23}$$

Quantising the classical one-dimensional harmonic oscillator

The best starting point is to first consider the fundamental system consisting of a particle of mass M attached to a spring with a spring constant k. This system is more commonly known as a harmonic oscillator and one can draw some fundamental analogies between the quantised electromagnetic field and the quantised harmonic oscillator.

One can readily write down an expression for the classical one-dimensional oscillator Hamiltonian by summing over kinetic and potential energies such that,

$$H \quad = \quad \frac{p^2}{2M} + \frac{1}{2}M\omega^2 x^2 \,, \tag{2.24}$$

where the frequency of oscillation ω is determined by the spring constant k and the mass of the particle mass M, such that $\omega = \sqrt{k/m}$. Understanding the harmonic oscillator in classical physics is crucial as the quantised harmonic oscillator plays a key role in quantum physics. One can write down the Hamiltonian for a quantum harmonic oscillator by making use of the correspondence principle [22–24] which states that a classical dynamic variable corresponds to a quantum mechanical Hermitian operator. Therefore, one can replace the momentum and position variables with their corresponding quantum mechanical operators to obtain the Hamiltonian for the one-dimensional oscillator

$$\hat{H} \quad = \quad \frac{\hat{p}^2}{2m} + \frac{1}{2}M\omega^2 \hat{x}^2 \,, \tag{2.25}$$

where

$$x \to \hat{x} \,, \qquad \text{and} \qquad p \to \hat{p} \,. \tag{2.26}$$

In the position representation these operators are defined such that $\hat{x} = x$ and $\hat{p} = -\mathrm{i}\hbar\partial_x$. The canonical commutation relation between the momentum and position (conjugate) variables arises from the Postulate 1 and is defined in the following way

$$[\hat{x}_i, \hat{p}_j] \quad = \quad \mathrm{i}\hbar\delta_{ij} \,, \tag{2.27}$$

where $i, j = 1, ..., n$ and δ_{ij} denotes the Kronecker delta function. One can justify Eq. (2.27) from classical physics as the Poisson bracket for position and momentum variables satisfies

$$\{x_i, p_j\} = \delta_{ij}, \tag{2.28}$$

where $i, j = 1, ..., n$. At this point, rather than attempt to solve Eq. (2.23), one can use the ladder operator method initially outlined by Dirac [25]. This method allows one to extract information regarding the energy eigenvalues of the system. This is achieved by defining the ladder operators as

$$\begin{aligned} \hat{a} &= \sqrt{\frac{M\omega}{2\hbar}} \left(\hat{x} + \frac{\mathrm{i}}{M\omega}\hat{p} \right), \\ \hat{a}^\dagger &= \sqrt{\frac{M\omega}{2\hbar}} \left(\hat{x} - \frac{\mathrm{i}}{M\omega}\hat{p} \right), \end{aligned} \tag{2.29}$$

where $\hat{a}$ and $\hat{a}^\dagger$ are also known as bosonic annihilation and creation operators. Moreover, these ladder operators obey the canonical commutation relation,

$$\left[\hat{a}, \hat{a}^\dagger \right] = 1. \tag{2.30}$$

From here, one can re-express the position and momentum operators in terms of these ladder operators,

$$\begin{aligned} \hat{x} &= \sqrt{\frac{\hbar}{2}\frac{1}{M\omega}} \left(\hat{a}^\dagger + \hat{a} \right), \\ \hat{p} &= \mathrm{i}\sqrt{\frac{\hbar}{2}M\omega} \left(\hat{a}^\dagger - \hat{a} \right). \end{aligned} \tag{2.31}$$

Substituting the expressions from Eq. (2.31) into Eq. (2.25) generates a new form for the quantised harmonic oscillator Hamiltonian in one-dimension. This substitution yields

$$\hat{H} = \hbar\omega \left(\hat{a}^\dagger \hat{a} + \frac{1}{2} \right), \tag{2.32}$$

where the constant represents the zero-point energy of the oscillator.

In order to understand Eq. (2.32), it is convenient to make use of the second quantisation notation [26]. This formalism looks at the occupation number
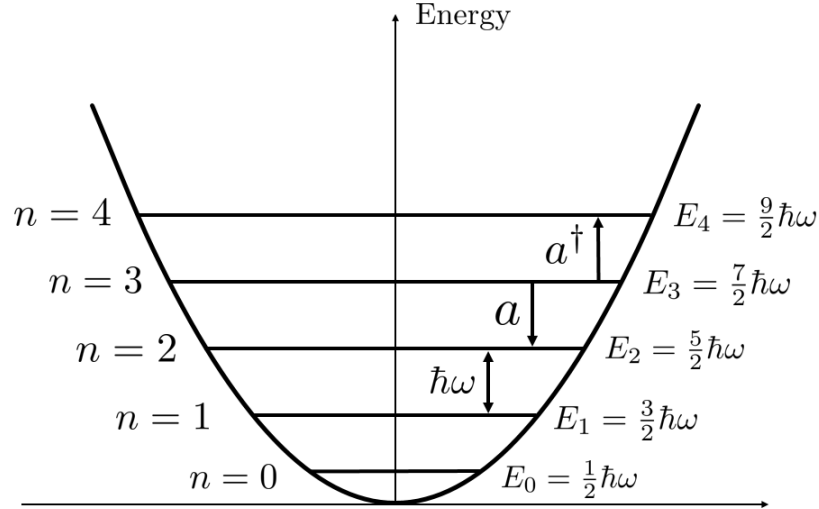
Figure 2.1: Energy-level diagram for a quantum-mechanical harmonic oscillator, where energy levels are equally separated by $\hbar\omega$. By applying the creation and annihilation operators $\hat{a}^\dagger$ and $\hat{a}$, one is able to move up or down these energy levels, which results in either adding or subtracting an amount $\hbar\omega$, respectively.

of particular states i.e. the number of particles or quanta in each state. This is particularly useful as it means one does not have to consider individual wave functions, especially since writing down the wave function of a photon in a particular representation is not a straight forward task. Implementing the second quantisation notation and substituting the Hamiltonian from Eq. (2.32) into the time-independent Schrödinger equation one finds

$$\hat{H}|n\rangle \;\;=\;\; \hbar\omega\left(\hat{a}^\dagger\hat{a} + \frac{1}{2}\right)|n\rangle = E_n|n\rangle\,, \tag{2.33}$$

for some arbitrary eigenstate $|n\rangle$ with the associated energy eigenvalue E_n. Eq. (2.33) takes the form of an eigenvalue equation, where the Fock state $|n\rangle$ is an eigenfunction of the Hamiltonian operator $\hat{H}$ with corresponding eigenvalue(s) E_n.

Multiplying from the left by the creation operator $\hat{a}^\dagger$ yields

$$\hbar\omega\left(\hat{a}^\dagger\hat{a}^\dagger\hat{a} + \frac{1}{2}\hat{a}^\dagger\right)|n\rangle = E_n\hat{a}^\dagger|n\rangle\,,$$

$$\hbar\omega\left(\hat{a}^\dagger\hat{a}\hat{a}^\dagger - \frac{1}{2}\hat{a}^\dagger\right)|n\rangle = E_n\hat{a}^\dagger|n\rangle\,,$$

$$\hbar\omega\left(\hat{a}^\dagger\hat{a} + \frac{1}{2}\right)\hat{a}^\dagger|n\rangle = (E_n + \hbar\omega)\,\hat{a}^\dagger|n\rangle\,. \tag{2.34}$$

From the last line of the above equation, one can write down the following energy eigenvalue-eigenstate equation

$$\hat{H}\hat{a}^\dagger|n\rangle = (E_n + \hbar\omega)\,\hat{a}^\dagger|n\rangle\,. \tag{2.35}$$

Eq. (2.35) demonstrates that by applying the creation operator $\hat{a}^\dagger$, one shifts up the ladder structure in Fig. 2.1, effectively moving to a higher energy level. Similarly, one can also apply the annihilation operator $\hat{a}$ to Eq. (2.33) which gives

$$\hat{H}\hat{a}|n\rangle = (E_n - \hbar\omega)\,\hat{a}|n\rangle\,. \tag{2.36}$$

From Eq. (2.36) it is evident that applying the annihilation operator $\hat{a}$ one shifts down the ladder structure in Fig. 2.1, effectively moving to a lower energy level. Denoting the ground state of the oscillator as $|0\rangle$, and using the Schrödinger equation, one can show that

$$\hat{H}\hat{a}|0\rangle = (E_n - \hbar\omega)\,\hat{a}|0\rangle\,, \tag{2.37}$$

which implies that

$$\hat{a}|0\rangle = 0\,, \tag{2.38}$$

as the ground state is the lowest possible eigenstate. In addition, it is also true

$$\hat{a}^\dagger|0\rangle = |1\rangle\,. \tag{2.39}$$

Moreover, using Eqs. (2.30), one can show

$$\langle n|\hat{a}\hat{a}^\dagger|n\rangle = \langle n|1 + \hat{a}^\dagger\hat{a}|n\rangle = n + 1\,, \tag{2.40}$$

meaning

$$
\begin{aligned}
\hat{a}^\dagger |n\rangle &= \sqrt{n+1}\,|n+1\rangle\,, \\
\hat{a} |n\rangle &= \sqrt{n}\,|n-1\rangle\,,
\end{aligned}
\tag{2.41}
$$

and

$$
|n\rangle = \frac{\left(\hat{a}^\dagger\right)^n}{\sqrt{n!}|0\rangle}\,. \tag{2.42}
$$

This allows one to define a Hermitian operator $\hat{n}$, which is known as the bosonic number operator or the occupation number operator, such that

$$
\hat{n} = \hat{a}^\dagger \hat{a}\,. \tag{2.43}
$$

Moreover, photons are an example of bosons and for this case, the number operator gives information regarding the number of photons occupying a certain state. In addition, the one-photon state $|1\rangle$ corresponds to a wavepacket with statistically one photon and the energy of one excitation. Importantly, this representation allows one to re-express Eq. (2.32) such that

$$
\langle \hat{H} \rangle = \hbar\omega \left(n + \frac{1}{2} \right) \quad \text{where } n = 0, 1, 2, 3... \tag{2.44}
$$

As it was demonstrated in Fig. 2.1 the energy spectrum of the harmonic oscillator is built up of discrete energy levels separated by an integer amount of $\hbar\omega$ and this description is confirmed by examining the form of Eq. (2.44). Finally, one can state that the number operator obeys the eigenvalue-eigenstate equation

$$
\hat{a}^\dagger \hat{a} |n\rangle = n|n\rangle \quad \text{where } n = 0, 1, 2, 3...\,, \tag{2.45}
$$

and the eigenstates $|n\rangle$ are known as number states or Fock states with the orthogonality property

$$
\langle n|n \rangle = \delta_{nn}\,, \tag{2.46}
$$

and the completeness relation

$$
\sum_{n=0}^{\infty} |n\rangle\langle n| = \hat{\mathbb{1}}\,, \tag{2.47}
$$

where $\hat{\mathbb{1}}$ denotes the identity operator. This completeness relation holds as any state of the system can be expressed as a superpositon of the number states $|n\rangle$.

19

2.2.2 Canonical field quantisation

The aim of this section is to present the quantisation of the electromagnetic field based on the canonical approach. The standard route was first laid out by Dirac who used the classical theory as a basis, and then replaced dynamical variables by corresponding quantum mechanical operators which obeyed commutation relations in analogy to the classical Poisson brackets [25].

A convenient starting point is the classical Maxwell equations (cf. Eq. (2.1)). Considering some electric field $\mathbf{E}_{\text{free}}(\mathbf{r}, t)$, one is able to express this field in terms of the gradient of the scalar potential $V(\mathbf{r}, t)$ such that

$$\mathbf{E}_{\text{free}}(\mathbf{r}, t) = -\nabla V(\mathbf{r}, t), \qquad (2.48)$$

which is possible since the potential is defined as the work required to bring a positive charge from infinity to some specific point, hence the minus sign. If the scalar potential in Eq. (2.48) was changed by some function constant which is spatially constant but time dependent, i.e. some periodic potential where $V(\mathbf{r}, t) \to V(\mathbf{r}, t) + C(t)$ then the equations of motion for the system are unaffected, which is more commonly known as *gauge freedom*. In other words, one can apply a mathematical operation to a system and the operation does not affect the system's dynamics. Implementing such an operation is called a *gauge transformation* [27]. The electric and magnetic fields $\mathbf{E}_{\text{free}}(\mathbf{r}, t)$ and $\mathbf{B}_{\text{free}}(\mathbf{r}, t)$ can be defined in terms the position- and time-dependent magnetic vector potential $\mathbf{A}(\mathbf{r}, t)$ such that

$$\begin{aligned}
\mathbf{E}_{\text{free}}(\mathbf{r}, t) &= -\nabla V(\mathbf{r}, t) - \partial_t \mathbf{A}(\mathbf{r}, t), \\
\mathbf{B}_{\text{free}}(\mathbf{r}, t) &= \nabla \times \mathbf{A}(\mathbf{r}, t).
\end{aligned} \qquad (2.49)$$

As the scalar potential $V(\mathbf{r}, t)$ and the magnetic vector potential $\mathbf{A}(\mathbf{r}, t)$ are not unique, one can define new potentials such that

$$\begin{aligned}
\mathbf{A}'(\mathbf{r}, t) &= \mathbf{A}(\mathbf{r}, t) + \nabla f(\mathbf{r}, t), \\
V'(\mathbf{r}, t) &= V(\mathbf{r}, t) - \partial_t f(\mathbf{r}, t),
\end{aligned} \qquad (2.50)$$

where the two are related through some function $f(\mathbf{r}, t)$ that depends on position and time and is twice differentiable. This function $f(\mathbf{r}, t)$ is more commonly

referred to as the *gauge function*, and introducing this function enforces a gauge transformation. In other words, when there are no sources or charges present Maxwells equations are *gauge invariant*. One can impose conditions on the potentials $\mathbf{A}(\mathbf{r}, t)$ and V that can be realised by a gauge transformation from an arbitrary pair of $\mathbf{A}(\mathbf{r}, t)$ and $V(\mathbf{r}, t)$, thereby specifying a gauge for the electromagnetic field. The most common and convenient choice of gauge for problems in quantum optics is the so-called Coulomb gauge,

$$\nabla \cdot \mathbf{A}(\mathbf{r}, t) = 0. \tag{2.51}$$

Field modes

Now let us have a closer look at what it means for the electromagnetic field to be quantised over all space and most importantly, derive the form of the quantised electromagnetic field observables.

Planck's key contribution to the modelling of this problem required treating a region of free-space as a cube with sides of length $L_x = L_y = L_z = L$. The walls of this cube provide periodic boundary conditions which are imposed to determine the travelling wave solutions of the electromagnetic field within that region of space. It is assumed that the wave function vanishes on the walls of the cube and the vector potential inside the cube satisfies $V(\mathbf{r}, t) = 0$. Therefore, the components of the wave vector $\mathbf{k}$ must have discrete values. The quantised wavevector is denoted by $\mathbf{k} = (k_x, k_y, k_z)$ such that

$$k_i = \sum_{i=x,y,z} \frac{2\pi n_i}{L}, \tag{2.52}$$

where the spatial dimensions x, y, z are summed over and n_i are integers or zeros. In addition, each wavevector carries a polarisation of either $\lambda = 1$ or $\lambda = 2$. The polarisation vectors $\hat{e}_{\mathbf{k}\lambda}$ satisfy the relations

$$\hat{e}_{\mathbf{k}\lambda} \cdot \mathbf{k} = 0,$$
$$\hat{e}_{\mathbf{k}\lambda} \cdot \hat{e}_{\mathbf{k}'\lambda'} = \delta_{\mathbf{k}\mathbf{k}'} \, \delta_{\lambda\lambda'}. \tag{2.53}$$

These solutions are more commonly referred to as modes, or field modes and they can be determined by obtaining a wave equation for the vector potential

$\mathbf{A}(\mathbf{r}, t)$, i.e. substituting the second expression of Eq. (2.49) into Ampères law (the fourth expression of Eq. (2.1)), which yields

$$\nabla^2 \mathbf{A}(\mathbf{r}, t) = \frac{1}{c^2} \partial_t^2 \mathbf{A}(\mathbf{r}, t) . \tag{2.54}$$

As this is the same form as Eq. (2.17), it is already known what form these modes take, and that they can be written as

$$\mathbf{A}(\mathbf{r}, t) = \mathbf{A}_{\mathbf{k}\lambda} e^{i\mathbf{k}\cdot\mathbf{r}} \hat{e}_{\mathbf{k}\lambda} + \mathbf{A}_{\mathbf{k}\lambda}^* e^{-i\mathbf{k}\cdot\mathbf{r}} \hat{e}_{\mathbf{k}\lambda} . \tag{2.55}$$

One can then expand the vector potential $\mathbf{A}(\mathbf{r}, t)$ to sum over contributions from all possible modes. This allows one to express the vector potential, the electric and the magnetic field observables in the following way

$$\begin{aligned}
\mathbf{A}(\mathbf{r}, t) &= \sum_{\mathbf{k}\lambda} \sqrt{\frac{\hbar}{2\omega_{\mathbf{k}}\varepsilon_0 V}} e^{i\mathbf{k}\cdot\mathbf{r}} a_{\mathbf{k}\lambda} \hat{e}_{\mathbf{k}\lambda} + \text{H.c.} , \\
\mathbf{E}(\mathbf{r}, t) &= \sum_{\mathbf{k}\lambda} \sqrt{\frac{\hbar\omega_{\mathbf{k}}}{2\varepsilon_0 V}} \, i \, e^{i\mathbf{k}\cdot\mathbf{r}} a_{\mathbf{k}\lambda} \hat{e}_{\mathbf{k}\lambda} + \text{H.c.} , \\
\mathbf{B}(\mathbf{r}, t) &= \sum_{\mathbf{k}\lambda} \sqrt{\frac{\hbar\omega}{2\varepsilon_0 V}} \, i \, e^{i\mathbf{k}\cdot\mathbf{r}} a_{\mathbf{k}\lambda} \left(\mathbf{k} \times \hat{e}_{\mathbf{k}\lambda} \right) + \text{H.c.} ,
\end{aligned} \tag{2.56}$$

where $\sqrt{\frac{\hbar}{2\omega\varepsilon_0 V}}$ and $\sqrt{\frac{\hbar}{2\omega V}}$ denote normalisation constants and V denotes the quantisation volume mapped out by the cube with sides of length L. Note that the expressions in Eq. (2.56) can also be derived without introducing a fictitious quantisation volume and instead consider all of space to be a part of an infinite quantisation volume. This is addressed in the next subsection which presents a physically-motivated approach to obtain consistent observables without introducing a quantisation volume.

2.2.3 A physically motivated field quantisation

In the previous subsection 2.2.2, the free-electromagnetic field was quantised through the canonical procedure, where discrete expressions for the electric and magnetic field observables were presented. In this subsection, an alternative approach is presented where experimental observation is used to state the main

result and one can then use the fundamentals to work backwards and obtain the necessary missing details [28]. Most importantly, the expressions derived using the physically-motivated approach are consistent with those derived through the canonical procedure, without having to introduce a certain gauge or a finite quantisation volume.

Field quantisation for propagation in one-dimension

In order to be able to quantise the electromagnetic field in free space in one dimension, it is important to first see what experimental evidence tells us. From experimental observations it is known that the free electromagnetic field consists of basic energy quanta (photons) which can be characterised by their (positive) frequency $\omega \in (0, \infty)$ and a direction of propagation $X = L, R$ [29–38]. Moreover, a photon with the frequency ω has an associated energy E, equal to

$$E \;=\; \hbar\omega \,, \tag{2.57}$$

with ω given in Eq. (2.14). In addition, there exist two possible polarisations $\lambda = 1, 2$, which indicate the direction of the respective electric field vectors. Looking at both polarisations, it is possible to fully describe the free-field using tensor product states of the form

$$\bigotimes_{\omega=0}^{\infty} \bigotimes_{X=L,R} \bigotimes_{\lambda=1,2} |n_{X\lambda}(\omega)\rangle \,, \tag{2.58}$$

as the free-electromagnetic field behaves as a collection of harmonic oscillator modes with number basis states of the form $|n_{X\lambda}(\omega)\rangle$. Moreover, the energy eigenstates of the electromagnetic field are the states defined in Eq. (2.58). Therefore, the form the field Hamiltonian $\hat{H}_{\text{field}}$ is such that

$$\hat{H}_{\text{field}}|n_{X\lambda}(\omega)\rangle \;=\; [\hbar\omega n_{X\lambda}(\omega) + H_{\text{zpe}}] \, |n_{X\lambda}(\omega)\rangle \,, \tag{2.59}$$

where the constant H_{zpe} denotes the zero point energy of the field. In addition, photons are characterised as bosons, therefore the annihilation and creation operators $\hat{a}_{X\lambda}(\omega)$ and $\hat{a}^\dagger_{X\lambda}(\omega)$ obey the bosonic commutation relation

$$\left[\hat{a}_{X\lambda}(\omega), \hat{a}^\dagger_{X'\lambda'}(\omega')\right] \;=\; \delta_{XX'}\delta_{\lambda\lambda'}\delta(\omega - \omega') \,. \tag{2.60}$$

Taking this into account it is possible to deduce the form of the field Hamiltonian $\hat{H}_{\text{field}}$ for light propagating along the x-axis, yielding

$$\hat{H}_{\text{field}} \quad = \quad \sum_{X=L,R}\sum_{\lambda=1,2}\int_0^\infty \mathrm{d}\omega\,\hbar\omega\,\hat{a}^\dagger_{X\lambda}(\omega)\hat{a}_{X\lambda}(\omega) + H_{\text{zpe}}\,, \qquad (2.61)$$

where all possible modes are summed over (X,ω,λ). One can easily check that the energy eigenvalues and eigenstates of Eq. (2.61) are consistent with those of Eq. (2.59).

If one considers the observable for the energy stored inside the free electromagnetic field $\hat{H}_{\text{field}}$, this can be expressed as

$$\hat{H}_{\text{field}} \quad = \quad \sum_{\lambda=1,2}\frac{1}{2}A\int_{-\infty}^\infty \mathrm{d}x\left[\varepsilon_0\,\hat{E}_{\text{free}}(x)^2 + \frac{1}{\mu_0}\,\hat{B}_{\text{free}}(x)^2\right], \qquad (2.62)$$

where A denotes the area in the y-z plane in which $\hat{H}_{\text{field}}$ is defined. Here $\hat{E}_{\text{free}}(x)$ and $\hat{B}_{\text{free}}(x)$ denote the free-space observables of the electric and the magnetic field amplitudes, respectively.

The next step is to determine full expressions for the quantised electric and magnetic field observables for propagation along the x-axis. To do so, one must compare the two Hamiltonian expressions from Eqs. (2.61) and (2.62), whilst also demanding that expectation values of $\hat{E}_{\text{free}}(x)$ and $\hat{B}_{\text{free}}(x)$ evolve according to Maxwell's equations. This allows one to calculate the remaining missing coefficients for the observables [28]. Immediately one can see by comparing the two equations, the electric field observable $\hat{E}_{\text{free}}(x)$ and the magnetic field observable $\hat{B}_{\text{free}}(x)$ are linear superpositions of annihilation and creation operators $\hat{a}_{X\lambda}(\omega)$ and $\hat{a}^\dagger_{X\lambda}(\omega)$. For this reason it is appropriate to adopt the following ansatz for the electric and magnetic fields $\hat{E}_{\text{free}}(x)$ and $\hat{B}_{\text{free}}(x)$,

$$\hat{E}_{\text{free}}(x) \quad = \quad \sum_{X=L,R}\sum_{\lambda=1,2}\int_0^\infty \mathrm{d}\omega\,f_{X\lambda}(x,\omega)\hat{a}_{X\lambda}(\omega) + \text{H.c.}\,,$$

$$\hat{B}_{\text{free}}(x) \quad = \quad \sum_{X=L,R}\sum_{\lambda=1,2}\int_0^\infty \mathrm{d}\omega\,g_{X\lambda}(x,\omega)\hat{a}_{X\lambda}(\omega) + \text{H.c.}\,, \qquad (2.63)$$

where $f_{X\lambda}(x,\omega)$ and $g_{X\lambda}(x,\omega)$ are complex coefficients and H.c. denotes the Hermitian conjugate (or adjoint).

One is able to calculate the time evolution of an expectation value with respect to a given Hamiltonian $\hat{H}$ through the following equation of motion

$$\partial_t \langle \hat{O} \rangle \;\; = \;\; -\frac{\mathrm{i}}{\hbar} \left\langle \left[\hat{O}, \hat{H} \right] \right\rangle . \tag{2.64}$$

Taking this into account and demanding that the expectation values of the electric and magnetic field observables evolve as predicted by Maxwell's equations whilst also maintaining the form of the field Hamiltonian in Eq. (2.61), consistency is maintained provided

$$
\begin{aligned}
\partial_x f_{X\lambda}(x,\omega) &= \pm \mathrm{i}\omega g_{X\lambda}(x,\omega) , \\
\partial_x g_{X\lambda}(x,\omega) &= \pm \mathrm{i}\varepsilon_0\mu_0\omega f_{X\lambda}(x,\omega) .
\end{aligned}
\tag{2.65}
$$

In Eq. (2.65), the minus and positive signs denote the different polarisations of light $\lambda = 1$ and $\lambda = 2$, respectively. More importantly, the general solutions of Eq. (2.65) can be written as

$$
\begin{aligned}
f_{X\lambda}(x,\omega) &= K_{X,1}(\omega)\mathrm{e}^{\mathrm{i}kx} + K_{X,2}(\omega)\mathrm{e}^{-\mathrm{i}kx} , \\
g_{X\lambda}(x,\omega) &= \mp\sqrt{\varepsilon_0\mu_0}\left[K_{X,1}(\omega)\mathrm{e}^{\mathrm{i}kx} - K_{X,2}(\omega)\mathrm{e}^{-\mathrm{i}kx} \right] ,
\end{aligned}
\tag{2.66}
$$

where the positive wave number k is defined in Eq. (2.14) and the constants K are complex functions of frequency and direction of propagation (ω and X) but independent of position, time and polarisation (x, t and λ). However, since the index X characterises the direction of propagation, it is only appropriate to keep certain solutions. In other words, looking at Eq. (2.66), the solutions with $K_{R,1}(\omega)$ and $K_{L,2}(\omega)$ are kept as these have an exponential term that is consistent with the correct direction of propagation. In turn, one can now set $K_{R,2}(\omega) = K_{L,1}(\omega) = 0$.

Next, one must determine the remaining constants $K_{R,1}(\omega)$ and $K_{L,2}(\omega)$. One can then normalise $\hat{E}_{\text{free}}(x)$ and $\hat{B}_{\text{free}}(x)$ by determining these constants through the two field Hamiltonians in Eqs. (2.61) and (2.62) coinciding. Therefore, one must use Eqs. (2.63) and (2.66) to generate expressions for the electric and magnetic free-field observables and then substitute these into the field Hamiltonian given in Eq. (2.62). Doing so, one notices that due to the prefactor in the second

line of Eq. (2.66), one obtains an equal contribution from both the electric and magnetic field. This yields the expression

$$
\hat{H}_{\text{field}} = \varepsilon_0 A \sum_{X=L,R} \sum_{\lambda=1,2} \int_{-\infty}^{\infty} \mathrm{d}x \int_0^{\infty} \mathrm{d}\omega \int_0^{\infty} \mathrm{d}\omega'
$$
$$
\times | \left(K_{X\lambda}(\omega)\mathrm{e}^{\mathrm{i}kx} + K_{X\lambda}(\omega)\mathrm{e}^{-\mathrm{i}kx} \right) + \text{H.c.}|^2. \qquad (2.67)
$$

Implementing the bosonic commutation relation from Eq. (2.60) and $K_{R,2}(\omega) = K_{L,1}(\omega) = 0$, one can re-arrange the expression in Eq. (2.67) to give

$$
\hat{H}_{\text{field}} = \varepsilon_0 A \sum_{\lambda=1,2} \int_{-\infty}^{\infty} \mathrm{d}x \int_0^{\infty} \mathrm{d}\omega \int_0^{\infty} \mathrm{d}\omega' \, F(k, k', \omega, \omega', \lambda), \qquad (2.68)
$$

where the function $F(k, k', \omega, \omega', \lambda)$ is defined as

$$
\begin{aligned}
F(k, k', \omega, \omega', \lambda) = {} & K_{R,1}(\omega)K_{R,1}^*(\omega)\mathrm{e}^{\mathrm{i}(k-k')x} \left(\hat{a}_{R\lambda}^{\dagger}(\omega')\hat{a}_{R\lambda}(\omega) + \delta(\omega - \omega') \right) \\
& + K_{R,1}^*(\omega)K_{R,1}(\omega)\mathrm{e}^{-\mathrm{i}(k-k')x}\hat{a}_{R\lambda}^{\dagger}(\omega')\hat{a}_{R\lambda}(\omega) \\
& + K_{L,2}(\omega)K_{L,2}^*(\omega)\mathrm{e}^{-\mathrm{i}(k-k')x} \left(\hat{a}_{L\lambda}^{\dagger}(\omega')\hat{a}_{L\lambda}(\omega) + \delta(\omega - \omega') \right) \\
& + K_{L,2}^*(\omega)K_{L,2}(\omega)\mathrm{e}^{\mathrm{i}(k-k')x}\hat{a}_{L\lambda}^{\dagger}(\omega')\hat{a}_{L\lambda}(\omega). \qquad (2.69)
\end{aligned}
$$

Making use of the definition of the Dirac delta function

$$
2\pi \, \delta(k - k') = \int_{-\infty}^{\infty} \mathrm{d}x \, \mathrm{e}^{\pm \mathrm{i}(k-k')x}, \qquad (2.70)
$$

one can then evaluate the ω'-integral and resolve the delta function to generate the following expression for the field Hamiltonian

$$
\begin{aligned}
\hat{H}_{\text{field}} = {} & 2\pi\varepsilon_0 Ac \sum_{\lambda=1,2} \int_0^{\infty} \mathrm{d}\omega \Big[|K_{R,1}(\omega)|^2 \big[2\hat{a}_{R\lambda}^{\dagger}(\omega)\hat{a}_{R\lambda}(\omega) + 1 \big] \\
& + |K_{L,2}(\omega)|^2 \big[2\hat{a}_{L\lambda}^{\dagger}(\omega)\hat{a}_{L\lambda}(\omega) + 1 \big] \Big]. \qquad (2.71)
\end{aligned}
$$

Finally, by demanding that the expectation value of the field Hamiltonian from Eq. (2.71) in the one-photon state ($\langle 1|\hat{H}_{\text{field}}|1\rangle = \hbar\omega$) is identical to the expectation value of the field Hamiltonian from Eq. (2.61) also in the one-photon state, one finds that

$$
|K_{R,1}(\omega)|^2 = |K_{L,2}(\omega)|^2 = \frac{\hbar\omega}{4\pi\varepsilon_0 Ac}. \qquad (2.72)
$$

In addition, from Eq. (2.71) it also possible to write down an expression for the zero-point energy of the field

$$H_{\text{zpe}} = \int_0^\infty \mathrm{d}\omega \, \frac{1}{2} \, \hbar\omega \, \delta(0) \,, \tag{2.73}$$

in relation to Eqs. (2.59) and (2.61). Finally, one can write down the expressions for the one-dimensional electric- and magnetic-field observables in the following way [28]

$$
\begin{aligned}
\hat{E}_{\text{free}}(x) &= \mathrm{i} \int_0^\infty \mathrm{d}\omega \, \sqrt{\frac{\hbar\omega}{4\pi\varepsilon_0 Ac}} \, \mathrm{e}^{\mathrm{i}kx} \left[\hat{a}_R(\omega) - \hat{a}_L^\dagger(\omega) \right] + \text{H.c.} \,, \\
\hat{B}_{\text{free}}(x) &= -\mathrm{i}\sqrt{\varepsilon_0\mu_0} \int_0^\infty \mathrm{d}\omega \, \sqrt{\frac{\hbar\omega}{4\pi\varepsilon_0 Ac}} \, \mathrm{e}^{\mathrm{i}kx} \left[\hat{a}_R(\omega) - \hat{a}_L^\dagger(\omega) \right] \text{sign(k)} + \text{H.c.}
\end{aligned}
\tag{2.74}
$$

Analogously, one can derive the electric and magnetic field observables for $\lambda = 2$ polarised light. These are of the same form as $\hat{E}_{\text{free}}(x)$ and $\hat{B}_{\text{free}}(x)$ in Eq. (2.74) up to an overall minus sign of the magnetic field.

One can simplify the expressions in Eq. (2.74) by stating that amplitudes propagating in the $-x$ direction have the associated wavenumber $-k$ and those propagating in the $+x$ direction have the associated wavenumber $+k$. Taking this into account, one can re-express Eq. (2.74) in the following way

$$
\begin{aligned}
\hat{E}_{\text{free}}(x) &= \mathrm{i} \int_{-\infty}^\infty \mathrm{d}k \, \sqrt{\frac{\hbar\omega}{4\pi\varepsilon_0 A}} \, \mathrm{e}^{\mathrm{i}kx} \, \hat{a}_k + \text{H.c.} \,, \\
\hat{B}_{\text{free}}(x) &= -\mathrm{i}\sqrt{\varepsilon_0\mu_0} \int_{-\infty}^\infty \mathrm{d}k \, \sqrt{\frac{\hbar\omega}{4\pi\varepsilon_0 A}} \, \mathrm{e}^{\mathrm{i}kx} \, \hat{a}_k \, \text{sign(k)} + \text{H.c.}
\end{aligned}
\tag{2.75}
$$

Note, the normalisation constant changes as the units of the $\hat{a}_X(\omega)$[1] operators differ from the $\hat{a}_k$ operators and the variable of integration changes from ω to k. As before, these observables apply to $\lambda = 1$ polarised light and they differ from $\lambda = 2$ polarised light by an overall minus sign for the magnetic field. Using the new form of the electromagnetic field observables from Eq. (2.75) and substituting the expressions into $\hat{H}_{\text{field}}$ in Eq. (2.62), one obtains

$$\hat{H}_{\text{field}} = \int_{-\infty}^\infty \mathrm{d}k \, \hbar\omega \, \hat{a}_k^\dagger \hat{a}_k \,. \tag{2.76}$$

---

[1] $X = L, R.$

Field quantisation for propagation in three-dimension

Finally, let us examine the quantised electromagnetic field in three dimensions. In free space, the electric field observable $\hat{\mathbf{E}}_{\text{free}}(\mathbf{r})$ and the magnetic field observable $\hat{\mathbf{B}}_{\text{free}}(\mathbf{r})$ at a position $\mathbf{r}$ for light propagation in three dimensions equal [28]

$$\hat{\mathbf{E}}_{\text{free}}(\mathbf{r}) = \frac{\mathrm{i}}{4\pi} \sum_{\lambda=1,2} \int_{\mathbb{R}^3} \mathrm{d}^3\mathbf{k} \sqrt{\frac{\hbar\omega_{\mathbf{k}}}{\pi\varepsilon}} \, \mathrm{e}^{\mathrm{i}\mathbf{k}\cdot\mathbf{r}} \, \hat{\mathbf{e}}_{\mathbf{k}\lambda} \, \hat{a}_{\mathbf{k}\lambda} + \text{H.c.}$$

$$\hat{\mathbf{B}}_{\text{free}}(\mathbf{r}) = -\frac{\mathrm{i}}{4\pi} \sum_{\lambda=1,2} \int_{\mathbb{R}^3} \mathrm{d}^3\mathbf{k} \sqrt{\frac{\hbar\omega}{\pi\varepsilon}} \, \mathrm{e}^{\mathrm{i}\mathbf{k}\cdot\mathbf{r}} \left(\hat{\mathbf{k}} \times \hat{\mathbf{e}}_{\mathbf{k}\lambda} \right) \hat{a}_{\mathbf{k}\lambda} + \text{H.c.} \quad (2.77)$$

which sum over all possible photon modes with wave vectors $\mathbf{k}$ and polarisations λ. Moreover, $\hat{a}_{\mathbf{k}\lambda}$ is the photon annihilation operator of the $(\mathbf{k}, \lambda)$ mode with the bosonic commutator relation

$$\left[\hat{a}_{\mathbf{k}\lambda}, \hat{a}_{\mathbf{k}'\lambda'}^{\dagger} \right] = \delta_{\lambda\lambda'} \, \delta(\mathbf{k} - \mathbf{k}') \,. \quad (2.78)$$

The normalised polarisation vectors $\hat{\mathbf{e}}_{\mathbf{k}\lambda}$ in Eq. (2.77) are pairwise orthogonal and $\hat{\mathbf{e}}_{\mathbf{k}\lambda} \cdot \mathbf{k} = 0$ for all $\mathbf{k}$. The frequency $\omega_{\mathbf{k}}$ can be found in Eq. (2.19) and the constant ε_0 denotes the permittivity of free space. Moreover, the Hamiltonian $\hat{H}_{\text{field}}$ of the electromagnetic field in free space in three dimensions can be expressed as

$$\hat{H}_{\text{field}} = \sum_{\lambda=1,2} \int_{-\infty}^{\infty} \mathrm{d}^3\mathbf{r} \left[\varepsilon_0 \, \hat{\mathbf{E}}_{\text{free}}(\mathbf{r})^2 + \frac{1}{\mu_0} \, \hat{\mathbf{B}}_{\text{free}}(\mathbf{r})^2 \right], \quad (2.79)$$

where A denotes the area in the y-z plane in which $\hat{H}_{\text{field}}$ is defined. Taking the three-dimensional observables for the electromagnetic field from Eq. (2.77) and substituting them into Eq. (2.79). One finds that the fields Hamiltonian $\hat{H}_{\text{field}}$ reduces to give [28]

$$\hat{H}_{\text{field}} = \sum_{\lambda=1,2} \int_{\mathbb{R}^3} \mathrm{d}^3\mathbf{k} \, \hbar\omega \, \hat{a}_{\mathbf{k}\lambda}^{\dagger} \hat{a}_{\mathbf{k}\lambda} \,, \quad (2.80)$$

in analogy to Eq. (2.61). Finally, in analogy to Eq. (2.73), one can now write down the three-dimensional expression for the zero-point energy of the electromagnetic field,

$$H_{\text{zpe}} = \int_0^{\infty} \mathrm{d}^3\mathbf{k} \, \frac{1}{2} \, \hbar\omega \, \delta(0) \,. \quad (2.81)$$

Most importantly, all the results derived here are consistent with the continuum limit of other authors, i.e. in the limit of an infinite quantisation volume [39–42].

2.3 Summary

In this chapter the classical theory of electromagnetism was used a starting point to then discuss the quantum description of electromagnetic radiation where the electromagnetic field consists of basic energy quanta known as photons. The first step in this part of the story is outlining what is more commonly known as the canonical approach to quantising the electromagnetic field. Contrasting this with a more physically-motivated approach where one uses experimental observations to state that the free-electromagnetic field behaves as a collection of quantum harmonic oscillators and photons with frequency ω have an associated energy $\hbar\omega$. Most importantly, the electric and magnetic field observables in Eqs. (2.74) and (2.77) are consistent with the findings of other authors.

Chapter 3

Atom-field interactions

In the previous chapter, the quantised electromagnetic field was explored and it was determined that it consists of basic energy quanta known as photons. At this stage it is possible to ask questions about how this field interacts with matter, such as individual atoms. It was Paul Dirac who first considered the interaction of light and matter through his newly developed interpretation of the quantum theory where dynamical variables are non-commutative [43]. Importantly, he noticed that the Schrödinger framework did not allow one to describe, nor does it give any useful information, regarding atomic transitions (cf. Postulate 4). In particular, the process of an atom spontaneously emitting a photon was not explainable within the framework of the Schrödinger equation because it is not sufficient to only understand how the energy levels of the atom are quantised - the electromagnetic field must also be quantised. This required extending quantum mechanics to also describe fields which are quantised at every point in space. One of the most famous quantum field theories is that of electrons and electromagnetic fields, or light-matter interactions, which is more commonly known as quantum electrodynamics (QED) [44, 45] and is one of the most successful theories ever developed in physics due to the high level of accuracy in its predictions.

If one considers the simple case of an isolated two-level atom, the Hamiltonian can be written in terms of its energy eigenstates which are orthogonal to one another (see Eq. (3.28)). In QED, one must explicitly consider the interaction between the atom and its surroundings, i.e. the quantised electromagnetic field. The result is that the free electromagnetic field perturbs the state of the atom

generating a finite probability that one photon will be emitted (the spontaneous emission rate of the atom) as well as inducing a level shift in the atoms excited state. The matrix elements which describe these atomic transitions were calculated by Fermi using his famous 'golden rule' [46], despite Dirac having achieved similar results some twenty years earlier. Moreover, it has been shown that quantum optical master equations are extremely useful tools to analyse the dynamics of atomic systems with spontaneous photon emission [15, 47–49].

The beginning of this chapter will present a brief overview of closed quantum systems and then contrast this by presenting an overview of open quantum systems, with a general master equation derivation in the following section. Finally, the master equation for a two-level atom interacting with the free-electromagnetic field is presented, with analytical expressions for the free-space spontaneous emission rate Γ_{free} and atomic level shift Δ_{free}.

3.1 Overview

If one wishes to understand how a closed quantum system with the time-dependent state vector $|\psi(t)\rangle$ evolves over time, one can use the time-dependent Schrödinger equation

$$|\dot{\psi}(t)\rangle \;\; = \;\; -\frac{\mathrm{i}}{\hbar}\,\hat{H}|\psi(t)\rangle\,, \tag{3.1}$$

where $\hat{H}$ represents the Hamiltonian describing the system of interest (cf. Postulate 4). More importantly, the closed system is an idealised case as it is assumed that the quantum system is completely decoupled from its surrounding environment. As a result, one is able to describe the dynamics of a closed quantum system using unitary operations. However, this idealised system is a simplified description of realistic physical systems.

In order to model more realistic scenarios one has to relax the assumptions used and one must explicitly consider the interaction of the system and the surroundings. In order to model the dynamics of open quantum systems and analyse their behaviour, one must introduce the quantum master equation [15, 47–49] as

unitary operations are no longer sufficient. In addition, one assumes a weak coupling between the system and its surroundings[1]. An N-dimensional system has the quantum optical master equation of Lindblad form

$$\dot{\rho}_{\mathrm{S}}(t) = -\frac{\mathrm{i}}{\hbar}\left[\hat{H}, \hat{\rho}_{\mathrm{S}}(t)\right] + \sum_{i=0}^{N}\sum_{j=0}^{N}\Gamma_{i,j}\left(\hat{L}_{j}\hat{\rho}_{\mathrm{S}}(t)\hat{L}_{i}^{\dagger} - \frac{1}{2}\left[\hat{L}_{i}^{\dagger}\hat{L}_{j}, \hat{\rho}_{\mathrm{S}}(t)\right]_{+}\right) \quad (3.2)$$

assuming the initial and final state of the system are uncorrelated. Here, $\hat{\rho}_{\mathrm{S}}(t)$ is the density operator describing the state of the system and the notation $[\hat{A}, \hat{B}]_{+}$ denotes the anti-commutator between some operators $\hat{A}$ and $\hat{B}$, such that $[\hat{A}, \hat{B}]_{+} = \hat{A}\hat{B} + \hat{B}\hat{A}$. The decay rate of the channel i, j is denoted by $\Gamma_{i,j}$ and the Lindblad operators $\hat{L}_{i,j}$ correspond to the transition $i \leftrightarrow j$. In the case where there is just a single decay channel, Eq. (3.2) simplifies to give

$$\dot{\rho}_{\mathrm{S}}(t) = -\frac{\mathrm{i}}{\hbar}\left[\hat{H}, \hat{\rho}_{\mathrm{S}}(t)\right] + \Gamma\left(\hat{L}\hat{\rho}_{\mathrm{S}}(t)\hat{L}^{\dagger} - \frac{1}{2}\left[\hat{L}^{\dagger}\hat{L}, \hat{\rho}_{\mathrm{S}}(t)\right]_{+}\right). \quad (3.3)$$

Although the time evolution of an open quantum system is non-trivial, the evolution is still characterised by linear differential equations. A general and in-depth derivation of a quantum optical master equation describing an atom-field interaction is presented in the next subsection.

3.2 Modelling open quantum systems

When modelling open quantum systems, there is an inherent connection between the quantum system under consideration and its surroundings, which is often referred to as a bath. As a result of this link, the total energy for the open system and is no longer conserved and one must use quantum master equations to accurately model the dynamics of the system.

3.2.1 The relevant Hamiltonians

Let us first have a closer look at the simplest case of an open quantum system. For this case, there is a quantum system interacting with the surrounding bath.

---

[1]Therefore, it is permissible to use perturbation theory.

One can then define the relevant Hamiltonians by considering the interacting and non-interacting (free) contributions. Therefore, one can write the overall Hamiltonian as

$$\hat{H} \;=\; \hat{H}_0 + \hat{H}_1 \,, \tag{3.4}$$

where the Hamiltonian $\hat{H}_0$ provides the description of the quantum system and bath in the absence of interactions, and is of the form

$$\hat{H}_0 \;=\; \hat{H}_{\mathrm{S}} + \hat{H}_{\mathrm{B}} \,, \tag{3.5}$$

whereas the Hamiltonian $\hat{H}_1$ is of the form

$$\hat{H}_1 \;=\; \hat{H}_{\mathrm{int}} + \hat{H}_{\mathrm{SB}} \,. \tag{3.6}$$

The Hamiltonian $\hat{H}_1$ has two contributions which arise due to interactions. The term $\hat{H}_{\mathrm{int}}$ describes the internal system dynamics and the term $\hat{H}_{\mathrm{SB}}$ describes interactions between the system and bath.
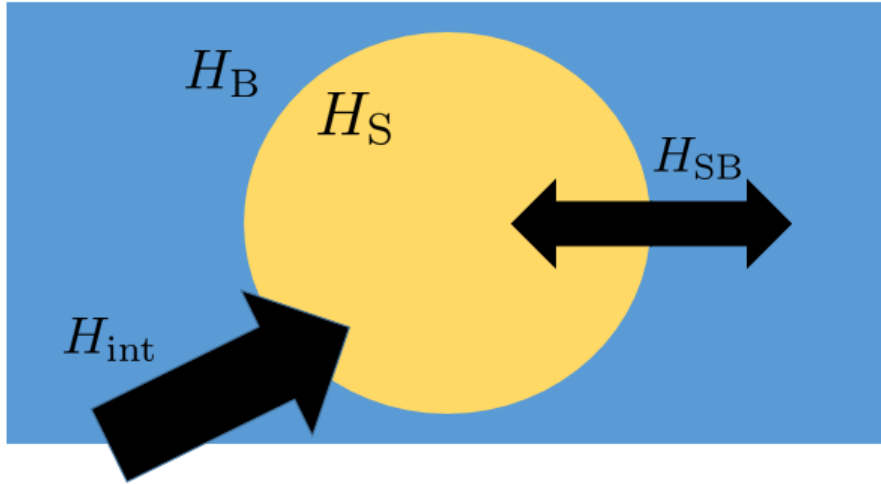
Figure 3.1: Schematic view of the total system with the different contributions annotated. The corresponding Hamiltonians for the system and bath are given by $\hat{H}_{\mathrm{S}}$ and $\hat{H}_{\mathrm{B}}$, with the system-bath interaction and internal dynamics given by $\hat{H}_{\mathrm{SB}}$ and $\hat{H}_{\mathrm{int}}$ respectively.

One can re-express the Hamiltonian in Eq. (3.4) by making use of unitary transformations. For example, these transformations can be used to move from the Schrödinger picture to the interaction picture. The Hamiltonian in Eq. (3.4) is currently in the Schrödinger picture and will be moved into the interaction picture, with respect to the free Hamiltonian $\hat{H}_0$ shown in Eq. (3.5). The interaction picture Hamiltonian $\hat{H}_{\mathrm{I}}(t)$ can be expressed as [42]

$$\hat{H}_{\mathrm{I}}(t) \;=\; \hat{U}_0^\dagger(t,0) \left(\hat{H} - \hat{H}_0 \right) \hat{U}_0(t,0) = \hat{U}_0^\dagger(t,0)\, \hat{H}_1\, \hat{U}_0(t,0) \,. \qquad (3.7)$$

The time evolution operator $\hat{U}_0(t,0)$ with respect to the Hamiltonian $\hat{H}_0$ is given by

$$\hat{U}_0(t,0) \;=\; \exp\left[-\frac{\mathrm{i}}{\hbar} \int_0^t \mathrm{d}t'\, \hat{H}_0(t') \right], \qquad (3.8)$$

which can be found by solving the Schrödinger equation in Eq. (3.1). The key result of this transformation allows one to ignore the trivial dynamics generated by the non-interacting Hamiltonian $\hat{H}_0$, and explicitly consider the non-trivial dynamics generated by the interaction between system and bath.

3.2.2 General derivation of the master equation

The starting point is to assume that the state of the quantum system is given by some density matrix, $\hat{\rho}(t)$ where the density matrix is defined as

$$\hat{\rho}(t) \;=\; \sum_j p_j |\psi_j(t)\rangle\langle\psi_j(t)| \,. \qquad (3.9)$$

In other words, the density matrix describes a mixed state - a statistical ensemble of various pure quantum states each with an associated probability p_j such that

$$\sum_j p_j \;=\; 1 \,. \qquad (3.10)$$

Suppose the bath (the free radiation field) surrounding the quantum system generally resides and resets to an environmentally preferred state - the so-called einselected state [49, 50]. In other words, when an excitation is emitted by the system it is absorbed by the bath, which could be the walls of a laboratory [51].

In general, the bath resets into an einselected state which corresponds to a minimum entropy state. In terms of the applications considered within this thesis, it is assumed that the einselected state coincides with the vacuum state $|0\rangle$ of the electromagnetic field[1]. Thus, one can write the general density matrix of the quantum system and bath at some given time t in the interaction picture as

$$\hat{\rho}_{\mathrm{SBI}}(t) \ = \ \hat{\rho}_{\mathrm{SI}}(t) \otimes |0_{\mathrm{B}}\rangle\langle 0_{\mathrm{B}}| = |0_{\mathrm{B}}\rangle\, \hat{\rho}_{\mathrm{SI}}(t)\, \langle 0_{\mathrm{B}}|\,. \tag{3.11}$$

The next step is to consider the system-bath interactions based on the interaction Hamiltonians from Eq. (3.7). Considering the evolution of these interactions on a short time scale Δt using the time evolution operator $\hat{U}_{\mathrm{I}}(t + \Delta t, t)$, one can evolve the system-bath density matrix $\rho_{\mathrm{SBI}}(t)$ to obtain the new density matrix $\hat{\rho}_{\mathrm{SBI}}(t + \Delta t)$ such that

$$\hat{\rho}_{\mathrm{SBI}}(t + \Delta t) \ = \ \hat{U}_{\mathrm{I}}(t + \Delta t, t)\, |0_{\mathrm{B}}\rangle\, \hat{\rho}_{\mathrm{SI}}(t)\, \langle 0_{\mathrm{B}}|\hat{U}_{\mathrm{I}}^{\dagger}(t + \Delta t, t)\,. \tag{3.12}$$

In addition, it is assumed that the system-bath interactions perturb the state of the bath but this time evolution is followed by a rapid resetting of the bath into its environmentally preferred state due to the fact that Δt is relatively small and that a typical bath has infinitely many degrees of freedom. This gives the new system-bath density matrix

$$\hat{\rho}_{\mathrm{SBI}}(t + \Delta t) \ = \ |0_{\mathrm{B}}\rangle\, \hat{\rho}_{\mathrm{SI}}(t + \Delta t)\, \langle 0_{\mathrm{B}}|\,. \tag{3.13}$$

By tracing over the modes of the bath, one obtains a density matrix $\hat{\rho}_{\mathrm{SI}}(t)$ which purely describes the state of the quantum system

$$\hat{\rho}_{\mathrm{SI}}(t + \Delta t) \ = \ \mathrm{Tr}_{\mathrm{B}}\left(\hat{\rho}_{\mathrm{SBI}}(t + \Delta t)\right)\,. \tag{3.14}$$

In the following, the coarse-grained dynamics are implied by a differential equation without coarse graining, i.e. an atomic master equation of the form,

$$\dot{\hat{\rho}}_{\mathrm{SI}}(t) \ = \ \frac{1}{\Delta t}\left(\hat{\rho}_{\mathrm{SI}}(t + \Delta t) - \hat{\rho}_{\mathrm{SI}}(t)\right)\,. \tag{3.15}$$

When calculating the terms on the right hand side of Eq. (3.15), it is necessary to consider a relatively short time interval Δt. However, Δt should not be too

---

[1]For the remainder of this derivation the vacuum state will be referred to as $|0_{\mathrm{B}}\rangle$.

short either, as it needs to be sufficient to allow for a transfer of information from the system to the bath.

Now, using Eqs. (3.12) – (3.14) and second-order perturbation theory, one can evaluate the right-hand side of Eq. (3.15). In addition, one can use the Dyson series [39] to obtain an expression for the time evolution operator $\hat{U}_\mathrm{I}(t + \Delta t, t)$, such that

$$\hat{U}_\mathrm{I}(t + \Delta t, t) \;=\; \mathcal{T} \exp\left[- \frac{\mathrm{i}}{\hbar} \int_{t_0}^{\tau} \mathrm{d}\tau \, \hat{H}_\mathrm{I}(\tau) \right], \tag{3.16}$$

where $\mathcal{T}$ denotes the time-ordered product of the Hamiltonians, $\hat{H}_\mathrm{I}(\tau)$. Up to second-order, this can be written as[1]

$$\hat{U}_\mathrm{I}(t + \Delta t, t) \simeq 1 - \frac{i}{\hbar} \int_{t}^{t+\Delta t} \mathrm{d}t' \, \hat{H}_\mathrm{I}(t') - \frac{1}{\hbar^2} \int_{t}^{t+\Delta t} \mathrm{d}t' \int_{t}^{t'} \mathrm{d}t'' \, \hat{H}_\mathrm{I}(t') \hat{H}_\mathrm{I}(t''). \tag{3.17}$$

Substituting Eq. (3.17) into Eq. (3.12) and using both Eqs. (3.14) and (3.15), one obtains the following expression

$$
\begin{aligned}
\dot{\hat{\rho}}_{\mathrm{S\,I}}(t) \;=\;\; & -\frac{1}{\Delta t} \frac{\mathrm{i}}{\hbar} \mathrm{Tr}_\mathrm{B} \left(\int_{t}^{t+\Delta t} \mathrm{d}t' \left[\hat{H}_{\mathrm{int\,I}}(t), \, |0_\mathrm{B}\rangle \hat{\rho}_{\mathrm{S\,I}}(t) \langle 0_\mathrm{B}| \right] \right) \\
& -\frac{1}{\Delta t} \frac{1}{\hbar^2} \mathrm{Tr}_\mathrm{B} \left(\int_{t}^{t+\Delta t} \mathrm{d}t' \int_{t}^{t'} \mathrm{d}t'' \left[\hat{H}_{\mathrm{SB\,I}}(t') \hat{H}_{\mathrm{SB\,I}}(t''), |0_\mathrm{B}\rangle \, \hat{\rho}_{\mathrm{S\,I}}(t) \langle 0_\mathrm{B}| \right]_{+} \right) \\
& +\frac{1}{\Delta t} \frac{1}{\hbar^2} \mathrm{Tr}_\mathrm{B} \left(\int_{t}^{t+\Delta t} \mathrm{d}t' \int_{t}^{t+\Delta t} \mathrm{d}t'' \, \hat{H}_{\mathrm{SB\,I}}(t') |0_\mathrm{B}\rangle \hat{\rho}_{\mathrm{S\,I}}(t) \langle 0_\mathrm{B}| \hat{H}_{\mathrm{SB\,I}}(t'') \right).
\end{aligned}
\tag{3.18}
$$

Finally, one can consider what happens when tracing out the bath modes in the above equation. The first term generates the internal dynamics of the quantum system, while the second and third line of Eq. (3.18) generate the open system dynamics. The term on the second line is only non-zero when the bath is projected into the vacuum state $|0_\mathrm{B}\rangle$ by the trace, where as the third line of Eq. (3.18) is only non-zero when the trace projects the bath into the one photon state $|1_\mathrm{B}\rangle$. Therefore, the terms on the second line corresponds to the situation where there is no emission by the system and the term on the third line corresponds to the situation where the system emits an excitation into the bath.

---

[1]Due to assuming a weak-coupling between the system and bath, terms higher than second-order do not contribute to $\dot{\hat{\rho}}_{\mathrm{S\,I}}(t)$ in the small Δt limit.

3.2.3 Unravelling of the master equation

The master equation describes the evolution of the ensemble average of the system. In other words, a master equation describes how a system will behave on average, whereas a single quantum system (or individual quantum trajectory) may evolve differently. Although individual quantum trajectories are not the main focus of the thesis, the following unravelling of Eq. (3.18) provides the necessary intuition and will be used throughout.

One denotes the unnormalised density matrix of the quantum system for which no excitation is exchanged and the bath remains in its environmentally preferred state $|0_B\rangle$ as $\rho_S^0(t)$. For the scenario where excitations are exchanged with the bath, this unnormalised density matrix is denoted as $\hat{\rho}_S^{\neq}(t)$. Taking this into account, one finds the time evolution of the density matrix has two contributions such that

$$\dot{\hat{\rho}}_{SI}(t) = \dot{\hat{\rho}}_{SI}^0(t) + \dot{\hat{\rho}}_{SI}^{\neq}(t), \tag{3.19}$$

where

$$\dot{\hat{\rho}}_{SI}^0(t) = -\frac{1}{\Delta t}\frac{i}{\hbar}\mathrm{Tr_B}\left(\int_t^{t+\Delta t}dt'\left[\hat{H}_{\mathrm{int\,I}}(t'),\,|0_B\rangle\hat{\rho}_{SI}(t)\langle0_B|\right]\right)$$
$$-\frac{1}{\Delta t}\frac{1}{\hbar^2}\mathrm{Tr_B}\left(\int_t^{t+\Delta t}dt'\int_t^{t'}dt''\left[\hat{H}_{\mathrm{SB\,I}}(t')\hat{H}_{\mathrm{SB\,I}}(t''),|0_B\rangle\,\hat{\rho}_{SI}(t)\langle0_B|\right]_+\right) \tag{3.20}$$

and

$$\dot{\hat{\rho}}_{SI}^{\neq}(t) = \frac{1}{\Delta t}\frac{1}{\hbar^2}\mathrm{Tr_B}\left(\int_t^{t+\Delta t}dt'\int_t^{t+\Delta t}dt''\,\hat{H}_{\mathrm{SB\,I}}(t')|0_B\rangle\hat{\rho}_{SI}(t)\langle0_B|\hat{H}_{\mathrm{SB\,I}}(t'')\right). \tag{3.21}$$

Now, one must use the Eqs. (3.20) and (3.21) and compare these with the master equation of Lindblad form given in Eq. (3.3). Doing so demonstrates that

$$\dot{\hat{\rho}}_{SI}^0(t) = -\frac{i}{\hbar}\left[\hat{H}_{\mathrm{int\,I}},\hat{\rho}_{SI}(t)\right] - \frac{1}{2}\Gamma\left[\hat{L}^\dagger\hat{L},\hat{\rho}_{SI}(t)\right]_+, \tag{3.22}$$
$$\dot{\hat{\rho}}_{SI}^{\neq}(t) = \Gamma\hat{L}\,\hat{\rho}_{SI}(t)\,\hat{L}^\dagger. \tag{3.23}$$

In addition, one can show that $\hat{\rho}_{\mathrm{S\,I}}(t)$ evolves according to

$$\dot{\hat{\rho}}_{\mathrm{S\,I}}(t) \;\; = \;\; -\frac{\mathrm{i}}{\hbar}\big[\hat{H}_{\mathrm{cond\,I}}(t)\,\hat{\rho}_{\mathrm{S\,I}}(t) - \hat{\rho}_{\mathrm{S\,I}}(t)\,\hat{H}_{\mathrm{cond\,I}}^{\dagger}(t)\big] + \mathcal{L}(\hat{\rho}_{\mathrm{S\,I}}(t))\,, \quad (3.24)$$

The conditional Hamiltonian $\hat{H}_{\mathrm{cond\,I}}(t)$ describes the time evolution of the system under the condition of no photon emission and is defined as [48, 52, 53][1]

$$\hat{H}_{\mathrm{cond\,I}}(t) \;\; = \;\; \frac{1}{\Delta t}\int\limits_{t}^{t+\Delta t}\mathrm{d}t'\,\langle 0_{\mathrm{B}}|\hat{H}_{\mathrm{int\,I}}(t')|0_{\mathrm{B}}\rangle$$
$$-\frac{\mathrm{i}}{\hbar\Delta t}\int_{t}^{t+\Delta t}\mathrm{d}t'\int_{t}^{t'}\mathrm{d}t''\,\langle 0_{\mathrm{B}}|\hat{H}_{\mathrm{SB\,I}}(t')\hat{H}_{\mathrm{SB\,I}}(t'')|0_{\mathrm{B}}\rangle + \mathrm{H.c.}$$
$$(3.25)$$

Finally, the reset operator $\mathcal{L}(\hat{\rho}_{\mathrm{S\,I}}(t))$ is defined as

$$\mathcal{L}(\hat{\rho}_{\mathrm{S\,I}}(t)) \;\; = \;\; \frac{1}{\hbar^2\Delta t}\,\mathrm{Tr}_{\mathrm{B}}\left(\int_{t}^{t+\Delta t}\mathrm{d}t'\int_{t}^{t+\Delta t}\mathrm{d}t''\,\hat{H}_{\mathrm{SB\,I}}(t')|0_{\mathrm{B}}\rangle\hat{\rho}_{\mathrm{S}}(t)\langle 0_{\mathrm{B}}|\hat{H}_{\mathrm{SB\,I}}(t'')\right),$$
$$(3.26)$$

which describes the un-normalised state of the quantum system in the case of an emission at time t [48, 52, 53].

In the following subsection, a master equation description for a two-level atom interacting with the surrounding free electromagnetic field will be presented, with the example demonstrating how to solve the various integrals within Eqs. (3.25) and (3.26).

3.3 Master equation for two-level atom-field interaction

The beginning of this chapter discussed the time evolution of both closed and open quantum systems, which allows one to present a description of a light-matter interaction where an atom couples to its surrounding environment, which

---

[1]In order to be completely general the Hamiltonian, $\hat{H}_{\mathrm{int\,I}}(t')$ which describes the internal dynamics of the quantum system has been included. However, for the scenarios studied within this thesis $\hat{H}_{\mathrm{int\,I}}(t') = 0$ is always the case.

in this case is the free electromagnetic field. In order to model this scenario, one can make use of the two-level approximation. This approximation means one only has to consider the two lowest energy levels, i.e. the ground state and first excited state. Any atomic transitions with energies very different from $\hbar\omega$ will be neglected.

3.3.1 The relevant Hamiltonians

As before, the first step is to identify the relevant Hamiltonians. In analogy to Eq. (3.4), we take the sum of three contributions such that

$$\hat{H} = \hat{H}_{\text{atom}} + \hat{H}_{\text{field}} + \hat{H}_{\text{SB}}, \tag{3.27}$$

where $\hat{H}_{\text{int}} = 0$ as there is no laser driving providing internal system dynamics. One can express the atom Hamiltonian in terms of the energy eigenstates $|n\rangle$ such that

$$\hat{H}_{\text{atom}} = \sum_{i=1}^{2} \hbar\omega_i |n_i\rangle\langle n_i|, \tag{3.28}$$

The form of this equation demonstrates why the number state representation is particularly useful as it is possible to simply read off the eigenvalues of a diagonal matrix. Similarly, the second term describes the free electromagnetic field

$$H_{\text{field}} = \sum_{j=1}^{\infty} \hbar\omega_j |n_j\rangle\langle n_j|, \tag{3.29}$$

to which the atom is coupled.

From Eq. (3.27), the first two terms can be identified as the system and the bath in the absence of interactions, respectively, with the last term representing the interaction between the atom and the free electromagnetic field. Therefore, in analogy to Eqs. (3.5) and (3.6), one can write

$$\begin{aligned}
\hat{H}_0 &= \hat{H}_{\text{atom}} + \hat{H}_{\text{field}}, \\
\hat{H}_1 &= \hat{H}_{\text{SB}}.
\end{aligned} \tag{3.30}$$

Moreover, the atom-field interaction can expressed as

$$\hat{H}_{\text{SB}} = \hat{\mathbf{D}} \cdot \hat{\mathbf{E}}_{\text{free}}(\mathbf{r}), \tag{3.31}$$

where $\hat{\mathbf{D}}_{12}$ denotes the dipole moment associated with the atomic transition $|2\rangle \rightarrow |1\rangle$ and $\hat{\mathbf{E}}_{\text{free}}(\mathbf{r})$ denotes the electric field at position $\mathbf{r}$. In order to arrive at Eq. (3.31) one must make use of the electric dipole approximation. In the previous chapter it was shown that one can satisfy Maxwell's equations with plane wave solutions. Since the wavelength of the emitted photon is much larger than the size of the atom, in the electric dipole approximation only the zeroth-order term contributes to the atom-field interaction, i.e. $e^{i\mathbf{k}\cdot\mathbf{r}} \approx 1$. Importantly, this approximation can be made regardless of the route taken to quantise the electromagnetic field. This is due to the electric field $\mathbf{E}_{\text{free}}(\mathbf{r}, t)$ being spatially uniform over the position of the atom. If one chooses a different gauge, this would then lead to a different atom-field interaction (see [49] and references herein). Moreover, to derive the full form of the dipole moment operator $\hat{\mathbf{D}}_{12}$ from Eq. (3.31), one can do so in the following way

$$\hat{\mathbf{D}}_{12} \;=\; e\hat{\mathbf{x}}\,, \tag{3.32}$$

where e denotes the quanta of charge (electric charge carried by a single proton or electron) and $\hat{\mathbf{x}}$ denotes the position operator. Expressing the dipole moment operator $\hat{\mathbf{D}}_{12}$ in terms of the identity operator such that

$$
\begin{aligned}
\hat{\mathbf{D}}_{12} \;&=\; \hat{\mathbb{1}}\hat{\mathbf{x}}\hat{\mathbb{1}} \\
&=\; (|1\rangle\langle 1| + |2\rangle\langle 2|)\hat{\mathbf{x}}(|1\rangle\langle 1| + |2\rangle\langle 2|) \\
&=\; \langle 1|\hat{\mathbf{x}}|1\rangle|1\rangle\langle 1| + \langle 1|\hat{\mathbf{x}}|2\rangle|1\rangle\langle 2| + \langle 2|\hat{\mathbf{x}}|1\rangle|2\rangle\langle 1| + \langle 2|\hat{\mathbf{x}}|2\rangle|2\rangle\langle 2|\,. \tag{3.33}
\end{aligned}
$$

Analysing the terms of the above equation, the diagonal elements describe permanent dipole moments e.g. an atom in a solid, and the off-diagonal elements describe transition dipole moments. Therefore, it is possible to say that $\langle 1|\hat{\mathbf{x}}|1\rangle = \langle 2|\hat{\mathbf{x}}|2\rangle = 0$ and due to the atom having inversion symmetry $\langle 1|\hat{\mathbf{x}}|2\rangle = \langle 2|\hat{\mathbf{x}}|1\rangle \neq 0$.

This generates the final form of the dipole moment operator

$$\hat{\mathbf{D}}_{12} \;=\; \langle 1|\hat{\mathbf{x}}|2\rangle\,|1\rangle\langle 2| + \langle 2|\hat{\mathbf{x}}|1\rangle\,|2\rangle\langle 1| = \mathbf{D}_{12}\,\hat{\sigma}^- + \mathbf{D}_{12}^*\,\hat{\sigma}^+\,, \tag{3.34}$$

where $\mathbf{D}_{12}$ and $\mathbf{D}_{12}^*$ are the matrix elements discussed above and $\hat{\sigma}^\pm$ represent the atomic raising and lowering operators, respectively. These operators are analogous to the ladder operators mentioned in the previous chapter. Finally, the

algebra of these operators can be defined in the following way

$$
\begin{aligned}
\hat{\sigma}^+ &= |2\rangle\langle 1| , \\
\hat{\sigma}^- &= |1\rangle\langle 2| ,
\end{aligned}
\tag{3.35}
$$

with

$$
\left[\hat{\sigma}^+, \hat{\sigma}^-\right] = \hat{\sigma}^+\hat{\sigma}^- - \hat{\sigma}^-\hat{\sigma}^+ = 2\hat{\sigma}_3 ,
\tag{3.36}
$$

where the operator $\hat{\sigma}_3 = \frac{1}{2}\big[|2\rangle\langle 2| - |1\rangle\langle 1|\big]$. Making use of Eqs. (3.32) – (3.34) and substituting this information into Eq. (3.31), one obtains

$$
\hat{H}_{\mathrm{SB}} = e\left[\mathbf{D}_{12}\,\hat{\sigma}^- + \mathbf{D}_{12}^*\,\hat{\sigma}^+\right] \cdot \hat{\mathbf{E}}_{\mathrm{free}}(\mathbf{r}) ,
\tag{3.37}
$$

where $\hat{\mathbf{E}}_{\mathrm{free}}(\mathbf{r})$ denotes the free electric field at position $\mathbf{r}$, the point at which the atom couples to this field. Using the expression obtained in Eq. (2.77), this generates the following atom-field Hamiltonian

$$
\hat{H}_{\mathrm{SB}}(t) = \frac{\mathrm{i}e}{4\pi} \sum_{\lambda=1,2} \int_{\mathbb{R}^3} \mathrm{d}^3\mathbf{k} \sqrt{\frac{\hbar\omega}{\pi\varepsilon}} \mathrm{e}^{\mathrm{i}(\mathbf{k}\cdot\mathbf{r}-\omega t)} \left[\mathbf{D}_{12}\,\hat{\sigma}^- + \mathbf{D}_{12}^*\,\hat{\sigma}^+\right] \hat{a}_{\mathbf{k}\lambda}\hat{\mathbf{e}}_{\mathbf{k}\lambda} + \mathrm{H.c.}
\tag{3.38}
$$

The next step is to use Eq. (3.7) to move the system-bath Hamiltonian from the Schrödinger picture into the interaction picture, with respect to the free Hamiltonian $\hat{H}_0$. To do so, one must use the spectral theorem to decompose the time evolution operator from Eq. (3.8) into the eigenvalues and eigenvectors of the Hamiltonian $\hat{H}_0$ such that

$$
\hat{U}_0(t,0) = \exp\left[-\frac{\mathrm{i}}{\hbar}\int_0^t \mathrm{d}t'\, \hat{H}_0(t')\right] = \sum_i \mathrm{e}^{-\mathrm{i}E_i t/\hbar}|E_i\rangle\langle E_i| ,
\tag{3.39}
$$

where E_i denotes the energy (eigenvalue) of the energy eigenstate $|E_i\rangle$. Implementing the above relation when evaluating Eq. (3.7) allows one to obtain an expression for the system-bath Hamiltonian within the interaction representa-

tion[1]. Performing this substitution yields

$$
\begin{aligned}
\hat{H}_{\mathrm{SBI}}(t) &= \frac{\mathrm{i}e}{4\pi} \sum_{\lambda=1,2} \int_{\mathbb{R}^3} \mathrm{d}^3\mathbf{k} \sqrt{\frac{\hbar\omega}{\pi\varepsilon}} \\
&\quad \times \left(\mathrm{e}^{\mathrm{i}(\omega+\omega_0)t} \mathbf{D}_{12} \hat{\sigma}^- + \mathrm{e}^{-\mathrm{i}(\omega-\omega_0)t} \mathbf{D}_{12}^* \hat{\sigma}^+ \right) \mathrm{e}^{\mathrm{i}\mathbf{k}\cdot\mathbf{r}} \hat{a}_{\mathbf{k}\lambda} \hat{\mathbf{e}}_{\mathbf{k}\lambda} + \mathrm{H.c.}
\end{aligned}
\tag{3.40}
$$

Finally, one must apply the rotating wave approximation in order to ensure the above Hamiltonian will return the appropriate physical dynamics[2]. Applying the rotating wave approximation to the above equation, one finds that the interaction picture Hamiltonian $\hat{H}_{\mathrm{SBI}}(t)$ takes the form

$$
\hat{H}_{\mathrm{SBI}}(t) = \frac{\mathrm{i}e}{4\pi} \sum_{\lambda=1,2} \int_{\mathbb{R}^3} \mathrm{d}^3\mathbf{k} \sqrt{\frac{\hbar\omega}{\pi\varepsilon}} \, \mathrm{e}^{-\mathrm{i}(\omega-\omega_0)t} \, \mathrm{e}^{\mathrm{i}\mathbf{k}\cdot\mathbf{r}} \, \mathbf{D}_{12}^* \, \hat{\sigma}^+ \, \hat{a}_{\mathbf{k}\lambda} \hat{\mathbf{e}}_{\mathbf{k}\lambda} + \mathrm{H.c.}
\tag{3.41}
$$

In the following section of this chapter, the Hamiltonian in Eq. (3.41) will be used to present a master equation description for the atom-field interaction.

3.3.2 Master equation

In order to obtain the master equation for a two-level atom coupled to the free electromagnetic field, one must substitute the interaction picture Hamiltonian $\hat{H}_{\mathrm{SBI}}(t)$ from Eq. (3.40) into the expressions for the conditional Hamiltonian $\hat{H}_{\mathrm{cond\,I}}(t)$ and the reset operator $\mathcal{L}(\hat{\rho}_{\mathrm{SI}}(t))$ in Eqs. (3.25) and (3.26), respectively.

---

[1]Moving into the interaction representation allows one to ignore the trivial dynamics and focus on the non-trivial (interacting) dynamics. This transformation is evident when comparing field operators in the Schrödinger and interaction representation. In the Schrödinger representation these operators take the form $\hat{a}_{\mathbf{k}\lambda}$ and $\hat{a}_{\mathbf{k}\lambda}^\dagger$. However, in the interaction representation, these operators now take the form $\hat{a}_{\mathbf{k}\lambda}\,\mathrm{e}^{-\mathrm{i}\omega_0 t}$ and $\hat{a}_{\mathbf{k}\lambda}^\dagger \mathrm{e}^{\mathrm{i}\omega_0 t}$.

[2]In Eq. (3.31), the dipole approximation was assumed and in order for this to remain a valid assumption, the electric field must be near resonance with the atomic transition, ω_0. Therefore, the exponentials in Eq. (3.40) which scale with $\mathrm{e}^{\pm\mathrm{i}(\omega+\omega_0)t}$ will be far from resonant with the field. These oscillations quickly average to 0 and therefore, these fast-oscillating terms may be neglected. Exponentials with $\mathrm{e}^{\pm\mathrm{i}(\omega-\omega_0)t}$ will be close to resonance with the field and are therefore kept.

Calculating $\hat{H}_{\text{cond I}}(t)$ for an atom in free space

Let us first take a closer look at how to calculate the non-Hermitian Hamiltonian $\hat{H}_{\text{cond I}}(t)$. The first step requires substituting the interaction picture Hamiltonian $\hat{H}_{\text{I}}(t)$ from Eq. (3.41) into the expression derived for the conditional Hamiltonian given in Eq. (3.25). Doing so, one finds that the conditional Hamiltonian $H_{\text{cond I}}(t)$ for an atom in free space equals[1]

$$
\hat{H}_{\text{cond I}}(t) = -\frac{\mathrm{i}\hbar}{\Delta t} \int\limits_{t}^{t+\Delta t} \mathrm{d}t' \int\limits_{t}^{t'} \mathrm{d}t'' \sum_{\lambda=1,2} \int_{\mathbb{R}^3} \mathrm{d}^3\mathbf{k}\, \frac{e^2\omega}{16\pi^3\varepsilon_0\hbar}\, \mathrm{e}^{-\mathrm{i}(\omega-\omega_0)(t'-t'')}
$$
$$
\times \left(\hat{\mathbf{D}}_{12}^* \cdot \hat{\mathbf{e}}_{\mathbf{k}\lambda}\right)\left(\hat{\mathbf{D}}_{12} \cdot \hat{\mathbf{e}}_{\mathbf{k}\lambda}\right) \hat{\sigma}^+\hat{\sigma}^- . \qquad (3.42)
$$

In free space, using a Cartesian coordinate system (x, y, z) it is possible express the atomic dipole moment $\hat{\mathbf{D}}_{12}$ without restrictions such that

$$
\frac{\hat{\mathbf{D}}_{12}}{\|\mathbf{D}_{12}\|} = \begin{pmatrix} d_1 \\ 0 \\ d_3 \end{pmatrix}, \qquad (3.43)
$$

with

$$
|d_1|^2 + |d_3|^2 = 1. \qquad (3.44)
$$

One can simplify Eq. (3.42) by noticing that the polarisation vectors $\hat{\mathbf{e}}_{\mathbf{k}\lambda}$ with $\lambda = 1, 2$ and the unit vector $\hat{\mathbf{k}} = \mathbf{k}/\|\mathbf{k}\|$ form a complete set of basis states in $\mathbb{R}^3$ which implies

$$
\sum_{\lambda=1,2} \|\mathbf{v} \cdot \hat{\mathbf{e}}_{\mathbf{k}\lambda}\|^2 = \|\mathbf{v}\|^2 - \|\mathbf{v} \cdot \hat{\mathbf{k}}\|^2, \qquad (3.45)
$$

for any vector $\mathbf{v}$. Moreover, to perform the integration in $\mathbf{k}$-space, one introduces the polar coordinates $(\omega, \vartheta, \phi)$ such that

$$
\mathbf{k} = k \begin{pmatrix} \cos(\vartheta) \\ \cos(\phi)\sin(\vartheta) \\ \sin(\phi)\sin(\vartheta) \end{pmatrix} = \frac{\omega}{c} \begin{pmatrix} \cos(\vartheta) \\ \cos(\phi)\sin(\vartheta) \\ \sin(\phi)\sin(\vartheta) \end{pmatrix}, \qquad (3.46)
$$

---

[1]Upon performing the substitution, it is evident from the perturbative expansion performed in Eq. (3.16), that one will obtain an integral over $\mathbf{k}$ and $\mathbf{k}'$. This is evaluated using the Dirac-delta function $\delta^3(\mathbf{k} - \mathbf{k}')$, when tracing out the bath modes. The significance of this delta function is that it ensures frequency-matching between the excitation emitted by the system and the excitation that is absorbed by the bath.

and

$$\int_{\mathbb{R}^3} \mathrm{d}^3\mathbf{k} \;=\; \int_{\mathbb{R}^3} \mathrm{d}k_x \, \mathrm{d}k_y \, \mathrm{d}k_z = \int_0^\infty \mathrm{d}k \, k^2 \int_0^\pi \mathrm{d}\vartheta \, \sin(\vartheta) \int_0^{2\pi} \mathrm{d}\phi \,, \quad (3.47)$$

where the spherical polar volume element is given by $\mathrm{d}k_x \, \mathrm{d}k_y \, \mathrm{d}k_z = k^2 \sin(\vartheta) \mathrm{d}k \, \mathrm{d}\vartheta \, \mathrm{d}\phi$. The above equation can be re-expressed using $\omega = ck$, which yields the expression

$$\int_{\mathbb{R}^3} \mathrm{d}^3\mathbf{k} \;=\; \int_0^\infty \mathrm{d}\omega \, \frac{\omega^2}{c^3} \int_0^\pi \mathrm{d}\vartheta \, \sin(\vartheta) \int_0^{2\pi} \mathrm{d}\phi \,. \quad (3.48)$$

Taking this into account and combining with the above equations yields

$$\hat{H}_{\mathrm{cond\,I}}(t) \;=\; -\frac{\mathrm{i}\hbar}{\Delta t} \int_t^{t+\Delta t} \mathrm{d}t' \int_t^{t'} \mathrm{d}t'' \int_0^\infty \mathrm{d}\omega \int_0^\pi \mathrm{d}\vartheta \, \sin(\vartheta) \int_0^{2\pi} \mathrm{d}\phi \, \frac{e^2 \, \|\mathbf{D}_{12}\|^2 \, \omega^3}{16\pi^3 \varepsilon_0 c^3 \hbar}$$

$$\times \left[|d_1|^2 \left(1 - \cos^2(\vartheta) \right) + |d_3|^2 \left(1 - \sin^2(\vartheta) \sin^2(\phi) \right) \right.$$

$$\left. + (d_1^* d_3 + d_3^* d_1) \sin(\vartheta) \cos(\vartheta) \sin(\phi) \right] \mathrm{e}^{-\mathrm{i}(\omega - \omega_0)(t' - t'')} \, \hat{\sigma}^+ \hat{\sigma}^- \,.$$

$$(3.49)$$

Performing the ϕ-integration, one finds that

$$\hat{H}_{\mathrm{cond\,I}}(t) \;=\; -\frac{\mathrm{i}\hbar}{\Delta t} \int_t^{t+\Delta t} \mathrm{d}t' \int_t^{t'} \mathrm{d}t'' \int_0^\infty \mathrm{d}\omega \int_0^\pi \mathrm{d}\vartheta \, \sin(\vartheta) \, \frac{e^2 \, \|\mathbf{D}_{12}\|^2 \, \omega^3}{16\pi^3 \varepsilon_0 c^3 \hbar}$$

$$\times 2\pi \left[|d_1|^2 \left(1 - \cos^2(\vartheta) \right) + \frac{1}{2} |d_3|^2 \left(1 + \cos^2(\vartheta) \right) \right]$$

$$\times \mathrm{e}^{-\mathrm{i}(\omega - \omega_0)(t' - t'')} \, \hat{\sigma}^+ \hat{\sigma}^- \,. \quad (3.50)$$

One can then simplify the ϑ-integration by introducing a new variable $s = \cos(\vartheta)$. Applying this substitution, one finds

$$\hat{H}_{\mathrm{cond\,I}}(t) \;=\; -\frac{\mathrm{i}\hbar}{\Delta t} \int_t^{t+\Delta t} \mathrm{d}t' \int_t^{t'} \mathrm{d}t'' \int_0^\infty \mathrm{d}\omega \int_{-1}^1 \mathrm{d}s \, \frac{e^2 \, \|\mathbf{D}_{12}\|^2 \, \omega^3}{8\pi^2 \varepsilon_0 c^3 \hbar}$$

$$\times \left[|d_1|^2 (1 - s^2) + \frac{1}{2} |d_3|^2 (1 + s^2) \right] \mathrm{e}^{-\mathrm{i}(\omega - \omega_0)(t' - t'')} \, \hat{\sigma}^+ \hat{\sigma}^- \,. (3.51)$$

Now, evaluating the s-integration and making use of the relation in Eq. (3.44), one obtains

$$\hat{H}_{\text{cond I}}(t) = -\frac{\mathrm{i}\hbar}{\Delta t} \int\limits_{t}^{t+\Delta t} \mathrm{d}t' \int\limits_{t}^{t'} \mathrm{d}t'' \int_{0}^{\infty} \mathrm{d}\omega \, \frac{e^2 \, \|\mathbf{D}_{12}\|^2 \, \omega^3}{6\pi^2 \varepsilon_0 c^3 \hbar} \, \mathrm{e}^{-\mathrm{i}(\omega - \omega_0)(t'-t'')} \, \hat{\sigma}^+ \hat{\sigma}^- \,.$$

$$(3.52)$$

The next step requires imposing Markovianity, i.e. the initial and final state of the system are uncorrelated meaning it is appropriate to replace the lower limit of the t'' integral with $-\infty$. Therefore, in Eq. (3.52) one can make the substitution

$$\int\limits_{t}^{t'} \mathrm{d}t'' \rightarrow \int\limits_{-\infty}^{t'} \mathrm{d}t'' \,,$$

$$(3.53)$$

which applies very well when $t \ll t + \Delta t$ and $\Delta t \gg 1/\omega_0$. In order to evaluate the resulting integral one must be aware of the singularity where $\omega = \omega_0$. This issue can be avoided through using a form of the Cauchy principle value theorem, where one introduces an infinitesimal term β (such that $\beta \in \mathbb{R}$). Therefore, looking the t''-integral from Eq. (3.52) whilst also considering Eq. (3.53), one finds that

$$\int_{-\infty}^{t'} \mathrm{d}t'' \, \mathrm{e}^{-\mathrm{i}(\omega - \omega_0)(t'-t'')}$$

$$= \lim_{\beta \to 0^+} \int_{t}^{t'} \mathrm{d}t'' \, \mathrm{e}^{-\mathrm{i}(\omega - \omega_0)(t'-t'') + \beta t''}$$

$$= \lim_{\beta \to 0^+} \frac{\mathrm{e}^{\beta t'}}{\beta + \mathrm{i}\,(\omega - \omega_0)}$$

$$= \lim_{\beta \to 0^+} \mathrm{e}^{\beta t'} \left(\frac{\beta}{\beta^2 + (\omega - \omega_0)^2} - \frac{\mathrm{i}\,(\omega - \omega_0)}{\beta^2 + (\omega - \omega_0)^2} \right)$$

$$= \lim_{\beta \to 0^+} \frac{\beta \, \mathrm{e}^{\beta t'}}{\beta^2 + (\omega - \omega_0)^2} - \frac{\mathrm{i}}{\omega - \omega_0} \,.$$

$$(3.54)$$

Considering the first term of the above equation, in the limit of $\beta \to 0^+$ this term is equivalent to a Dirac-delta distribution, which can be defined as

$$\lim_{\beta \to 0^+} \frac{1}{\pi} \frac{\beta}{x^2 + \beta^2} = \delta\,(x) \,,$$

$$(3.55)$$

where

$$\int_{-\infty}^{\infty} \mathrm{d}x\, \delta(x) \;=\; 1\,. \tag{3.56}$$

Therefore, one can state that

$$\int_{-\infty}^{t'} \mathrm{d}t''\, \mathrm{e}^{-\mathrm{i}(\omega-\omega_0)(t'-t'')} \;=\; \pi\delta\left(\omega-\omega_0\right) - \frac{\mathrm{i}}{(\omega-\omega_0)}\,. \tag{3.57}$$

Looking at the above equation, the first term is real and this is the contribution that gives rise to the spontaneous emission rate of the system. The second term is imaginary and describes a level shift for the atom's excited state. However, this level shift can be dealt with by absorbing it into the definition of the system's free energy. Now, one can make use of Eq. (3.57) to simplify Eq. (3.52). Doing so and performing the t'-integration, one obtains the conditional Hamiltonian

$$\hat{H}_{\mathrm{cond\,I}}(t) \;=\; -\frac{\mathrm{i}\hbar}{2}\int_0^{\infty} \mathrm{d}\omega\, \frac{e^2\, \|\mathbf{D}_{12}\|^2\, \omega^3}{3\pi^2\varepsilon_0 c^3\hbar} \left[\pi\delta\left(\omega-\omega_0\right) - \frac{\mathrm{i}\mathcal{P}}{(\omega-\omega_0)}\right]\hat{\sigma}^+\hat{\sigma}^-\,, \tag{3.58}$$

where the Cauchy-principal value $\mathcal{P}$ allows one to evaluate improper integrals, which otherwise would be undefined e.g. due to a singularity in the integrand [54]. Evaluating the ω-integral generates the following expression

$$\hat{H}_{\mathrm{cond\,I}}(t) \;=\; -\frac{\mathrm{i}\hbar}{2}\left[\Gamma_{\mathrm{free}} - \mathrm{i}\Delta_{\mathrm{free}}\right]\hat{\sigma}^+\hat{\sigma}^-\,, \tag{3.59}$$

where the spontaneous decay rate of the system is equal to Γ_{free} and the atomic level shift is given by Δ_{free}. The above equation simplifies to give

$$\hat{H}_{\mathrm{cond\,I}}(t) \;=\; \hbar\left(\Delta_{\mathrm{free}} - \frac{\mathrm{i}}{2}\Gamma_{\mathrm{free}}\right)\hat{\sigma}^+\hat{\sigma}^-\,. \tag{3.60}$$

As stated earlier, one can absorb the atomic level shift into the definition of ω_0, thereby absorbing it into the atomic Hamiltonian H_{atom} in Eq. (3.28). This simplifies the conditional Hamiltonian in Eq. (3.60) to give

$$\hat{H}_{\mathrm{cond\,I}}(t) \;=\; -\frac{\mathrm{i}\hbar}{2}\Gamma_{\mathrm{free}}\,\hat{\sigma}^+\hat{\sigma}^-\,, \tag{3.61}$$

where the spontaneous decay rate of the system is expressed as

$$\Gamma_{\text{free}} = \frac{e^2 \left\| \mathbf{D}_{12} \right\|^2 \omega_0^3}{3\pi \varepsilon_0 c^3 \hbar} . \tag{3.62}$$

This is the spontaneous emission rate of a two-level atom in free space. In addition, one can define the atomic level shift Δ_{free} as

$$\Delta_{\text{free}} = \mathcal{P} \int_0^\infty \mathrm{d}\omega \, \frac{2}{\pi} \frac{\Gamma_{\text{free}}}{\omega_0^3} \frac{\omega^3}{(\omega_0 - \omega)} . \tag{3.63}$$

However, the exact form of this free-space level shift is not important for the work presented in this thesis[1].

Calculating $\mathcal{L}(\hat{\rho}_{\text{SI}}(t))$ for an atom in free space

The next step requires obtaining an expression for the reset operator $\mathcal{L}(\hat{\rho}_{\text{SI}}(t))$, which is achieved by substituting the interaction picture Hamiltonian $\hat{H}_{\text{SBI}}(t)$ from Eq. (3.41) into the reset operator expression given in Eq. (3.26). Doing so, one finds[2]

$$\begin{aligned}
\mathcal{L}(\hat{\rho}_{\text{SI}}(t)) &= (-1)^2 \int_t^{t+\Delta t} \mathrm{d}t' \int_t^{t+\Delta t} \mathrm{d}t'' \int_{\mathbb{R}^3} \mathrm{d}^3\mathbf{k} \, \frac{e^2 \omega}{16\pi^3 \varepsilon_0 \hbar \Delta t} \\
&\quad \times e^{i(\omega - \omega_0)(t' - t'')} \left(\hat{\mathbf{D}}_{12}^* \cdot \hat{\mathbf{e}}_{\mathbf{k}\lambda} \right) \left(\hat{\mathbf{D}}_{12} \cdot \hat{\mathbf{e}}_{\mathbf{k}\lambda} \right) \\
&\quad \times \langle 1_{\mathbf{k}\lambda} | \hat{a}_{\mathbf{k}\lambda}^\dagger | 0_{\mathbf{k}\lambda} \rangle \, \hat{\sigma}^- \hat{\rho}_{\text{SI}}(t) \hat{\sigma}^+ \langle 0_{\mathbf{k}\lambda} | \hat{a}_{\mathbf{k}\lambda} | 1_{\mathbf{k}\lambda} \rangle .
\end{aligned} \tag{3.64}$$

Implementing the relations from Eqs. (3.45) – (3.48), one finds that the above equation simplifies to give

$$\begin{aligned}
\mathcal{L}(\hat{\rho}_{\text{SI}}(t)) &= \int_t^{t+\Delta t} \mathrm{d}t' \int_t^{t+\Delta t} \mathrm{d}t'' \int_0^\infty \mathrm{d}\omega \int_0^\pi \mathrm{d}\vartheta \sin(\vartheta) \int_0^{2\pi} \mathrm{d}\phi \, \frac{e^2 \|\mathbf{D}_{12}\|^2 \omega^3}{16\pi^3 \varepsilon_0 c^3 \hbar \Delta t} \\
&\quad \times \left[|d_1|^2 \left(1 - \cos^2(\vartheta) \right) + |d_3|^2 \left(1 - \sin^2(\vartheta) \sin^2(\phi) \right) \right. \\
&\quad \left. + (d_1^* d_3 + d_3^* d_1) \sin(\vartheta) \cos(\vartheta) \sin(\phi) \right] e^{i(\omega - \omega_0)(t' - t'')} \, \hat{\sigma}^- \, \hat{\rho}_{\text{SI}}(t) \, \hat{\sigma}^+ .
\end{aligned} \tag{3.65}$$

---

[1]The free-space level shift Δ_{free} is highly divergent when treated non-relativistically.

[2]As with Eq. (3.42), strictly one obtains two integrals; one over $\mathbf{k}$ and one over $\mathbf{k}'$. However, frequency matching is required when one traces over the bath modes hence, one obtains Eq. (3.64).

From Eq. (3.50), it is evident that evaluating the ϕ-integral generates a factor of 2π, which yields the expression

$$
\begin{aligned}
\mathcal{L}(\hat{\rho}_{\mathrm{SI}}(t)) \;=\;& \int_t^{t+\Delta t} \mathrm{d}t' \int_t^{t+\Delta t} \mathrm{d}t'' \int_0^\infty \mathrm{d}\omega \int_0^\pi \mathrm{d}\vartheta \sin(\vartheta) \frac{e^2 \|\mathbf{D}_{12}\|^2 \omega^3}{8\pi^2 \varepsilon_0 c^3 \hbar \Delta t} \\
& \times \left[|d_1|^2 \left(1 - \cos^2(\vartheta)\right) + |d_3|^2 \left(1 - \sin^2(\vartheta)\sin^2(\phi)\right) \right] \\
& \times \mathrm{e}^{\mathrm{i}(\omega-\omega_0)(t'-t'')} \hat{\sigma}^- \hat{\rho}_{\mathrm{SI}}(t) \hat{\sigma}^+ .
\end{aligned}
\tag{3.66}
$$

Again making use of the substitution $s = \cos(\vartheta)$, one finds that

$$
\begin{aligned}
\mathcal{L}(\hat{\rho}_{\mathrm{SI}}(t)) \;=\;& \int_t^{t+\Delta t} \mathrm{d}t' \int_t^{t+\Delta t} \mathrm{d}t'' \int_0^\infty \mathrm{d}\omega \int_{-1}^1 \mathrm{d}s \, \frac{e^2 \|\mathbf{D}_{12}\|^2 \omega^3}{8\pi^2 \varepsilon_0 c^3 \hbar \Delta t} \\
& \times \left[|d_1|^2 \left(1 - s^2\right) + \frac{1}{2}|d_3|^2 \left(1 + s^2\right) \right] \mathrm{e}^{\mathrm{i}(\omega-\omega_0)(t'-t'')} \hat{\sigma}^- \hat{\rho}_{\mathrm{SI}}(t) \hat{\sigma}^+ .
\end{aligned}
\tag{3.67}
$$

Evaluating the s-integral yields the expression

$$
\begin{aligned}
\mathcal{L}(\hat{\rho}_{\mathrm{SI}}(t)) \;=\;& \int_t^{t+\Delta t} \mathrm{d}t' \int_t^{t+\Delta t} \mathrm{d}t'' \int_0^\infty \mathrm{d}\omega \, \frac{e^2 \|\mathbf{D}_{12}\|^2 \omega^3}{6\pi^2 \varepsilon_0 c^3 \hbar \Delta t} \\
& \times \mathrm{e}^{\mathrm{i}(\omega-\omega_0)(t'-t'')} \hat{\sigma}^- \hat{\rho}_{\mathrm{SI}}(t) \hat{\sigma}^+ .
\end{aligned}
\tag{3.68}
$$

Note that the above expression can be re-written such that[1]

$$
\begin{aligned}
\mathcal{L}(\hat{\rho}_{\mathrm{SI}}(t)) \;=\;& \Gamma_{\mathrm{free}} \int_t^{t+\Delta t} \mathrm{d}t' \int_t^{t+\Delta t} \mathrm{d}t'' \int_0^\infty \mathrm{d}\omega \, \frac{1}{\Delta t} \frac{1}{2\pi} \frac{\omega^3}{\omega_0^3} \mathrm{e}^{\mathrm{i}(\omega-\omega_0)(t'-t'')} \\
& \times \hat{\sigma}^- \hat{\rho}_{\mathrm{SI}}(t) \hat{\sigma}^+ .
\end{aligned}
\tag{3.70}
$$

In order to evaluate the t''-integral, one makes use of the substitution $\xi = t' - t''$. Through this substitution one is able to state that

$$
\int_t^{t+\Delta t} \mathrm{d}t'' \;=\; \int_{t'-(t+\Delta t)}^{t'-t} \mathrm{d}\xi \, ,
\tag{3.71}
$$

---

[1]As the final Lindblad form of the master equation is known, one can also say that

$$
\Gamma = \Gamma_{\mathrm{free}} \int_t^{t+\Delta t} \mathrm{d}t' \int_t^{t+\Delta t} \mathrm{d}t'' \int_0^\infty \mathrm{d}\omega \, \frac{1}{\Delta t} \frac{1}{2\pi} \frac{\omega^3}{\omega_0^3} \mathrm{e}^{\mathrm{i}(\omega-\omega_0)(t'-t'')} \, .
\tag{3.69}
$$

and by making the Markov approximation, it is possible to say that

$$\int\limits_{t'-(t+\Delta t)}^{t'-t} \mathrm{d}\xi \, \mathrm{e}^{\mathrm{i}(\omega-\omega_0)\xi} = \int_{-\infty}^{\infty} \mathrm{d}\xi \, \mathrm{e}^{\mathrm{i}(\omega-\omega_0)\xi} = 2\pi \, \delta(\omega-\omega_0) \,. \qquad (3.72)$$

Through the above identity one can obtain the final form of the reset operator, $\mathcal{L}(\hat{\rho}_{\mathrm{S\,I}}(t))$. This is shown to be equal to

$$\mathcal{L}(\hat{\rho}_{\mathrm{S\,I}}(t)) \;=\; \Gamma_{\mathrm{free}} \, \hat{\sigma}^- \, \hat{\rho}_{\mathrm{S\,I}}(t) \, \hat{\sigma}^+ \,, \qquad (3.73)$$

where Γ_{free} is consistent with Eq. (3.62).

Finally, in order to obtain the master equation in Lindblad form, one must substitute the expressions for the conditional Hamiltonian and the reset operator from Eqs. (3.61) and (3.73), respectively, into the quantum jump master equation given in Eq. (3.24). This generates the following equation

$$\dot{\hat{\rho}}_{\mathrm{S\,I}}(t) \;=\; \Gamma_{\mathrm{free}} \left(\hat{\sigma}^- \, \hat{\rho}_{\mathrm{S\,I}}(t) \, \hat{\sigma}^+ - \frac{1}{2} \left[\hat{\sigma}^+ \hat{\sigma}^-, \hat{\rho}_{\mathrm{S\,I}}(t) \right]_+ \right) \,. \qquad (3.74)$$

The first term of Eq. (3.74) arises due to the spontaneous emission of a photon by the atom and the second term corresponds to no photon emission.

3.4 Summary

In this chapter, the behaviour and modelling of closed quantum systems is contrasted with that of open quantum systems. Open quantum systems posses a coupling to the surrounding environment and one way to accurately model open quantum systems is through the use of quantum optical master equations. By considering the well-understood example of a two-level atom interacting with the free electromagnetic field, a master equation description with analytical expressions for the free-space spontaneous emission rate Γ_{free} (cf. Eq. (3.62)) and atomic level shift for the excited state Δ_{free} (cf. Eq. (3.63)) was presented. Moreover, both results are consistent with the findings of other authors [49].

Chapter 4

Dipole-dipole interactions in free space

Dipole interactions are ubiquitous in quantum physics. Moreover, interacting dipole systems have shown practicality in the real world, e.g. quantum information processing and designing quantum gates for quantum information processing [55–57]. Experimental observations have shown that Ryberg atoms (i.e. atoms with high quantum numbers n which are extremely sensitive to small perturbations) are excellent candidates for dipole-dipole interactions [55–59]. Tanas & Ficek [60] provide an in-depth review where entanglement and quantum effects in two-atom systems are investigated (see references herein as well as Refs. [61–65] for more discussion on interacting dipole-dipole systems and entanglement). In addition, it has been demonstrated that arranging atoms in an ordered array, such as a lattice, makes it possible to achieve strong enhancement of emission [66] - a result that has been confirmed experimentally [67]. For a recent study looking at finite size effects in dipole systems see Ref. [68] and references within. More importantly, these scenarios have previously been shown to be successfully described using both the Heisenberg formalism [69] as well as quantum jump approaches [70–72], with a recent study demonstrated a gauge-invariant master equation approach for strongly interacting dipoles [73].

This chapter will focus on considering the interaction between two dipoles (or atoms) in free space. As it will be demonstrated later, the origin of this interaction stems from interference effects experienced by both atoms due to

coupling to the same electromagnetic field. The result of the interaction leads to corrections in the spontaneous emission rates of each atom as well as both atoms experiencing a level shift. Both these rates depend strongly on the orientation of their respective dipoles and the interatomic separation x, if x is of the same order of magnitude as the wavelength λ_0 of the emitted light. Unfortunately, these types of atomic interactions are usually relatively short-range. However, as it shall be demonstrated in Chapter 7, one is able to maintain and even increase the strength of this interaction when separating the atoms with a thin semi-transparent mirror.

4.1 Overview

The interaction of two dipoles in free space is a well-understood problem. Dicke was first to demonstrate that a collection of identical atoms can interact with one another through the electromagnetic field generating sub- or super-radiance [74], provided the atoms are separated by a distance that is much shorter than the wavelength of the emitted radiation, λ_0. As a result of interference effects, the collective spontaneous emission rate of the total system can be enhanced or suppressed and this generally depends on the initial state that the system is prepared in. In other words, depending on whether the system was initially prepared in a symmetric or an anti-symmetric state, one either observes an enhanced or suppressed emission rate. Following this, studying the behaviours of these collective systems gained a fair amount of interest [75–82] as well as studies considering non-identical atoms and the effect of retardation [83, 84].

Considering the case of two identical atoms (i.e. atoms with ground state $|1\rangle$ and excited state $|2\rangle$) in free space, as shown in Fig. 4.3, it is well-known that this scenario can be modelled as a single four-level system consisting of a ground, an excited, a symmetric and an anti-symmetric state which are denoted by $|g\rangle, |e\rangle, |s\rangle$ and $|a\rangle$ respectively (see Fig. 4.2). These states are known as *Dicke*
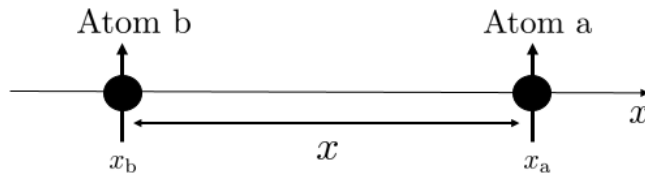
Figure 4.1: Schematic view of two interacting atoms in free space, where the atoms are placed along the x-axis with atom a and atom b being placed at the positions x_a and x_b, respectively. One can then define the separation between the atoms as some distance $x = |x_a - x_b| = |x_b - x_a|$.

states and can be expressed in the following way,

$$
\begin{aligned}
|g\rangle &= |11\rangle, \\
|e\rangle &= |22\rangle, \\
|s\rangle &= \frac{1}{\sqrt{2}} \left(|12\rangle + |21\rangle \right), \\
|a\rangle &= \frac{1}{\sqrt{2}} \left(|12\rangle - |21\rangle \right).
\end{aligned} \tag{4.1}
$$

Interpreting the above equations, the ground state $|g\rangle$ denotes the state where both atoms are de-excited and the excited state $|e\rangle$ denotes the state where both atoms are excited. The symmetric and anti-symmetric state $|s\rangle$ and $|a\rangle$ respectively, then denote states which are a superposition of atom one excited, atom two de-excited and vice versa.

As one shall see later in this chapter, in the limit of atomic separation $x \to 0$, the associated spontaneous decay rate of two atoms in the symmetric Dicke states $|s\rangle$ or $|e\rangle$ is twice as large as the decay rate of a single atom in free space. However, the antisymmetric state $|a\rangle$ forms a different superposition of atom one excited, atom two de-excited and vice versa. The associated spontaneous decay rate of two atoms in the anti-symmetric Dicke states $|a\rangle$ is suppressed such that they are no longer able to emit a photon. This means the dipole-dipole interaction is a manifestation of the indistinguishability of nearby atomic emitters. Moreover, for very large atomic separation $x \gg \lambda_0$, both atoms decay independently and exactly as in free space, as one would expect.
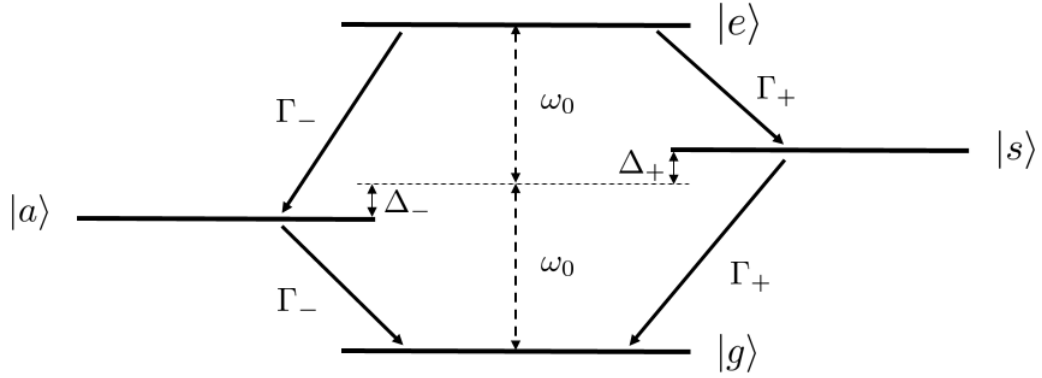
Figure 4.2: Level scheme for a dipole-dipole interaction between a pair of identical two-level atoms. This figure illustrates that such a system can be described by a single four-level configuration. The possible states of the system are denoted as; $|e\rangle$, $|g\rangle$, $|s\rangle$ and $|a\rangle$, where the $|s\rangle$ and $|a\rangle$ are the symmetric and anti-symmetric states, respectively. Each arrow denotes a one-photon transition, with Γ_+ and Γ_- denoting the spontaneous emission rate of the symmetric and anti-symmetric states, respectively. In addition, the level shifts for the symmetric and anti-symmetric states are denoted by Δ_+ and Δ_-, respectively.

4.2 Master equation for dipole-dipole interactions in free space

In order to present a master equation description for two interacting dipoles (or atoms), one is required to make use of the assumptions previously used in Chapters 2 and 3, i.e. the two-level approximation as well as the electric dipole and Markov approximation. This allows one to obtain analytical expressions for the spontaneous emission rates and atomic level shifts of the system.

4.2.1 The relevant Hamiltonians

Following the same procedure outlined in Chapter 3 and making use of the well-known dipole approximation, one can express the relevant Hamiltonian for two

interacting dipoles as

$$\hat{H} = \hat{H}_{\text{atom a}} + \hat{H}_{\text{atom b}} + \hat{H}_{\text{field}} + \hat{H}_{\text{SB}}, \qquad (4.2)$$

where $\hat{H}_{\text{atom a}}, \hat{H}_{\text{atom b}}$ and $\hat{H}_{\text{field}}$ describe the non-interacting contributions of the two atoms and the free electromagnetic field, respectively. The final term $\hat{H}_{\text{SB}}$ describes the interaction between the atoms and the surrounding free electromagnetic field. As before, it is necessary to move into the interaction picture with respect to the free Hamiltonian $\hat{H}_0$. Here, $\hat{H}_0$ has been chosen such that

$$\hat{H}_0 = \hat{H}_{\text{atom a}} + \hat{H}_{\text{atom b}} + \hat{H}_{\text{field}}, \qquad (4.3)$$

and the interaction Hamiltonian $\hat{H}_{\text{SB}}$ can again be defined through the dipole approximation in the following way

$$\hat{H}_{\text{SB}} = e \sum_{i=a,b} \hat{\mathbf{D}}_{12}^{(i)} \cdot \hat{\mathbf{E}}(\mathbf{r}_i), \qquad (4.4)$$

where $\hat{\mathbf{E}}(\mathbf{r}_i)$ represents the electric field observable at the position of atom i. In free space, this observable equals $\hat{\mathbf{E}}_{\text{free}}(\mathbf{r}_i)$ (cf. Eq. (2.77)). Therefore, one can say that the atom-field interaction Hamiltonian $\hat{H}_{\text{SB}}$ of two atoms at positions $\mathbf{r}_a$ and $\mathbf{r}_b$ and with dipole moments $\hat{\mathbf{D}}_{12}^{(a)}$ and $\hat{\mathbf{D}}_{12}^{(b)}$ is equal to

$$\hat{H}_{\text{SB}} = e\left[\hat{\mathbf{D}}_{12}^{(a)}\hat{\sigma}_a^- + \hat{\mathbf{D}}_{12}^{(a)*}\hat{\sigma}_a^+\right] \cdot \hat{\mathbf{E}}_{\text{free}}(\mathbf{r}_a) + e\left[\hat{\mathbf{D}}_{12}^{(b)}\hat{\sigma}_b^- + \hat{\mathbf{D}}_{12}^{(b)*}\hat{\sigma}_b^+\right] \cdot \hat{\mathbf{E}}_{\text{free}}(\mathbf{r}_b).$$
$$(4.5)$$

Without restrictions, the dipole moments $\hat{\mathbf{D}}_{12}^{(i)}$ are defined in the following way

$$\frac{\hat{\mathbf{D}}_{12}^{(a)}}{\|\mathbf{D}_{12}\|} = \begin{pmatrix} d_1^{(a)} \\ 0 \\ d_3^{(a)} \end{pmatrix}, \quad \frac{\hat{\mathbf{D}}_{12}^{(b)}}{\|\mathbf{D}_{12}\|} = \begin{pmatrix} d_1^{(b)} \\ d_2^{(b)} \\ d_3^{(b)} \end{pmatrix} \qquad (4.6)$$

with

$$|d_1^{(i)}|^2 + |d_2^{(i)}|^2 + |d_3^{(i)}|^2 = 1. \qquad (4.7)$$

Combining Eqs. (2.77) and (4.5), one is then able to move into the interaction picture via Eq. (3.7). One finds that the interaction picture Hamiltonian $\hat{H}_{\text{SB I}}(t)$

takes the form

$$
\hat{H}_{\mathrm{SBI}}(t) = \frac{\mathrm{i}e}{4\pi} \sum_{i=a,b} \sum_{\lambda=1,2} \int_{\mathbb{R}^3} \mathrm{d}^3\mathbf{k} \sqrt{\frac{\hbar\omega}{\pi\varepsilon}} \times \left[\mathrm{e}^{\mathrm{i}(\omega+\omega_0)t} \left(\hat{\mathbf{D}}_{12}^{(i)} \cdot \hat{\mathbf{e}}_{\mathbf{k}\lambda} \right) \hat{\sigma}_i^- \right.
$$
$$
\left. + \mathrm{e}^{-\mathrm{i}(\omega-\omega_0)t} \left(\hat{\mathbf{D}}_{12}^{(i)*} \cdot \hat{\mathbf{e}}_{\mathbf{k}\lambda} \right) \hat{\sigma}_i^+ \right] \hat{a}_{\mathbf{k}\lambda} + \mathrm{H.c.},
$$
(4.8)

in analogy to Eq. (3.40). Finally, applying the rotating wave approximation, one finds that

$$
\hat{H}_{\mathrm{SBI}}(t) = \frac{\mathrm{i}e}{4\pi} \sum_{i=a,b} \sum_{\lambda=1,2} \int_{\mathbb{R}^3} \mathrm{d}^3\mathbf{k} \sqrt{\frac{\hbar\omega}{\pi\varepsilon}} \, \mathrm{e}^{-\mathrm{i}(\omega-\omega_0)t} \left(\hat{\mathbf{D}}_{12}^{(i)*} \cdot \hat{\mathbf{e}}_{\mathbf{k}\lambda} \right) \mathrm{e}^{\mathrm{i}\mathbf{k}\cdot\mathbf{r}_i} \, \hat{\sigma}_i^+ \hat{a}_{\mathbf{k}\lambda} + \mathrm{H.c.}.
$$
(4.9)

This Hamiltonian describes the simultaneous interaction of atom a and atom b with the electric fields $\hat{\mathbf{E}}_{\mathrm{free}}(\mathbf{r}_a)$ and $\hat{\mathbf{E}}_{\mathrm{free}}(\mathbf{r}_b)$. The indistinguishability of the two atoms arises as both atoms couple to the same field.

4.2.2 Master equation

In order to determine the master equation for this system, one must substitute the interaction-picture Hamiltonian $\hat{H}_{\mathrm{SBI}}(t)$ into the expressions derived for the conditional Hamiltonian $\hat{H}_{\mathrm{condI}}(t)$ and the reset operator $\mathcal{L}(\hat{\rho}_{\mathrm{SI}}(t))$ in Eqs. (3.25) and (3.26). Evaluating the various integrals by proceeding as described in App. A, one obtains expressions for the conditional Hamiltonian $\hat{H}_{\mathrm{condI}}(t)$ and the reset operator $\mathcal{L}(\hat{\rho}_{\mathrm{SI}}(t))$ for two interacting atoms. The conditional Hamiltonian is given by

$$
\hat{H}_{\mathrm{condI}}(t) = -\frac{\mathrm{i}\hbar}{2} \left[\Gamma_{\mathrm{free}} \left(\hat{\sigma}_a^+ \hat{\sigma}_a^- + \hat{\sigma}_b^+ \hat{\sigma}_b^- \right) + C(x) \left(\hat{\sigma}_a^+ \hat{\sigma}_b^- + \hat{\sigma}_b^+ \hat{\sigma}_a^+ \right) \right], \quad (4.10)
$$

where $C(x)$ is a complex function which corresponds to an inter-system decay rate. This results in a reset operator of the form

$$
\mathcal{L}(\hat{\rho}_{\mathrm{SI}}(t)) = \Gamma_{\mathrm{free}} \left[\hat{\sigma}_a^- \hat{\rho}_{\mathrm{SI}}(t)\hat{\sigma}_a^+ + \hat{\sigma}_b^- \hat{\rho}_{\mathrm{SI}}(t)\hat{\sigma}_b^+ \right]
$$
$$
+ \mathrm{Re}(C(x)) \left[\hat{\sigma}_b^- \hat{\rho}_{\mathrm{SI}}(t)\hat{\sigma}_a^+ + \hat{\sigma}_a^- \hat{\rho}_{\mathrm{SI}}(t)\hat{\sigma}_b^+ \right], \quad (4.11)
$$

Both Eqs. (4.10) and (4.11) depend on the complex dipole-coupling constant $C(x)$ which is defined as (cf. Eq. (A.12))

$$C(x) \;=\; \frac{3}{2}\,\mathrm{e}^{\mathrm{i}k_0 x}\left[\frac{c_1}{\mathrm{i}k_0 x} + \frac{c_2}{(k_0 x)^2} - \frac{c_2}{\mathrm{i}(k_0 x)^3}\right]\Gamma_{\mathrm{free}}\,, \tag{4.12}$$

where

$$x \equiv |x_a - x_b| \equiv |x_b - x_a|\,, \tag{4.13}$$

denotes the distance between atom a and atom b. In the above equations, Γ_{free} denotes the spontaneous emission rate of an atom in free space (cf. Eq. (3.62)), $k_0 = \omega_0/c$, x denotes the always positive distance between the atoms, and c_1 and c_2 equal[1]

$$
\begin{aligned}
c_1 &\equiv \left(\hat{\mathbf{D}}_{12}^{(a)}\cdot\hat{\mathbf{D}}_{12}^{(b)}\right) - \left(\hat{\mathbf{D}}_{12}^{(a)}\cdot\hat{\mathbf{x}}\right)\left(\hat{\mathbf{D}}_{12}^{(b)}\cdot\hat{\mathbf{x}}\right),\\
c_2 &\equiv \left(\hat{\mathbf{D}}_{12}^{(a)}\cdot\hat{\mathbf{D}}_{12}^{(b)}\right) - 3\left(\hat{\mathbf{D}}_{12}^{(a)}\cdot\hat{\mathbf{x}}\right)\left(\hat{\mathbf{D}}_{12}^{(b)}\cdot\hat{\mathbf{x}}\right).
\end{aligned}
\tag{4.14}
$$

where the atomic dipole moment can be defined as[2]

$$
\begin{aligned}
\mu^{(a)} &= \|\hat{\mathbf{D}}_{12}^{(a)}\cdot\hat{\mathbf{x}}\|^2\,,\\
\mu^{(b)} &= \|\hat{\mathbf{D}}_{12}^{(b)}\cdot\hat{\mathbf{x}}\|^2\,.
\end{aligned}
\tag{4.15}
$$

As a consequence, the spontaneous decay rates and level shifts of the atoms can exhibit an intricate distance-dependence, especially, when their dipole moment vectors are complex or different from each other.

When substituting Eqs. (4.10) and (4.11) into the expression for the quantum jump master equation, one finds that it is necessary to perform the following change of basis,

$$
\begin{aligned}
|1\rangle &= \text{Both atom a and atom b in ground state}\,,\\
|2\rangle &= \text{Atom b excited and atom a in ground state}\,,\\
|3\rangle &= \text{Atom a excited and atom b in ground state}\,,\\
|4\rangle &= \text{Both atom a and atom b in excited state}\,,
\end{aligned}
\tag{4.16}
$$

---

[1]Both dipole moments are assumed to be real.

[2]Here, $\hat{\mathbf{x}}$ denotes the normalised vector $\hat{\mathbf{x}} = \frac{\mathbf{x}}{\|\mathbf{x}\|}$.

in order to maintain Lindblad form. In addition, one can define the atomic lowering and raising operators

$$
\begin{aligned}
\hat{\sigma}_a^- &= |1_a\rangle\langle 2_a| \big[|1_b\rangle\langle 1_b| + |2_b\rangle\langle 2_b|\big] = |1\rangle\langle 3| + |2\rangle\langle 4|, \\
\hat{\sigma}_b^- &= |1_b\rangle\langle 2_b| \big[|1_a\rangle\langle 1_a| + |2_a\rangle\langle 2_a|\big] = |1\rangle\langle 2| + |3\rangle\langle 4|,
\end{aligned}
\tag{4.17}
$$

and

$$
\begin{aligned}
\hat{\sigma}_a^+ &= |3\rangle\langle 1| + |4\rangle\langle 2|, \\
\hat{\sigma}_b^+ &= |2\rangle\langle 1| + |4\rangle\langle 3|.
\end{aligned}
\tag{4.18}
$$

Using this notation and the conditional Hamiltonian in Eq. (4.10), one finds that

$$
\hat{H}_{\text{cond I}}(t) = -\frac{i\hbar}{2}\left[\Gamma_{\text{free}}\left(|2\rangle\langle 2| + |3\rangle\langle 3|\right) + C(x)\left(|2\rangle\langle 3| + |3\rangle\langle 2|\right) + 2\,\Gamma_{\text{free}}|4\rangle\langle 4|\right].
\tag{4.19}
$$

Using the above equation and Eq. (4.16), it is evident that the state $|1\rangle$ has a zero associated eigenvalue (spontaneous emission rate) where as the state $|4\rangle$ has the spontaneous emission rate of $2\Gamma_{\text{free}}$ as it should. Considering the central block of this Hamiltonian separately, one obtains the additional eigenvalues

$$
\lambda_\pm = \Gamma_{\text{free}} \pm C(x),
\tag{4.20}
$$

corresponding to the eigenstates[1]

$$
\begin{aligned}
|\lambda_+\rangle &= \frac{1}{\sqrt{2}}\left(|2\rangle + |3\rangle\right), \\
|\lambda_-\rangle &= \frac{1}{\sqrt{2}}\left(|2\rangle - |3\rangle\right).
\end{aligned}
\tag{4.21}
$$

In the above equation, the state $|\lambda_+\rangle$ corresponds to the symmetric state of the system, where as the state $|\lambda_-\rangle$ corresponds to the anti-symmetric state of the

---

[1]One can check these are the correct eigenstates by applying the states in Eq. (4.21) to the conditional Hamiltonian in Eq. (4.19). Doing so gives an eigenvalue-eigenvector equation where the spontaneous emission rates $\Gamma_\pm$ correspond to the states $|\lambda_\pm\rangle$.

system. Returning to the notation in Eq. (4.1),

$$
\begin{aligned}
|g\rangle &= |1\rangle, \\
|e\rangle &= |4\rangle, \\
|s\rangle &= \frac{1}{\sqrt{2}}\left(|2\rangle + |3\rangle\right), \\
|a\rangle &= \frac{1}{\sqrt{2}}\left(|2\rangle - |3\rangle\right),
\end{aligned}
\tag{4.22}
$$

it is possible to write the conditional Hamiltonian $\hat{H}_{\text{cond I}}(t)$ from Eq. (4.19) in terms of these basis states,

$$
\hat{H}_{\text{cond I}}(t) = -\frac{\mathrm{i}\hbar}{2}\left[\left(\Gamma_{\text{free}} + C(x)\right)|s\rangle\langle s| + \left(\Gamma_{\text{free}} - C(x)\right)|a\rangle\langle a| + 2\Gamma_{\text{free}}|e\rangle\langle e|\right].
\tag{4.23}
$$

Comparing Eqs. (4.19) and (4.23), one finds that

$$
\begin{aligned}
\hat{\sigma}_a^- &= \frac{1}{\sqrt{2}}\left[|g\rangle\langle s| + \mathrm{i}|s\rangle\langle a| + |s\rangle\langle e| + \mathrm{i}|a\rangle\langle e|\right], \\
\hat{\sigma}_b^- &= \frac{1}{\sqrt{2}}\left[|g\rangle\langle s| - \mathrm{i}|s\rangle\langle a| + |s\rangle\langle e| - \mathrm{i}|a\rangle\langle e|\right],
\end{aligned}
\tag{4.24}
$$

and

$$
\begin{aligned}
\hat{\sigma}_a^+ &= \frac{1}{\sqrt{2}}\left[|s\rangle\langle g| - \mathrm{i}|a\rangle\langle s| + |e\rangle\langle s| - \mathrm{i}|e\rangle\langle a|\right], \\
\hat{\sigma}_b^+ &= \frac{1}{\sqrt{2}}\left[|s\rangle\langle g| + \mathrm{i}|a\rangle\langle s| + |e\rangle\langle s| + \mathrm{i}|e\rangle\langle a|\right].
\end{aligned}
\tag{4.25}
$$

From Eqs. (4.24) and (4.25), one can define two new operators $\hat{L}_\pm$ and $\hat{L}_\pm^\dagger$ which are linear superpositions of the atomic operators $\hat{\sigma}_{a,b}^-$ and $\hat{\sigma}_{a,b}^+$. These new operators are defined in the following way

$$
\begin{aligned}
\hat{L}_\pm &= \frac{1}{\sqrt{2}}\left(\hat{\sigma}_a^- \pm \hat{\sigma}_b^-\right), \\
\hat{L}_\pm^\dagger &= \frac{1}{\sqrt{2}}\left(\hat{\sigma}_a^+ \pm \hat{\sigma}_b^+\right),
\end{aligned}
\tag{4.26}
$$

where the plus sign corresponds to the symmetric state and the minus sign corresponds to the anti-symmetric state. These states yield the conditional Hamiltonian

$$
\hat{H}_{\text{cond I}}(t) = -\frac{\mathrm{i}\hbar}{2}\left[\left(\Gamma_{\text{free}} + C(x)\right)\hat{L}_+^\dagger\hat{L}_+ + \left(\Gamma_{\text{free}} - C(x)\right)\hat{L}_-^\dagger\hat{L}_-\right].
\tag{4.27}
$$

Moreover, these operators can be expressed in terms of the collective atomic states (Dicke states) $|g\rangle$, $|e\rangle$, $|s\rangle$ and $|a\rangle$ from Eq. (4.1), such that[1]

$$
\begin{aligned}
\hat{L}_+ &= |g\rangle\langle s| + |s\rangle\langle e|\,, \\
\hat{L}_- &= -|g\rangle\langle a| + |a\rangle\langle e|\,,
\end{aligned}
\tag{4.28}
$$

and

$$
\begin{aligned}
\hat{L}_+^\dagger &= |s\rangle\langle g| + |e\rangle\langle s|\,, \\
\hat{L}_-^\dagger &= -|a\rangle\langle g| + |e\rangle\langle a|\,.
\end{aligned}
\tag{4.29}
$$

In addition, this allows the reset operator $\mathcal{L}(\hat{\rho}_{\mathrm{S\,I}}(t))$ in Eq. (4.11) to be expressed in the following way

$$
\begin{aligned}
\mathcal{L}(\hat{\rho}_{\mathrm{S\,I}}(t)) &= [\Gamma_{\mathrm{free}} + \mathrm{Re}(C(x))]\,\hat{L}_+\,\hat{\rho}_{\mathrm{S\,I}}(t)\,\hat{L}_+^\dagger \\
&\quad + [\Gamma_{\mathrm{free}} - \mathrm{Re}(C(x))]\,\hat{L}_-\,\hat{\rho}_{\mathrm{S\,I}}(t)\,\hat{L}_-^\dagger\,.
\end{aligned}
\tag{4.30}
$$

Considering the form of Eqs. (4.27) and (4.30), it is evident that the basis transformation outlined in Eqs. (4.16) – (4.18) and Eq. (4.22) generate a master equation of Lindblad form. More importantly, the above calculations show that two interacting atoms effectively have two decay channels. The spontaneous emission of a photon transfers symmetrically into symmetric states with an emission rate given by $\Gamma_{\mathrm{free}} + \mathrm{Re}(C(x))$ and anti-symmetric states have an associated emission rate given by $\Gamma_{\mathrm{free}} - \mathrm{Re}(C(x))$. The imaginary part of the dipole coupling constant $C(x)$ describes atomic level shifts which apply to the collective atomic states $|s\rangle$ and $|a\rangle$, respectively, as illustrated by the combined atomic level scheme in Fig. 4.2.

To obtain the master equation of Lindblad form, one must substitute the expressions for the conditional Hamiltonian and the reset operator from Eqs. (4.27) and (4.30) respectively, into the quantum jump master equation given in Eq. (3.24).

---

[1]For the schematic setup shown in Fig. 4.3, there exists a certain symmetry. For example, the Hamiltonian is unchanged if one exchanges the labels 'atom a' and 'atom b'. One could use this interpretation to deduce the form of the operators in Eqs. (4.28) and (4.29).

This generates the following master equation

$$
\begin{aligned}
\dot{\hat{\rho}}_{\mathrm{SI}}(t) \;=\;& \Gamma_+ \left(\hat{L}_+ \, \hat{\rho}_{\mathrm{SI}}(t) \, \hat{L}_+^\dagger - \frac{1}{2} \left[\hat{L}_+^\dagger \hat{L}_+, \hat{\rho}_{\mathrm{SI}}(t) \right]_+ \right) \\
&+ \Gamma_- \left(\hat{L}_- \, \hat{\rho}_{\mathrm{SI}}(t) \, \hat{L}_-^\dagger - \frac{1}{2} \left[\hat{L}_-^\dagger \hat{L}_-, \hat{\rho}_{\mathrm{SI}}(t) \right]_+ \right),
\end{aligned} \tag{4.31}
$$

where $\Gamma_\pm = \Gamma_{\mathrm{free}} \pm \mathrm{Re}(C(x))$.

4.2.3 Spontaneous emission rates and atomic level shifts

From Eqs. (4.12), (4.27) and (4.30), one can determine full analytical expressions for the spontaneous emission rates of the system as well as atomic level shifts.

The spontaneous emission rates of two interacting dipoles are

$$
\Gamma_\pm \;\equiv\; \Gamma_{\mathrm{free}} \pm \mathrm{Re}(C(x)), \tag{4.32}
$$

with the $\pm$ sign denoting the symmetric and the anti-symmetric decay channels, respectively. The distance-dependent dipole-coupling constant $C(x)$ is given in Eq. (4.12). Moreover, the decay channels from Eq. (4.32) can be expressed as

$$
\Gamma_\pm \;=\; \left[1 \pm \frac{3}{2} \left[\frac{\sin(k_0 x)}{k_0 x} c_1 + \left(\frac{\cos(k_0 x)}{(k_0 x)^2} - \frac{\sin(k_0 x)}{(k_0 x)^3} \right) c_2 \right] \right] \Gamma_{\mathrm{free}}, \tag{4.33}
$$

where c_1 and c_2 are defined in Eq. (4.14). In addition, one can obtain the atomic level shift from the imaginary part of the dipole-coupling constant. Examining the imaginary coefficient, one finds that atomic level shift takes the following form[1]

$$
\Delta_\pm \;=\; \frac{3}{4} \left[\frac{\cos(k_0 x)}{k_0 x} c_1 - \left(\frac{\sin(k_0 x)}{(k_0 x)^2} + \frac{\cos(k_0 x)}{(k_0 x)^3} \right) c_2 \right] \Gamma_{\mathrm{free}}. \tag{4.34}
$$

Limiting cases

To gain a better understanding of the physical behaviour described by the above equations, one can look at some limiting cases.

---

[1] The exact form of these level shifts is not important for the work presented in this thesis.
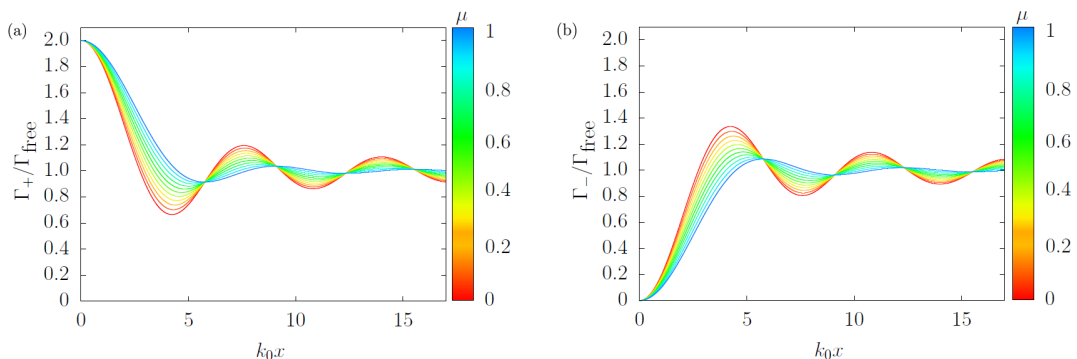
Figure 4.3: [Colour online] The spontaneous decay rates $\Gamma_\pm$ for the (a) symmetric and (b) anti-symmetric states as a function of the atomic separation x for different orientations of the atomic dipole moment, where $\hat{\mathbf{D}}_{12}^{(a)} = \hat{\mathbf{D}}_{12}^{(b)}$. For distances x of the same order of magnitude as the wavelength λ_0 of the emitted light, the last few terms in Eq. (4.33) are no longer negligible and $\Gamma_\pm$ depend strongly on x and μ. As shown in Eq. (4.38), the decay rates $\Gamma_+ \to 2\,\Gamma_{\text{free}}$ and $\Gamma_- \to 0$ when $x \to 0$. Moreover, for $k_0 x \gg 1$, we have $\Gamma_\pm = \Gamma_{\text{free}}$, as it should (c.f. Eq. (4.38)).

Behaviour for large atomic separation

First, let us consider the physical behaviour of Eqs. (4.33) and (4.34) when $x \to \infty$, i.e. when the atoms are separated over large distances. In other words, for the case where $x \to \infty$, then one finds that $C(x) \to 0$ and each atom decays independently and as in free space. As a result, the spontaneous emission rates $\Gamma_\pm$ reduce to give

$$\Gamma_\pm = \Gamma_{\text{free}}\,, \qquad (4.35)$$

and the atomic level shifts reduce to give

$$\Delta_\pm = 0\,. \qquad (4.36)$$

Strictly, the separation cannot be taken to infinity as this would violate the Markovian approximation used earlier. This atomic separation $\widetilde{x}$ can be taken to approximately $0.03cm$ provided the time period under consideration Δt is approximately $10^{-13}s$.

Behaviour for small atomic separation

Finally, let us consider the behaviour of Eqs. (4.33) and (4.34) when the two atoms are separated over very small distances. In other words, for the case where $x \to 0$, one finds

$$\Gamma_\pm = \left[1 \pm \frac{3}{2} \left[(1 - \mu) - \frac{1}{3}(1 - 3\mu) \right] \right] \Gamma_{\text{free}} . \qquad (4.37)$$

For both cases of $\mu = 0$ and $\mu = 1$, one finds that the spontaneous emission rates reduce to

$$\Gamma_\pm = [1 \pm 1] \, \Gamma_{\text{free}} , \qquad (4.38)$$

which is consistent with the spontaneous emission rates for the symmetric and anti-symmetric states illustrated in Fig. 4.3. Finally, for the atomic level shifts in this limit, one finds that[1]

$$\Delta_\pm = \infty . \qquad (4.39)$$

4.3 Summary

In this chapter, the behaviour and modelling of two interacting atoms in free space is presented through a master equation description. This allows one to obtain analytical expressions for the spontaneous emission rates $\Gamma_\pm$ (cf. Eq. (4.33)) and atomic level shifts $\Delta_\pm$ (cf. Eq. (4.34)), respectively. These rates arise due to interference effects as the atoms interact through the electromagnetic field, generating collective spontaneous emission rates. These spontaneous emission rates can be enhanced or suppressed depending on the initial state of the system, i.e. if the system is initially prepared in a symmetric state this leads to an enhanced emission rate given by Γ_+, and preparing in the anti-symmetric leads to a suppressed emission rate given by Γ_-. The symmetric and anti-symmetric states have an associated atomic level shift given by Δ_+ and Δ_-, respectively. The main results from this chapter and the process applied should aid the understanding of the long-range dipole-dipole interaction detailed in Chapter 7.

---

[1]This is due to assuming that the electron is a point particle orbiting around the atomic nuclei. In reality, one finds finite level shifts e.g. Lamb shift (see Ref. [49] for details).

Part II

Novel Theoretical Models

Chapter 5

Modelling the electromagnetic field in the presence of two-sided mirrors

Quantising the electromagnetic field in the presence of perfectly-conducting surfaces is well-understood due to the strict boundary conditions imposed on the electromagnetic field by the interface. However, quantising the electromagnetic field near semi-transparent mirrors is less straightforward as these boundary conditions are not as strictly enforced. Moreover, within the postulates of quantum physics, there is no information given about how one should impose these boundary conditions. In this chapter it will be shown this can be done in different ways.

Sommerfeld laid the foundation for quantising the electromagnetic field near semi-transparent mirrors in 1909 when he examined the propagation of surface waves above a flat lossy ground for applications in wireless communication [85]. In 1971, Carniglia and Mandel [86] considered a semi-transparent mirror with finite transmission and reflection rates and identified a set of elementary orthogonal light modes of travelling waves, so-called triplet modes. These are formed by incident, transmitted and reflected electromagnetic waves, as illustrated in Fig. 5.1. Quantising these triplet modes, Carniglia and Mandel obtained an electromagnetic field Hamiltonian, which is the sum of independent harmonic oscillator

Hamiltonians, and electromagnetic field observables, which are superpositions of free space observables (see Refs. [87–91] for more recent related work).

In 1974, Agarwal used quantum electrodynamics to calculate the level shift and spontaneous decay rate of an atom near a dielectric medium [92, 93]. Subsequently, he published a series of papers on quantum electrodynamics in the presence of dielectrics and conductors [94–99]. In these papers, Agarwal uses linear response functions to indirectly deduce the properties of the electromagnetic field observables. His implicit approach to field quantisation helped to lay the foundations of a research area now known as macroscopic quantum electrodynamics [100, 101]. Other authors are more interested in the direct canonical quantisation of the electromagnetic field [8–10, 102–109] or prefer purely phenomenological approaches to model light scattering through semi-transparent mirrors, like the so-called input-output formalism [3–5] and different continuous-mode model approaches [2, 110]. When modelling the transmission of single photons through linear optics networks, we usually employ scattering matrices [101, 111]. Unfortunately, the consistency and relationship between these different methods is not yet always well understood [112].

This chapter models light scattering through thin, conducting, flat surfaces with finite transmission, reflection and absorption rates, where light approaches the mirror from both sides (cf. Fig. 5.1). The physically-motivated description presented in Chapter 2 provides the basis and allows one to characterise photons as in free space. The uniqueness of this model then arises by explicitly considering the exchange of energy between the electromagnetic field and the mirror surface and the presence of *mirror images*.

5.1 Overview of the image-detector method

The basic idea of realising boundary conditions through the *image-detector method* maps the problem onto analogous free space scenarios. In other words, when considering a wave packet incident on a reflective surface such as a mirror, one can realise the boundary condition by replacing the mirror with a wave packet of opposite amplitude and propagating in the opposite direction. As it will be shown in this chapter, the field quantisation scheme applies to a wide range of optical

Figure 5.1: Schematic view of a semi-transparent mirror with light incident from both sides. Depending on the direction of the incoming light, the (real) transmission and reflection rates of the mirror are denoted by t_a, t_b, r_a and r_b, respectively. In this model, the possible absorption of light in the mirror surface is explicitly taken into account. However, for simplicity it is assumed that these rates are angle-independent and the medium on both sides of the mirror is assumed to be the same.

mirrors and is strongly motivated by the method-of-images [17]. This model details an approach that describes the electromagnetic field near semi-transparent mirrors using the same Hamiltonian as in free space and assume that incoming wave packets evolve exactly as they would in the absence of mirrors [28]. However, the presence of mirrors changes how and where electric and magnetic field amplitudes are measured. Adopting this point of view, one finds that detectors observe superpositions of free-space observables which can be associated with incoming, reflected and transmitted waves.

Although the approach has some similarities with the so-called triplet or normal mode field quantisation schemes of previous authors [86–91], it also provides novel insight into their origin and extends the potential use of these modes. As it will be shown later in this chapter, the triplet modes derived here differ from

the triplet modes of Carniglia and Mandel [86] by phase factors which coincide with the phase factors of the beamsplitter transformations that are routinely used to describe linear optics experiments [101, 111]. The phase factors are crucial components as they guarantee energy conservation on the mirror surface. As a result, this model applies not only to one-sided but also to two-sided semi-transparent mirrors unlike Ref. [86]. As it is demonstrated later in this chapter, the energy of the mirror surface, i.e. the energy of mirror images, is explicitly taken into account. Therefore, the harmonic oscillator system Hamiltonian $\hat{H}_{\mathrm{sys}}$ can be decomposed into a Hamiltonian $\hat{H}_{\mathrm{field}}$ which describes the energy of the electromagnetic field and a Hamiltonian $\hat{H}_{\mathrm{mirr}}$ which describes the energy of the mirror surface,

$$\hat{H}_{\mathrm{sys}} \;\;=\;\; \hat{H}_{\mathrm{field}} + \hat{H}_{\mathrm{mirr}} \,. \tag{5.1}$$

For example, when placing a wave packet in front of a perfect mirror, one finds that half of the energy of the system belongs to the wave packet and the other half belongs to its mirror image. However, when wave packets approach a mirror simultaneously from both sides, then the expectation values of $\hat{H}_{\mathrm{field}}$ and $\hat{H}_{\mathrm{mirr}}$ are in general not the same. Moreover, the squares of the electric field amplitudes of reflected and transmitted waves do not have to add up to one, meaning

$$t_a{}^2 + r_a{}^2 \le 1 \quad \text{and} \quad t_b{}^2 + r_b{}^2 \le 1 \,, \tag{5.2}$$

thereby the possible absorption of light by the mirror surface is taken into account. It is assumed that the mirror surface does not alter the coherent properties of the incoming light, it only reduces the amplitude of incoming wave packets. In addition, the medium on both sides of the mirror is assumed to be the same.

In order to test the validity of this model and determine the normalisation factors η_a and η_b, a closer examination of a radiating atom near a two-sided semi-transparent mirror is presented in the following chapter, with analytical expressions for the spontaneous decay rate Γ_{mirr} and the level shift Δ_{mirr} of the system (see Chapter 6).

5.2 Classical physics

This section will review the scenario of light incident on a single, thin mirror using a classical description. Throughout this treatment it is assumed that the transmission and reflection coefficients describing the quality of the mirror surface are independent of the angle of incident light and these coefficients are assumed to be real and readily determined from experimental observation.

5.2.1 One-sided perfect mirror

First, let us have a closer look at the case of a perfect mirror in one-dimension and understand what happens when light is incident on it. Placing the mirror at $x = 0$, only considering wave packets which propagate along the x-axis and approach the perfect mirror from one side of the setup, the right-hand side, i.e. $x > 0$. Strict boundary conditions are imposed by the mirror surface, such that the electric field obeys the condition

$$E_{\text{mirr}}(0, t) \;\;=\;\; 0 \tag{5.3}$$

at all times t, as the mirror surface charges move freely and are able to immediately compensate for any non-zero electric field contributions. In a similar fashion to the standard method-of-images approach of satisfying boundary conditions as discussed earlier, a *mirror-image detector* (see later) is introduced.

The easiest way of deriving electric and magnetic field solutions in this situation is to apply the mirror image method [17]. This method suggests to write the electric field $E_{\text{mirr}}(x, t)$ and its accompanying magnetic field $B_{\text{mirr}}(x, t)$ as

$$
\begin{aligned}
E_{\text{mirr}}(x, t) &= \left[E_{\text{free}}(x, t) - E_{\text{free}}(-x, t) \right] \Theta(x), \\
B_{\text{mirr}}(x, t) &= \left[B_{\text{free}}(x, t) + B_{\text{free}}(-x, t) \right] \Theta(x)
\end{aligned}
\tag{5.4}
$$

with the Heaviside step function $\Theta(x)$ defined as

$$
\Theta(x) = \begin{cases} 1 & \text{for } x \geq 0, \\ 0 & \text{for } x < 0. \end{cases}
\tag{5.5}
$$

An interpretation of Eq. (5.4) is to say that the mirror produces a mirror-image of any incoming wave packet (see Fig. 5.2). The mirror image has the

same shape as the original wave packet but its components travel with negative electric field amplitudes in the opposite direction. Propagating any incoming wave packet *and* its mirror image simultaneously as in free space and adding the respective field amplitudes of both contributions yields exactly the same electric and magnetic fields as Eq. (5.4), provided one restricts to looking at the $x \geq 0$ half space. In Fig. 5.2 (a)–(c) and Fig. 5.2 (d)–(f) demonstrate a left-moving and a right-moving wave packet, respectively, at three different times. The two wave packets cross over the mirror location at $x = 0$ at the same time. Adding the electric field contributions on the right side of the mirror, as done in Fig. 5.2 (g)–(i), reproduces the dynamics of an incoming wave packet approaching a perfect mirror from the right.

An alternative way of interpreting Eq. (5.4) is to say that the mirror introduces *mirror-image detectors* while assuming that any incoming wave packets propagate exactly as they would in free space. The presence of the image detectors changes where and how the electromagnetic field is observed. In this description, it is assumed that the image detectors of the electric field measure $-E_{\text{free}}(-x,t)$, while the original detectors measure $E_{\text{free}}(x,t)$. Moreover, the total electric field $E_{\text{mirr}}(x,t)$ in the presence of a one-sided perfect mirror is the sum of the free-fields seen by both the original and the image-detector. This approach also reproduces $E_{\text{mirr}}(x,t)$ in Eq. (5.4), and analogously, one can also construct mirror image-detectors for magnetic field measurements.

Looking closer at Eq. (5.4), more specifically the second terms of $E_{\text{mirr}}(x,t)$ and $B_{\text{mirr}}(x,t)$, why is a pre-factor of ± 1 attributed to describe reflection? Since the model maps the mirror scenario onto an analogous free space scenario with two wave packets, then in order to satisfy Eq. (5.3) the phase shift between the incident and reflected wave packet must be equal to π. It is well-known that the general form of a plane wave is

$$e^{i(kx-\omega t+\varphi)} = e^{i(kx-\omega t)} e^{i\varphi}, \qquad (5.6)$$

and it is also true that

$$e^{i\varphi} = \cos(\varphi) + i\sin(\varphi) = -1 \quad \text{when } \varphi = \pi. \qquad (5.7)$$

Therefore, this minus sign should not be surprising as the mirror imposes a strict boundary condition on the electric field meaning the phase factor must satisfy $\varphi = \pi$. As the mirror does not impose any conditions on the magnetic field, and more importantly, in order to be consistent with Maxwell's equations, the free-field magnetic field solutions can be 'stitched together' through a pre-factor of $+1$. Most importantly, in the presence of a mirror, the electric field $E_{\mathrm{mirr}}(x, t)$ still needs to obey Maxwell's equations (cf. Eq. (2.1)).

One can easily check that, at all times, the solution in Eq. (5.4) obeys Eq. (5.3) and Maxwell's equations, since it is a superposition of free-field solutions. Upon reflection, the electric field changes sign, while the magnetic field amplitude remains the same[1].

5.2.2 Two-sided perfect mirror

The next step is looking at how to model the scenario where light is incident on a perfect mirror from both sides. Doing so is fairly straightforward, since wave packets on different sides of the mirror never meet and therefore, never interfere. Proceeding as previously, one finds that the electric field amplitude $E_{\mathrm{mirr}}(x, t)$ can now be written as

$$
\begin{aligned}
E_{\mathrm{mirr}}(x, t) &= \left[E_{\mathrm{free}}^{(a)}(x, t) - E_{\mathrm{free}}^{(a)}(-x, t)\right] \Theta(x) \\
&\quad + \left[E_{\mathrm{free}}^{(b)}(x, t) - E_{\mathrm{free}}^{(b)}(-x, t)\right] \Theta(-x)
\end{aligned}
\tag{5.8}
$$

in analogy to Eq. (5.4). The superscripts in this equation help to distinguish free space solutions corresponding to opposite sides of the mirror. Here, the superscript (a) denotes free-field solutions originating on the right-hand side of the mirror $(x > 0)$ and the superscript (b) denotes free-field solutions originating on the left-hand side of the mirror $(x < 0)$. One can easily check that this general electric field solution satisfies the wave equation in Eq. (2.6) and also the boundary condition in Eq. (5.3) at all times.

---

[1]Notice that, if $E_{\mathrm{free}}(x, t)$ and $B_{\mathrm{free}}(x, t)$ are consistent with Maxwell's equations, then the same applies to $E_{\mathrm{free}}(-x, t)$ and $-B_{\mathrm{free}}(x, t)$ due to symmetry.
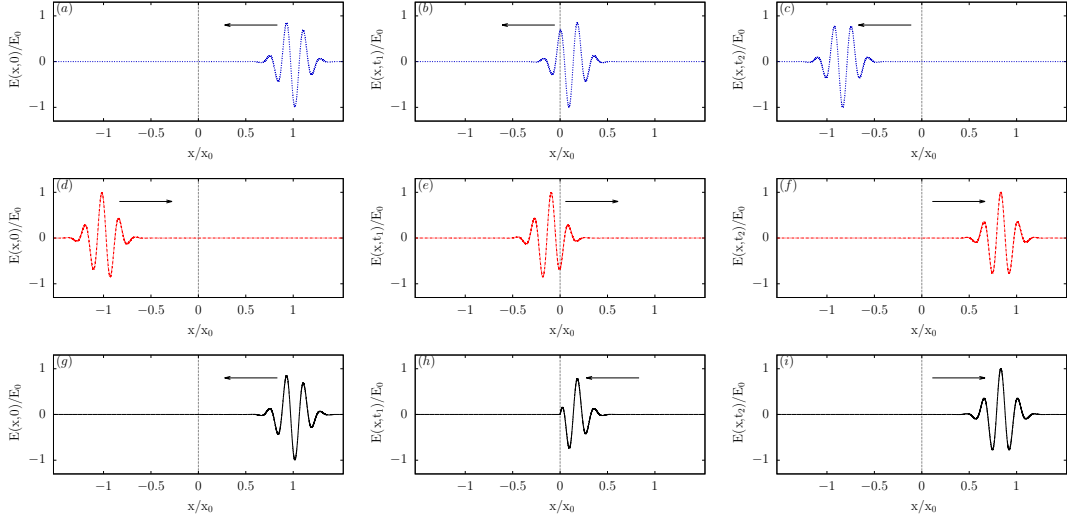
Figure 5.2: Plots (a)–(c) show a left-travelling Gaussian wave packet with $E_{\text{free}}(x,0) = E_0\, \mathrm{e}^{-(x-x_0)^2/2\sigma^2}\, \mathrm{e}^{\mathrm{i}k_0 x} + \text{c.c.}$ where E_0 and x_0 are free parameters and where $k_0 x_0 = -6$, $\sigma = \left(1/\sqrt{2}\right) x_0$, $t_1 = 0.89 x_0/c$ and $t_2 = 1.83 x_0/c$. Moreover, plots (d)–(f) show a right-travelling Gaussian wave packet. At $t = 0$, the blue wave packet ((a)–(c)) can be interpreted as a real wave packet, while the red wave packet ((d)–(f)) constitutes its mirror image. When the wave packets cross over at $x = 0$, the red wave packet becomes real, while the blue one becomes the image. Moreover, plots (g)–(i) show the sum of the red and the blue electric field contribution on the right side of the mirror, which evolves like a wave packet approaching a perfectly reflecting mirror.

5.2.3 Two-sided semi-transparent mirror

Next, let us examine what happens when wave packets, which travel along the x-axis, approach a semi-transparent mirror from both sides. This scenario is more complicated to model as semi-transparent mirrors do not impose such strict boundary conditions, unlike the perfect mirror. Therefore, for all times t, the condition in Eq. (5.3) is not satisfied.

As illustrated in Fig. 5.1, we denote the (real) transmission and reflection rates of the mirror by t_a, t_b, r_a and r_b, respectively. Assuming that the mirror only affects the amplitudes but not the coherence properties of incoming wave packets, we can again write the electric field amplitude $E_{\text{mirr}}(x,t)$ as a sum of

free-space solutions,

$$
\begin{aligned}
E_{\mathrm{mirr}}(x,t) &= \left[E_{\mathrm{free}}^{(a)}(x,t) + r_a\, E_{\mathrm{free}}^{(a)}(-x,t,\varphi_1) + t_b\, E_{\mathrm{free}}^{(b)}(x,t,\varphi_2) \right] \Theta(x) \\
&\quad + \left[E_{\mathrm{free}}^{(b)}(x,t) + r_b\, E_{\mathrm{free}}^{(b)}(-x,t,\varphi_3) + t_a\, E_{\mathrm{free}}^{(a)}(x,t,\varphi_4) \right] \Theta(-x)\,,
\end{aligned}
\tag{5.9}
$$

where each term is weighted with its respective rate. Again, one requires superscripts to distinguish electric field contributions which originate from different sides of the mirror. As before, the superscripts (a) and (b) are chosen such that, at $t = 0$,

$$
\begin{aligned}
E_{\mathrm{free}}^{(a)}(x,0) &= E_{\mathrm{mirr}}(x,0)\,\Theta(x)\,, \\
E_{\mathrm{free}}^{(b)}(x,0) &= E_{\mathrm{mirr}}(x,0)\,\Theta(-x)\,.
\end{aligned}
\tag{5.10}
$$

Moreover, $E_{\mathrm{free}}^{(s)}(x,t,\varphi)$ is defined such that its amplitude differs from $E_{\mathrm{free}}^{(s)}(x,t)$ only by a phase shift φ, where $s = a,b$. Unfortunately, Eq. (5.9) applies only for positive times t. For $t < 0$, the weighting of the individual electric field contributions becomes incorrect. When evolving a wave packet backwards in time, its amplitude should increases whenever it passes through the mirror surface, however, the rates in Eq. (5.9) are all smaller than unity (cf. Eq. (5.2)).

The expression in Eq. (5.9) solves Maxwell's equations, since it is again a superposition of free-field solutions. It also produces the expected long-term dynamics for the scattering of incoming wave packets through a two-sided semi-transparent mirror. However, $E_{\mathrm{mirr}}(x,t)$ no longer satisfies the boundary condition in Eq. (5.3). A physical explanation of this is that semi-transparent mirrors do not have enough surface charges to compensate all electric field amplitudes. To ensure that maximum interference of the electric field on one side of the mirror implies minimum interference on the other, one assumes that

$$
\varphi_1 - \varphi_2 + \varphi_3 - \varphi_4 = \pm(2n+1)\,\pi\,,
\tag{5.11}
$$

where n is an integer (cf. App. B for more details). In addition, there are another two constraints placed on the phase factors such that

$$
\begin{aligned}
\varphi_1 - \varphi_4 &= \pm\frac{\pi}{2}\,, \\
\varphi_3 - \varphi_2 &= \pm\frac{\pi}{2}\,.
\end{aligned}
\tag{5.12}
$$

These conditions only apply to lossless semi-transparent mirrors [113, 114] and are required to ensure energy conversation between transmitted and reflected wave packets.

Looking closer at Eq. (5.9), one can see this includes free space as a limiting case which corresponds to $r_a = r_b = 0$, $t_a = t_b = 1$ and $\varphi_1 = \varphi_2 = \varphi_3 = \varphi_4 = 0$. In addition, Eq. (5.9) reproduces the one-sided perfect mirror case (cf. Eq. (5.4)), if one chooses $r_a = r_b = 1$, $t_a = t_b = 0$ with phase factors $\varphi_1 = \varphi_3 = \pi$ and $\varphi_2 = \varphi_4 = \pi/2$. In general, three of the phase factors φ_i depend on the properties of the mirror surface but can be determined relatively easily experimentally. The remaining fourth parameter is established when the interference of wave packets originating from different sides of the mirror is first observed.

As pointed out already in Sec. 5.1, the possible absorption of light by the mirror surface is explicitly taken into account in this model. The only assumption is that absorption does not affect the shape of the incoming wave packets, it only reduces their amplitudes. Moreover, it is assumed that the reflection and transmission rates of the mirror do not depend on the frequency or angle of the incoming light[1]. For simplicity, one also ignores the existence of evanescent wave solutions of Maxwell's equations, i.e. the electromagnetic field is only considered at a certain distance away from the mirror surface [86].

5.2.4 Generalisation to three dimensions

Finally, the dynamics of the electromagnetic field near a semi-transparent mirror with light approaching the mirror at any possible angle, cf. Fig. 5.3, is analysed. Again, one assumes that the mirror does not affect the dynamics of incoming wave packets but only changes how and where the electric and magnetic field amplitudes $\mathbf{E}_{\mathrm{mirr}}(\mathbf{r}, t)$ and $\mathbf{B}_{\mathrm{mirr}}(\mathbf{r}, t)$ are detected. Suppose an electric field detector observes incoming and transmitted wave packets at a position $\mathbf{r} = (x, y, z)$. Then the detector sees the electric field amplitudes of incident and of reflected

---

[1]One can make the transmission and reflection rates functions of frequency and also factor in the angle of the incident light, however, this would make master equations calculations highly non-trivial, particularly solving the necessary integrals. Therefore, monochromatic light is assumed throughout this model.

wave packets which are equal to the electric field amplitudes of freely-propagating wave packets at a position $\widetilde{\mathbf{r}}$ with

$$\widetilde{\mathbf{r}} = (-x, y, z). \tag{5.13}$$

The latter contributions need to be multiplied by their respective transmission and reflection rates. Moreover, parallel electric field amplitudes need to be multiplied with a factor -1 upon reflection, as illustrated in Fig. 5.3.
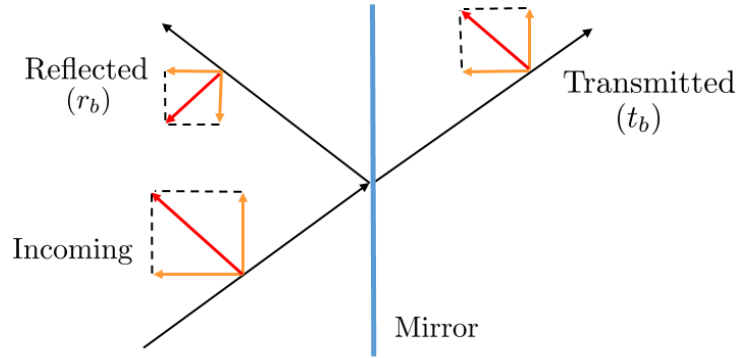
Figure 5.3: Schematic view of a semi-transparent mirror with light incident from the left. The red lines indicate the direction of the wave vector of the incoming light, while the perpendicular orange vectors indicate electric field amplitudes. To predict the effect of the mirror, the electric field amplitudes of incoming wave packets are decomposed into parallel and perpendicular components with respect to the mirror surface. As illustrated, transmission and reflection reduces these components by a factor which equals the corresponding transmission and reflection rate. Notice that these rates have to be the same for parallel and perpendicular field amplitudes. Otherwise, the electric field vector would not remain orthogonal to the corresponding wave vector $\mathbf{k}$. However, parallel electric field components obtain a minus sign upon reflection due to the rearrangement of mirror surface charges.

Taking this into account, placing the mirror again into the $x = 0$ plane, one now finds that the electric field $\mathbf{E}_{\mathrm{mirr}}(\mathbf{r}, t)$ is the sum of six contributions,

$$
\begin{aligned}
\mathbf{E}_{\mathrm{mirr}}(\mathbf{r}, t) &= \left[\mathbf{E}_{\mathrm{free}}^{(a)}(\mathbf{r}, t) + r_a \, \widetilde{\mathbf{E}}_{\mathrm{free}}^{(a)}(\widetilde{\mathbf{r}}, t, \varphi_1) + t_b \, \mathbf{E}_{\mathrm{free}}^{(b)}(\mathbf{r}, t, \varphi_2) \right] \Theta(x) \\
&\quad + \left[\mathbf{E}_{\mathrm{free}}^{(b)}(\mathbf{r}, t) \, \Theta(-x) + r_b \, \widetilde{\mathbf{E}}_{\mathrm{free}}^{(b)}(\widetilde{\mathbf{r}}, t, \varphi_3) + t_a \, \mathbf{E}_{\mathrm{free}}^{(a)}(\mathbf{r}, t, \varphi_4) \right] \Theta(-x) ,
\end{aligned}
$$

$$(5.14)$$

where x refers to the x-component of $\mathbf{r}$. Here $\mathbf{E}_{\mathrm{free}}^{(s)}(\mathbf{r}, t)$ denotes an electric field free-space solution of Maxwell's equations, where $s = a, b$. Moreover, $\widetilde{\mathbf{E}}_{\mathrm{free}}^{(s)}(\mathbf{r}, t)$ is defined such that it differs from $\mathbf{E}_{\mathrm{free}}^{(s)}(\mathbf{r}, t)$ only by the sign of the x-component. The superscripts (a) and (b) help again to distinguish initial electric field contributions on the left- and on the right-side of the mirror and the phase factors φ_i indicate shifts of electric field amplitudes in agreement with the discussion in the previous subsection. Notice that the same transmission and reflection rates need to apply to vertical and horizontal electric field components. Otherwise, one would obtain electric field vectors which are no longer orthogonal to their wave vectors $\mathbf{k}$[1].

5.3 Quantum physics

In the previous section, the scattering of light through a two-sided semi-transparent mirror onto an analogous free-space scenario with both real and mirror-image detectors, using classical physics. In this section, the classical model is used as an analogy to quantise the electromagnetic field in the presence of a two-sided semi-transparent mirror. In the following, expression for the system Hamiltonian $\hat{H}_{\mathrm{sys}}$ (cf. Eq. (5.1)) as well as the electric and magnetic field observables $\hat{\mathbf{E}}_{\mathrm{mirr}}(\mathbf{r})$ and $\hat{\mathbf{B}}_{\mathrm{mirr}}(\mathbf{r})$ as a function of the transmission and reflection rates of the mirror are presented.

---

[1]Treating the problem in this way could potentially allow one to build refraction into this model.

5.3.1 One-sided perfect mirror

As before, the starting point is to consider a one-sided perfect mirror which is placed in the $x = 0$ plane with light incident from the right-hand side of the setup, as in Fig. 5.2 (a) – (c). From experimental observation, it is known that a photon of frequency ω has the associated energy $\hbar\omega$, even in the presence of a mirror. Hence, when using the same notion of photons as in free space, one finds that the system Hamiltonian $\hat{H}_{\mathrm{sys}}$ in the presence of a perfect mirror must be the same as the free space Hamiltonian $\hat{H}_{\mathrm{sys}}$ in Eq. (2.61). Moreover, as demonstrated previously, wave packets evolve essentially as in free space, even in the presence of mirrors. What changes is how and where electromagnetic field amplitudes are measured. These are now the sum of the field amplitudes seen by original detectors and the field amplitudes seen by mirror-image detectors in the corresponding free-space scenario. Taking this into account, Eq. (5.4) suggests that

$$
\begin{aligned}
\hat{E}_{\mathrm{mirr}}(x) &= \frac{1}{\eta}\left[\hat{E}_{\mathrm{free}}(x) - \hat{E}_{\mathrm{free}}(-x)\right]\Theta(x)\,, \\
\hat{B}_{\mathrm{mirr}}(x) &= \frac{1}{\eta}\left[\hat{B}_{\mathrm{free}}(x) + \hat{B}_{\mathrm{free}}(-x)\right]\Theta(x)\,,
\end{aligned}
\tag{5.15}
$$

with $\hat{E}_{\mathrm{free}}(x)$ and $\hat{B}_{\mathrm{free}}(x)$ given in Eq. (2.74) and with η denoting a normalisation factor. As it will be demonstrated later, a perfect mirror has

$$
\eta = \sqrt{2}\,.
\tag{5.16}
$$

To show that this is the case, a radiating atom placed near a perfectly reflecting mirror is examined (see Chapter 6).

Taking this into account, introducing standing-wave photon annihilation operators ξ_k,

$$
\hat{\xi}_k = \frac{1}{\sqrt{2}}\left(\hat{a}_k - \hat{a}_{-k}\right) \quad \text{with} \quad \hat{\xi}_{-k} = -\hat{\xi}_k\,,
\tag{5.17}
$$

and combining Eqs. (2.74) and (5.15), the field operators $\hat{E}_{\mathrm{mirr}}(x)$ and $\hat{B}_{\mathrm{mirr}}(x)$ simplify to

$$
\begin{aligned}
\hat{E}_{\mathrm{mirr}}(x) &= \mathrm{i}\int_{-\infty}^{\infty}\mathrm{d}k\,\sqrt{\frac{\hbar\omega}{4\pi\varepsilon_0 A}}\,\mathrm{e}^{\mathrm{i}kx}\,\hat{\xi}_k\,\Theta(x) + \mathrm{H.c.}\,, \\
\hat{B}_{\mathrm{mirr}}(x) &= \mp\mathrm{i}\sqrt{\varepsilon_0\mu_0}\int_{-\infty}^{\infty}\mathrm{d}k\,\sqrt{\frac{\hbar\omega}{4\pi\varepsilon_0 A}}\,\mathrm{e}^{\mathrm{i}kx}\,\hat{\xi}_k\,\mathrm{sign}(k)\,\Theta(x) + \mathrm{H.c.}\,,
\end{aligned}
\tag{5.18}
$$

with the sign of the magnetic field depending on the polarisation of the field. Moreover, it is known that the energy of the electromagnetic field on the right-hand side of the mirror equals

$$\hat{H}_{\text{field}} \quad = \quad \sum_{\lambda=1,2} \frac{1}{2} A \int_0^\infty \mathrm{d}x \left[\varepsilon_0 \, \hat{E}_{\text{mirr}}(x)^2 + \frac{1}{\mu_0} \, \hat{B}_{\text{mirr}}(x)^2 \right]. \tag{5.19}$$

Proceeding as described in App. C, one finds that

$$\hat{H}_{\text{field}} \quad = \quad \int_0^\infty \mathrm{d}k \, \hbar\omega \, \hat{\xi}_k^\dagger \hat{\xi}_k \tag{5.20}$$

up to a constant. One can easily check that this field Hamiltonian commutes with $\hat{H}_{\text{sys}}$ and that its expectation values are conserved.

However, notice that $\hat{H}_{\text{sys}}$ and $\hat{H}_{\text{field}}$ are no longer the same. For example, suppose a wave packet approaches the mirror from the right. In this case, exactly half of the population of the electromagnetic field is in the antisymmetric $\hat{\xi}_k$ modes. All other population is in orthogonal (symmetric) modes and

$$\langle \hat{H}_{\text{field}} \rangle \quad = \quad \frac{1}{2} \langle \hat{H}_{\text{sys}} \rangle . \tag{5.21}$$

Only half of the energy of the system is stored in the electromagnetic field in this case. The other half belongs to the mirror image of the incoming wave packet. As illustrated in Fig. 5.2, the mirror scenario is indeed equivalent to having two wave packets travelling in opposite directions in free space. The difference between $\hat{H}_{\text{sys}}$ and $\hat{H}_{\text{field}}$ is the observable $\hat{H}_{\text{mirr}}$ for the energy of the mirror surface charges, cf. Eq. (5.1).

Previous quantisation schemes for the electromagnetic field in front of a perfect mirror do not account for the energy of the mirror surface (see e.g. Refs. [115–120]). Nevertheless, they are consistent with this approach. If one considers the scenario where a wave packet approaches a one-sided perfect mirror from the right, as illustrated in Fig. 5.2 (a)–(c), then one can extend the initial state to the left-side of the setup ($x < 0$), as only the electromagnetic field on the right-side of the mirror ($x > 0$) is of interest. By doing so, one introduces the *mirror-image* shown in Fig. 5.2 (d)–(f), which is equivalent to having an initial state with population only in the $\hat{\xi}_k$ modes. For these modes, the field observables $\hat{H}_{\text{sys}}$, $\hat{E}_{\text{mirr}}(x)$ and

$\hat{B}_{\mathrm{mirr}}(x)$ are exactly the same as in free space. However, this approach does not restrict the Hilbert space of the electromagnetic field to a subset of possible initial states. This means it is possible to model a mirror scenario where light is incident from both sides of the mirror.

5.3.2 Two-sided perfect mirror

As pointed out in Subsection 5.2.2, wave packets approaching a perfectly-reflecting two-sided mirror from different sides never meet. Therefore, in order to quantise the electromagnetic field, one can treat each side of the mirror separately. This requires dividing the overall Hilbert space $\mathcal{H}$ into the tensor product of two free-space Hilbert spaces $\mathcal{H}^{(a)}$ and $\mathcal{H}^{(b)}$, such that

$$\mathcal{H} \quad \rightarrow \quad \mathcal{H}^{(a)} \otimes \mathcal{H}^{(b)} \,. \tag{5.22}$$

Denoting the annihilation operators for photons on different sides by $\hat{a}_k$ and $\hat{b}_k$, respectively, the system Hamiltonian $\hat{H}_{\mathrm{sys}}$ of the mirror surfaces and the electromagnetic fields equals

$$\hat{H}_{\mathrm{sys}} \;\; = \;\; \int_{-\infty}^{\infty} \mathrm{d}k \, \hbar\omega \left[\hat{a}_k^\dagger \hat{a}_k + \hat{b}_k^\dagger \hat{b}_k \right] \,. \tag{5.23}$$

Moreover, in analogy to Eq. (5.15), one finds that the electric field observable $\hat{E}_{\mathrm{mirr}}(x)$ in front of a two-sided perfect mirror is equal to

$$\begin{aligned}
\hat{E}_{\mathrm{mirr}}(x) \;\; = \;\; & \frac{1}{\sqrt{2}} \left[\hat{E}_{\mathrm{free}}^{(a)}(x) - \hat{E}_{\mathrm{free}}^{(a)}(-x) \right] \Theta(x) \\
& + \frac{1}{\sqrt{2}} \left[\hat{E}_{\mathrm{free}}^{(b)}(x) - \hat{E}_{\mathrm{free}}^{(b)}(-x) \right] \Theta(-x) \,,
\end{aligned} \tag{5.24}$$

where $\hat{E}_{\mathrm{free}}^{(a)}(x)$ and $\hat{E}_{\mathrm{free}}^{(b)}(x)$ are electric field free space observables. As before, superscripts indicate whether the respective field contribution initially belongs in the right- or left-half space, respectively.

5.3.3 Two-sided semi-transparent mirror

From 5.2.4, the dynamics of wave packets which approach a semi-transparent mirror from both sides depends on whether they originate from the left or from

the right side. As above, the Hilbert space $\mathcal{H}$ becomes a tensor product of two free-space Hilbert spaces $\mathcal{H}^{(a)}$ and $\mathcal{H}^{(b)}$ as in Eq. (5.22).

Considering only light travelling along the x-axis and denoting the corresponding photon annihilation operators belonging to $\mathcal{H}^{(a)}$ and $\mathcal{H}^{(b)}$ by $\hat{a}_k$ and $\hat{b}_k$, respectively, then in analogy to Eq. (5.23), one finds that the system Hamiltonian $\hat{H}_{\text{sys}}$ describing the mirror surfaces and the surrounding electromagnetic fields is again given by Eq. (5.23). As before, the superscripts (a) and (b) indicate contributions which originate from the right and the left half space of the mirror, respectively.

Moreover, Eq. (5.9) suggests that the observable $\hat{E}_{\text{mirr}}(x)$ of the electric field near a semi-transparent mirror is a superposition of free-space observables,

$$
\begin{aligned}
\hat{E}_{\text{mirr}}(x) &= \frac{1}{\eta_a}\left[\hat{E}_{\text{free}}^{(a)}(x) + \frac{r_a}{\eta_a}\hat{E}_{\text{free}}^{(a)}(-x,\varphi_1) + \frac{t_b}{\eta_b}\hat{E}_{\text{free}}^{(b)}(x,\varphi_2)\right]\Theta(x) \\
&\quad + \frac{1}{\eta_b}\left[\hat{E}_{\text{free}}^{(b)}(x) + \frac{r_b}{\eta_b}\hat{E}_{\text{free}}^{(b)}(-x,\varphi_3) + \frac{t_a}{\eta_a}\hat{E}_{\text{free}}^{(a)}(x,\varphi_4)\right]\Theta(-x). \quad (5.25)
\end{aligned}
$$

The additional argument in $\hat{E}_{\text{free}}^{(s)}(x,\varphi)$ indicates a φ phase shift of the electric amplitude with respect to the field amplitude of $\hat{E}_{\text{free}}^{(s)}(x)$. Moreover, the constants η_a and η_b are normalisation factors. To determine them one needs to specify not only transmission and reflection rates but also the type of medium on either side of the semi-transparent mirror. Again, this will be done later when looking at the spontaneous emission of an atom placed near the mirror.

As in classical physics, the expectation value of $\hat{E}_{\text{mirr}}(x)$ no longer always vanishes at $x = 0$ and the transmission of light through a semi-transparent mirror surface can result in the exchange of energy between the electromagnetic field and mirror. Only the energy of the electromagnetic field and the mirror surface, i.e. the expectation value of the system Hamiltonian $\hat{H}_{\text{sys}}$ in Eq. (5.23), is conserved. However, the expectation value of the electromagnetic field Hamiltonian $\hat{H}_{\text{field}}$ can change in time. In general, there is a continuous exchange of energy between the electromagnetic field and the mirror surface. For example, suppose a wave packet approaches the mirror from the right. After a sufficiently long time, this wave packet turns into two wave packets: one on the left and one on the right side of the mirror. This implies a reduction of the energy stored inside the electromagnetic field by a factor which can be smaller than one (cf. Eq. (5.2)).

5.3.4 Generalisation to three dimensions

To model a two-sided semi-transparent mirror in the $x = 0$ plane, one again doubles the Hilbert space compared to the free-space description. Denoting the corresponding photon annihilation operators by $\hat{a}_{\mathbf{k}\lambda}$ and $\hat{b}_{\mathbf{k}\lambda}$, respectively, the system Hamiltonian $\hat{H}_{\text{sys}}$ of the electromagnetic field and the mirror surface equals

$$\hat{H}_{\text{sys}} \;=\; \sum_{\lambda=1,2} \int_{\mathbb{R}^3} \mathrm{d}^3\mathbf{k}\,\hbar\omega \left[\hat{a}^{\dagger}_{\mathbf{k}\lambda}\hat{a}_{\mathbf{k}\lambda} + \hat{b}^{\dagger}_{\mathbf{k}\lambda}\hat{b}_{\mathbf{k}\lambda} \right] , \tag{5.26}$$

in analogy to Eq. (5.23). To obtain the observable $\hat{\mathbf{E}}_{\text{mirr}}(\mathbf{r})$ of the electric field at position $\mathbf{r}$, one makes use of the previously introduced quantum 'image detector method'. Again, it is assumed that wave packets evolve as in free space but that an electric field detector at position $\mathbf{r}$ observes electric field contributions of incoming, transmitted and reflected wave packets. Reflection changes the sign of the y-and the z-component of the electric field of incoming wave packets, while their x-component remains unaffected. Hence

$$\begin{aligned}
\hat{\mathbf{E}}_{\text{mirr}}(\mathbf{r}) \;=\;& \frac{1}{\eta_a} \left[\hat{\mathbf{E}}^{(a)}_{\text{free}}(\mathbf{r}) + \frac{r_a}{\eta_a} \widetilde{\hat{\mathbf{E}}}^{(a)}_{\text{free}}(\widetilde{\mathbf{r}}, \varphi_1) + \frac{t_b}{\eta_b} \hat{\mathbf{E}}^{(b)}_{\text{free}}(\mathbf{r}, \varphi_2) \right] \Theta(x) \\
&+ \frac{1}{\eta_b} \left[\hat{\mathbf{E}}^{(b)}_{\text{free}}(\mathbf{r}) + \frac{r_b}{\eta_b} \widetilde{\hat{\mathbf{E}}}^{(b)}_{\text{free}}(\widetilde{\mathbf{r}}, \varphi_3) + \frac{t_a}{\eta_a} \hat{\mathbf{E}}^{(a)}_{\text{free}}(\mathbf{r}, \varphi_4) \right] \Theta(-x) ,
\end{aligned} \tag{5.27}$$

in analogy to Eq. (5.14). The definition of $\widetilde{\mathbf{r}}$ can be found in Eq. (5.13) and $\widetilde{\hat{\mathbf{E}}}^{(s)}_{\text{free}}(\mathbf{r})$ differs from $\hat{\mathbf{E}}^{(s)}_{\text{free}}(\mathbf{r})$ only by the sign of its x-component, where $s = a, b$. The argument in $\Theta(x)$ refers again to the x-component of $\mathbf{r}$ and the factors η_a and η_b are again normalisation factors.

5.4 Conclusions

The main result of this chapter is the quantisation of the electromagnetic field in the presence of a semi-transparent mirror. Using an 'image-detector' method allowed expressions for the system Hamiltonian $\hat{H}_{\text{sys}}$ (describes the field and mirror) and for the electric field observable $\hat{\mathbf{E}}_{\text{mirr}}(\mathbf{r})$ (cf. Eqs. (5.26) and (5.27) with η_a and η_b as in Eq. (6.12)) to be derived. In contrast to $\hat{H}_{\text{sys}}$, which is independent of the transmission and reflection rates t_a, t_b, r_a and r_b of the mirror, the electric

field observable $\hat{\mathbf{E}}_{\mathrm{mirr}}(\mathbf{r})$ depends strongly on these rates. As it is assumed that wave packets remain coherent after interacting with the mirror, then the possible absorption of light in the mirror surface is explicitly taken into account, since the squares of the absorption and transmission coefficients, i.e. $r_a^2 + t_a^2$ and $r_b^2 + t_b^2$, do not have to add up to one for this model to work. However, it is assumed that the reflection and the transmission rates of the mirror do not depend on the frequency and the angle of the incoming light.

Before quantising the electromagnetic field, classical electrodynamics is used to discuss the scattering of light on flat surfaces. Throughout this section the scattering process is mapped onto an analogous free space scenario. The presence of the mirror changes how and where the amplitudes of the electromagnetic field are measured. Adopting this point of view when deriving the observables of the quantised electromagnetic field in the presence of a two-sided semi-transparent mirror, it is found that the system Hamiltonian $\hat{H}_{\mathrm{sys}}$ is the sum of two free-space field Hamiltonians $\hat{H}_{\mathrm{free}}$. Moreover, $\hat{\mathbf{E}}_{\mathrm{mirr}}(\mathbf{r})$ is now a sum of electric field free-space observables which can be associated with incoming, reflected and transmitted waves. These contributions are properly normalised through the normalisation factors η_a and η_b. In addition, phase factors need to be introduced such that maximum interference on one side of the mirror implies minimum interference on the other. Our field observables have some similarities with previously proposed observables [86–91] but can be used to model not only one-sided but two-sided semi-transparent mirrors.

Another difference between this field quantisation scheme and the schemes of other authors is that the energy of the mirror surface, i.e. the energy of the mirror images, is explicitly taken into account. For example, when placing a single wave packet in front of a one-sided perfect mirror, half of the energy of the system belongs to the original wave packet and the other half belongs to its mirror image and is stored in mirror surface charges. In general, there is a difference between the system Hamiltonian $\hat{H}_{\mathrm{sys}}$ and the Hamiltonian $\hat{H}_{\mathrm{field}}$ of the electromagnetic field surrounding the semi-transparent mirror. Energy can flow from the field onto the mirror surface and back. In the case of absorption, the interaction with the mirror surface reduces the energy of incoming wave packets without changing their coherence properties.

Part III

Applications

Chapter 6

Radiating atom in the presence of a two-sided semi-transparent mirror

The spontaneous photon emission of atoms in the presence of perfect mirrors has been extensively studied in the literature [115–125]. When considering this problem, boundary conditions of vanishing electric field amplitudes along the mirror surface must be imposed. This is usually done by reducing the state space of the electromagnetic field to a subset of photon modes. As a result, the spontaneous decay rate Γ_{mirr} of an atom in front of a perfect mirror differs strongly from its free-space decay rate Γ_{free} in Eq. (3.62), when the distance x of the atom from the mirror surface is of the same order of magnitude as the wavelength λ_0 of the emitted light. Although the effect of the mirror is relatively short-range, the sub- and super-radiance of atomic systems near perfect mirrors has already been verified experimentally [126–128].

In this chapter, the well-understood problem of a radiating atom in the presence of a perfect mirror is used in order to test the validity of the model presented in Chapter 5. In this description, the spontaneous emission rate Γ_{mirr} and atomic level shift Δ_{mirr} of an atom at a fixed distance x from a semi-transparent mirror as a function of its transmission and reflection rates are deterined, through the image-detector method. In the following, it is assumed that the atom-mirror distance does not become so large that delay terms have to be taken into account

[119]. In addition, it should not be too short in order to avoid the interaction of the system with evanescent field modes. The only other assumptions made in this section are standard quantum optical approximations which were introduced in the theoretical background (see Chapters 2 and 3).

As one would expect, it is shown that a radiating atom near a perfect mirror has the same effect as the dipole-dipole interaction between an atom and a mirror atom [70]. In the limit of relatively large atom-mirror distances x, the spontaneous emission rate Γ_{mirr} of the atom coincides with its free-space emission rate Γ_{free} in Eq. (3.62). Imposing this as a condition allows one to calculate the normalisation factors η_a and η_b in Eq. (5.27) as a function of the reflection and transmission rates of the two-sided semi-transparent mirror. The validity of this model is then confirmed by reproducing known results for a radiating atom in the presence of a perfect mirror as well as obtaining describing previously unknown results for a radiating atom in the presence of a two-sided semi-transparent mirror.

6.1 Master equation for an atom near a two-sided mirror

In this section, a master equation description of an atom radiating in the presence of a two-sided semi-transparent mirror using the quantum image-detector method outlined in Chapter 5 as well as the procedures outlined in Chapter 3.

6.1.1 The relevant Hamiltonians

As before, the starting point is to identify the relevant Hamiltonians. In analogy to Eq. (3.4), there are contributions from the atom, the field and the interaction between the two. This gives the following Hamiltonian

$$\hat{H} \;\; = \;\; \hat{H}_{\mathrm{atom}} + \hat{H}_{\mathrm{sys}} + \hat{H}_{\mathrm{SB}} \,. \tag{6.1}$$

Supposing $|1\rangle$ denotes the ground state of the atom and $|2\rangle$ is its excited state with energy $\hbar\omega_0$, then the form of the atom Hamiltonian $\hat{H}_{\mathrm{atom}}$ is given in Eq. (3.28). The system Hamiltonian $\hat{H}_{\mathrm{sys}}$ for the electromagnetic field and the

semi-transparent mirror can be found in Eq. (5.26). Moreover, in analogy to Eq. (3.31), the atom-field interaction Hamiltonian $\hat{H}_{\mathrm{SB}}$ equals

$$\hat{H}_{\mathrm{SB}} \;=\; \hat{\mathbf{D}} \cdot \hat{\mathbf{E}}_{\mathrm{mirr}}(\mathbf{r})\,, \tag{6.2}$$

where instead of the free electric field $\hat{\mathbf{E}}_{\mathrm{free}}(\mathbf{r})$, the atom now couples to a slightly different electric field $\hat{\mathbf{E}}_{\mathrm{mirr}}(\mathbf{r})$ due to the presence of the mirror. The form of the semi-transparent mirror electric field observable $\hat{\mathbf{E}}_{\mathrm{mirr}}(\mathbf{r})$ can be found in Eq. (5.27). Here, $\hat{\mathbf{D}}$ represents the complex atomic dipole moment and is defined in Eq. (3.34). As before, one moves into the interaction picture with respect to the free Hamiltonian $\hat{H}_0 = \hat{H}_{\mathrm{atom}} + \hat{H}_{\mathrm{sys}}$ and exploits Eqs. (3.7), (3.39) and the rotating wave approximation. This yields the interaction Hamiltonian

$$
\begin{aligned}
\hat{H}_{\mathrm{SB\,I}}(t) \;=\; & \frac{\mathrm{i}e}{4\pi} \sum_{\lambda=1,2} \int_{\mathbb{R}^3} \mathrm{d}^3\mathbf{k} \, \sqrt{\frac{\hbar\omega}{\pi\varepsilon}} \, \mathrm{e}^{-\mathrm{i}(\omega-\omega_0)t} \\
& \times \Bigg[\left(\hat{\mathbf{D}}_{12}^* \cdot \hat{\mathbf{e}}_{\mathbf{k}\lambda} \right) \mathrm{e}^{\mathrm{i}\mathbf{k}\cdot\mathbf{r}} \left(\frac{1}{\eta_a} \, \hat{a}_{\mathbf{k}\lambda} + \frac{t_b \mathrm{e}^{\mathrm{i}\varphi_2}}{\eta_b} \, \hat{b}_{\mathbf{k}\lambda} \right) \\
& \qquad\qquad + \left(\hat{\tilde{\mathbf{D}}}_{12}^* \cdot \hat{\mathbf{e}}_{\mathbf{k}\lambda} \right) \mathrm{e}^{\mathrm{i}\mathbf{k}\cdot\tilde{\mathbf{r}}} \, \frac{r_a \mathrm{e}^{\mathrm{i}\varphi_1}}{\eta_a} \, \hat{a}_{\mathbf{k}\lambda} \Bigg] \hat{\sigma}^+ + \mathrm{H.c.}
\end{aligned}
\tag{6.3}
$$

As a specific example, when determining the master equation the interaction Hamiltonian will be expressed using the phases,

$$\varphi_1 = \pi \quad \text{and} \quad \varphi_2 = \frac{\pi}{2}\,. \tag{6.4}$$

In this way, the model contains the free-space and the one-sided perfect mirror scenario as limiting cases. However, in general, φ_1 and φ_2 might be different from the above choice and depend on the optical properties of the mirror surface. Moreover, the atomic dipole moment $\hat{\tilde{\mathbf{D}}}_{12}$ is defined such that it differs from $\hat{\mathbf{D}}_{12}$ only by the sign of its x-component (cf. Eq. (D.2)).

6.1.2   Master equation

The next step is to make use of the quantum jump approach outlined in Sec. 3.2.3. One must substitute the expression for the interaction picture Hamiltonian $\hat{H}_{\mathrm{SB\,I}}(t)$

from Eq. (6.3) into the expressions for the conditional Hamiltonian $\hat{H}_{\mathrm{cond\,I}}(t)$ and the reset operator $\mathcal{L}(\hat{\rho}_{\mathrm{S\,I}}(t))$, which are given in Eqs. (3.25) and (3.26), respectively. Again, in the case of an environment that monitors the spontaneous emission of photons, the non-Hermitian Hamiltonian $\hat{H}_{\mathrm{cond\,I}}(t)$ describes the time evolution of the atom under the condition of no photon emission, while the reset operator $\mathcal{L}(\hat{\rho}_{\mathrm{S\,I}}(t))$ denotes the un-normalised state of the atom in the case of an emission at t [48].

Substituting in the interaction picture Hamiltonian $\hat{H}_{\mathrm{I}}(t)$ from Eq. (6.3) and proceeding as described in App. D whilst using standard quantum optical approximations to evaluate integrals, one obtains

$$
\begin{aligned}
\hat{H}_{\mathrm{cond\,I}}(t) &= \hbar\left(\Delta_{\mathrm{mirr}} - \frac{\mathrm{i}}{2}\,\Gamma_{\mathrm{mirr}}\right)\hat{\sigma}^+\hat{\sigma}^-\,, \\
\mathcal{L}(\hat{\rho}_{\mathrm{S\,I}}(t)) &= \Gamma_{\mathrm{mirr}}\,\hat{\sigma}^-\,\hat{\rho}_{\mathrm{S\,I}}(t)\,\hat{\sigma}^+
\end{aligned}
\tag{6.5}
$$

As a final step, one can ignore the level shift Δ_{mirr} and substitute the expressions from Eq. (6.5) into the quantum jump expression for the master equation given in Eq. (3.24). Doing so, generates the following master equation for the atom-mirror configuration,

$$
\dot{\rho}_{\mathrm{S\,I}}(t) = \Gamma_{\mathrm{mirr}}\left(\hat{\sigma}^-\hat{\rho}_{\mathrm{S\,I}}(t)\hat{\sigma}^+ - \frac{1}{2}\left[\hat{\sigma}^+\hat{\sigma}^-,\hat{\rho}_{\mathrm{S\,I}}(t)\right]_+\right).
\tag{6.6}
$$

The master equation in Eq. (6.6) takes the same form as Eq. (3.2), however, the form of the spontaneous emission rate and atomic level shift (cf. Sec. 6.1.3) differ strongly from the free-space results (cf. Sec. 3.3) due to the presence of the mirror.

6.1.3   Spontaneous emission rate and atomic level shift

The spontaneous emission rate and the atomic level shift are denoted by Γ_{mirr} and Δ_{mirr}, respectively. The mirror alters the spontaneous emission rate of an atom near a semi-transparent mirror and causes a level shift of the excited atomic state $|2\rangle$. The expressions for these differ strongly from the free-space results presented in Sec. 3.3 due to the presence of the mirror. The atom now couples to a different field, as the surface effectively changes the electromagnetic environment.

Following the steps outlined in App. D, one finds that

$$
\begin{aligned}
\Gamma_{\mathrm{mirr}} &= \left[\frac{1 + r_a^2}{\eta_a^2} + \frac{t_b^2}{\eta_b^2} \right] \Gamma_{\mathrm{free}} \\
&\quad - \frac{3 r_a}{\eta_a^2} \left[\frac{\sin(2 k_0 x)}{2 k_0 x} (1 - \mu) + \left(\frac{\cos(2 k_0 x)}{(2 k_0 x)^2} - \frac{\sin(2 k_0 x)}{(2 k_0 x)^3} \right) (1 + \mu) \right] \Gamma_{\mathrm{free}}, \\
\Delta_{\mathrm{mirr}} &= \frac{3 r_a}{2 \eta_a^2} \left[\frac{\cos(2 k_0 x)}{2 k_0 x} (1 - \mu) - \left(\frac{\sin(2 k_0 x)}{(2 k_0 x)^2} + \frac{\cos(2 k_0 x)}{(2 k_0 x)^3} \right) (1 + \mu) \right] \Gamma_{\mathrm{free}}.
\end{aligned}
\tag{6.7}
$$

Here $k_0 = \omega_0 / c$ and the constant μ denotes the orientation of the atomic dipole moment relative to the x-axis such that,

$$
\mu = \| \hat{\mathbf{D}}_{12} \cdot \hat{\mathbf{x}} \|^2
\tag{6.8}
$$

When deriving the above level shift a self-interaction term, which is also present in free space, has been neglected. This form of this term is presented in Sec. 3.3 and it is independent of the mirror. As previously stated, the free-space level shift can be absorbed into the definition of ω_0 [49].

6.1.4 Limiting cases

To gain more intuition for the results in Eq. (6.7), let us now have a closer look at some limiting cases and concrete scenarios.

Considering an atom placed on the right-hand of the mirror setup ($x > 0$), assuming atom-mirror distances x which are much larger than the wavelength λ_0 of the emitted light, we have $k_0 x \gg 1$ and Eq. (6.7) simplify to give $\Delta_{\mathrm{mirr}} \sim 0$, while

$$
\Gamma_{\mathrm{mirr}} = \left[\frac{1 + r_a^2}{\eta_a^2} + \frac{t_b^2}{\eta_b^2} \right] \Gamma_{\mathrm{free}}.
\tag{6.9}
$$

In order to determine the normalisation factors η_a and η_b, one must assume that on both sides the mirror borders a medium with permittivity ε_0 and demand that

$$
\Gamma_{\mathrm{mirr}} = \Gamma_{\mathrm{free}} \quad \text{when } k_0 |x| \gg 1.
\tag{6.10}
$$

Analogously, one can show that the spontaneous decay rate for an atom placed on the left-hand side of the mirror ($x < 0$) is equal to

$$\Gamma_{\text{mirr}} = \left[\frac{1 + r_b^2}{\eta_b^2} + \frac{t_a^2}{\eta_a^2} \right] \Gamma_{\text{free}} , \tag{6.11}$$

when $k_0|x| \gg 1$. Following the condition outlined in Eq. (6.10), one can solve Eqs. (6.9) and (6.11) simultaneously to find that the normalisation factors η_a and η_b are in general given by

$$\eta_a^2 = \frac{(1 + r_a^2)(1 + r_b^2) - (t_a t_b)^2}{1 + r_b^2 - t_b^2} ,$$
$$\eta_b^2 = \frac{(1 + r_a^2)(1 + r_b^2) - (t_a t_b)^2}{1 + r_a^2 - t_a^2} . \tag{6.12}$$

The (real) transmission and reflection rates in these equations can be determined experimentally. From above, one can determine the normalisation factors for the case of a symmetric mirror using the energy conservation condition from Eq. (5.2). Doing so, one finds

$$\eta_a^2 = \eta_b^2 = \frac{(1 + r^2)^2 - t^4}{1 + r^2 - t^2} = 2 . \tag{6.13}$$

Perfect mirrors

Now le us consider the example of a perfect mirror, where this means maximum reflection ($r_a = r_b = 1$) and zero transmission ($t_a = t_b = 0$). Using Eq. (6.12), one finds that in this case $\eta_a = \eta_b = \sqrt{2}$, as stated in Eqs. (5.16) and (5.24). Substituting these parameters into Eq. (6.7) yields

$$\Gamma_{\text{mirr}} = \left[1 - \frac{3}{2} \left[\frac{\sin(2k_0 x)}{2k_0 x}(1 - \mu) + \left(\frac{\cos(2k_0 x)}{(2k_0 x)^2} - \frac{\sin(2k_0 x)}{(2k_0 x)^3} \right)(1 + \mu) \right] \right] \Gamma_{\text{free}} ,$$

$$\Delta_{\text{mirr}} = \frac{3}{4} \left[\frac{\cos(2k_0 x)}{(2k_0 x)}(1 - \mu) - \left(\frac{\sin(2k_0 x)}{(2k_0 x)^2} + \frac{\cos(2k_0 x)}{(2k_0 x)^3} \right)(1 + \mu) \right] \Gamma_{\text{free}} . \tag{6.14}$$

The altered spontaneous decay rate Γ_{mirr} and the level shift Δ_{mirr} can be thought of as arising from a dipole-dipole interaction between the atom and its mirror image [70]. However, as one can see from Eq. (6.3), the x-component of the atomic dipole moment of the mirror image, $\hat{\tilde{\mathbf{D}}}_{12}$, and the dipole moment $\hat{\mathbf{D}}_{12}$ of the original atom have different signs.
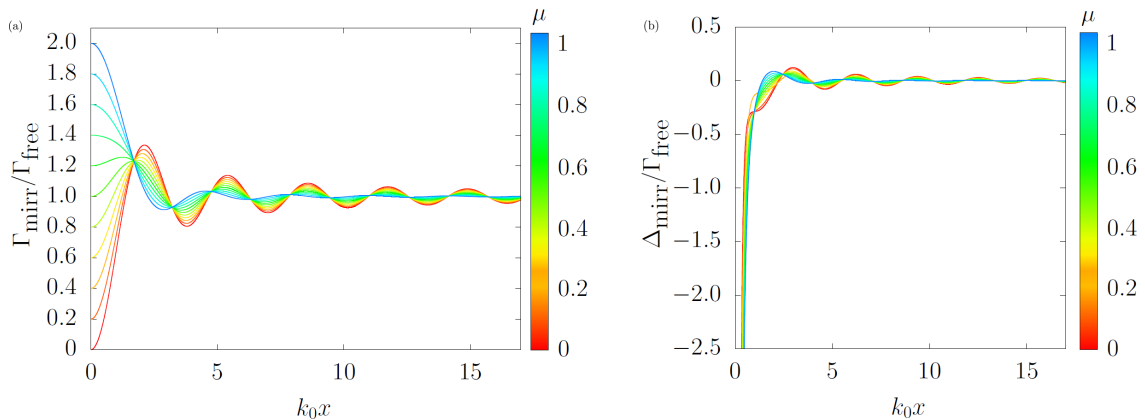
Figure 6.1: The spontaneous emission rate Γ_{mirr} (a) and the atomic level shift Δ_{mirr} (b) of an atom in front of a perfect mirror (cf. Eq. (6.14)) as a function of the atom-mirror distance x for different orientations of the atomic dipole moment $\hat{\mathbf{D}}_{12}$. For $\mu = 0$, $\hat{\mathbf{D}}_{12}$ is parallel and, for $\mu = 1$, $\hat{\mathbf{D}}_{12}$ is perpendicular to the mirror surface. In all cases, we have $\Gamma_{\text{mirr}} = 0$ while Δ_{mirr} diverges for $x = 0$ (due to Taylor expansion of Eq. (6.14)). Moreover, for $k_0 x \gg 1$, we have $\Gamma_{\text{mirr}} = \Gamma_{\text{free}}$ and $\Delta_{\text{mirr}} = 0$, as it should.

Fig. 6.1 shows the x-dependence of the spontaneous emission rate Γ_{mirr} and the level shift Δ_{mirr} of an atom in the presence of a perfect mirror for different dipole orientations μ. For distances x of the same order of magnitude as the wavelength λ_0 of the emitted light, the last terms in Eq. (6.14) are no longer negligible and Γ_{mirr} and Δ_{mirr} both depend strongly on x and μ. As one would expect, this dependence is most pronounced and most long-range when $\mu = 0$, i.e. in the case of an atomic dipole moment that is parallel to the mirror surface. In contrast to this, the decay rate Γ_{mirr} approaches Γ_{free} much more quickly when $\mu = 1$. In both cases, we have $\Gamma_{\text{mirr}} = 0$ for $x = 0$, since the electric field amplitude vanishes on the surface of a perfectly conducting mirror (cf. Eq. (5.3)).

Symmetric mirrors

The case of a symmetric mirror gives rise to transmission and reflection rates equal for both sides of the mirror,

$$t_a = t_b = t \quad \text{and} \quad r_a = r_b = r\,. \tag{6.15}$$

This results in the normalisation factors η_a and η_b from Eq. (6.12) becoming the same. In this case, one can deduce from Eq. (6.15) that $\eta_a^2 = \eta_b^2 = 2$. Substituting back into Eq. (6.7), one can show that

$$
\begin{aligned}
\Gamma_{\text{mirr}} &= \Gamma_{\text{free}} - \frac{3r}{2}\left[\frac{\sin(2k_0 x)}{2k_0 x}\left(1-\mu\right)\right.\\
&\qquad\qquad \left. + \left(\frac{\cos(2k_0 x)}{(2k_0 x)^2} - \frac{\sin(2k_0 x)}{(2k_0 x)^3}\right)(1+\mu)\right]\Gamma_{\text{free}}\,,\\
\Delta_{\text{mirr}} &= \frac{3r}{4}\left[\frac{\cos(2k_0 x)}{2k_0 x}\left(1-\mu\right)\right.\\
&\qquad\qquad \left. - \left(\frac{\sin(2k_0 x)}{(2k_0 x)^2} + \frac{\cos(2k_0 x)}{(2k_0 x)^3}\right)(1+\mu)\right]\Gamma_{\text{free}}\,. \tag{6.16}
\end{aligned}
$$

Again, Γ_{mirr} and Δ_{mirr} depend strongly on μ and r for relatively short atom-mirror distances x but tend to their respective free-space rates when x becomes much larger than λ_0. This is illustrated in Fig. 6.2 which show Γ_{mirr} and and Δ_{mirr} as a function of x for different values of r and t, while $\mu = 0$.

Highly absorbing mirrors

Finally, let us have a closer look at the example where a mirror absorbs all incoming light. This case is equivalent to a perfectly-transmitting mirror where $t_a = 1$ and $r_a = 0$, as no emitted light is reflected back towards the atom. Therefore, this yields (cf. Eq. (6.7))

$$\Gamma_{\text{mirr}} = \Gamma_{\text{free}} \quad \text{and} \quad \Delta_{\text{mirr}} = 0 \tag{6.17}$$

independent of the atom-mirror distance x and the orientation μ of the atomic dipole moment. As one would expect, an atom in the presence of an absorbing medium does not see any of the emitted light return from the surface and emits exactly as it would in free space. This is illustrated in Fig. 6.2, where the spontaneous emission rate and atomic level shift both show a flat line for $r_a = 0$.
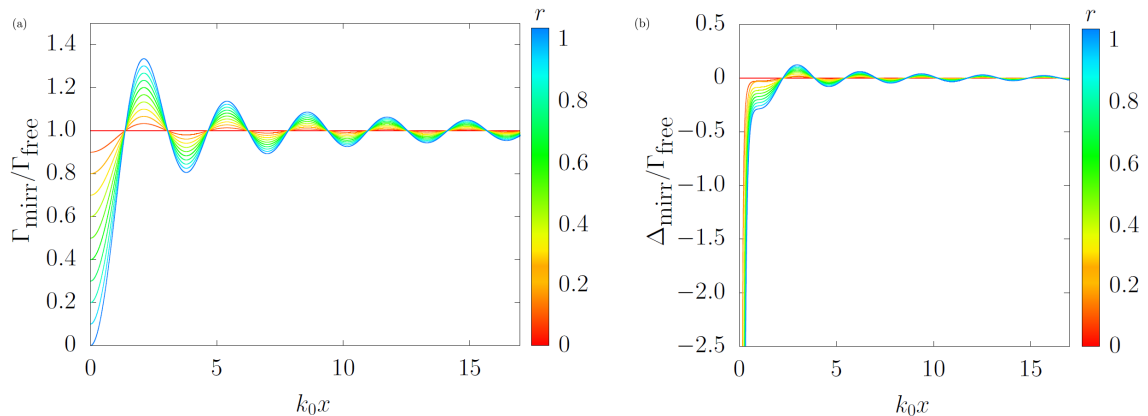
Figure 6.2: The spontaneous emission rate Γ_{mirr} (a) and the atomic level shift Δ_{mirr} (b) of an atom in the presence of a non-absorbing symmetric mirror (cf. Eqs. (6.16)) as a function of the atom-mirror distance x for different values of r. Again it is assumed $\mu = 0$, while $t^2 = 1 - r^2$. Here, the $r = 0$ case corresponds to free space, while $r = 1$ models a perfect mirror.

6.2 Conclusions

In this chapter, the validity of the image-detector method outlined in Chapter 5 is tested by presenting a master equation description of a radiating atom in the presence of a two-sided semi-transparent mirror. The master equation description provides analytical expressions for the spontaneous emission rate Γ_{mirr} and the level shift Δ_{mirr} (cf. Eq. (6.7)) of an atom in the presence of a two-sided semi-transparent mirror. In general, Γ_{mirr} and Δ_{mirr} depend in a relatively complex way on transmission and reflection rates and other relevant system parameters, i.e. normalisation factors η_a and η_b, which in general depend on the optical properties of the mirror (cf. Eq. (6.12)). Most importantly, the model reproduced the expected behaviour in the limiting cases, e.g. perfect mirrors and highly absorbing mirrors [115–125] and is in good agreement with experimental findings of other authors [126–128].

Chapter 7

Long-range dipole-dipole interaction mediated by two-sided mirror

In Chapter 4 the interaction of two dipoles in free space was reviewed and Chapter 6 demonstrated that a radiating atom in the presence of a two-sided semi-transparent mirror can be thought of as arising from a dipole-dipole interaction between an atom and its mirror image [70]. The next step is to build on the work presented in Chapter 6 and introduce a second atom in order to demonstrate that it is possible to induce atomic long-range interactions with the help of thin semi-transparent mirrors.

Suppose an atom is placed on either side of a thin semi-transparent mirror with finite transmission and reflection rates. As it will be demonstrated below, this situation is equivalent to having two atoms and two mirror images at certain locations in a free space scenario as illustrated in Fig. 7.1. From Fig. 7.1, it is evident that one can use the mirror to induce a dipole-dipole interaction between an atom and a mirror-image atom provided the following condition is maintained

$$\widetilde{x} \equiv |\mathbf{r}_a - \widetilde{\mathbf{r}}_b| \equiv |\widetilde{\mathbf{r}}_a - \mathbf{r}_b| \sim \lambda_0 \ . \tag{7.1}$$

This means as long as the relative distance between an atom and a mirror-image atom, $\widetilde{x}$ is approximately of the same order as the emitted radiation λ_0, a dipole-dipole interaction is induced - even when the actual distance of the atoms is

several orders of magnitude larger[1]. To show that this is the case, one adopts the continuous-mode field quantisation in front of a semi-transparent mirror presented in Chapter 5. Through this field quantisation scheme one is able to obtain an expression for the electric field observable $\hat{\mathbf{E}}_{\mathrm{mirr}}(\mathbf{r})$ (cf. Eq. (5.27)) which allows one to derive a master equation for the system and obtain analytical expressions for the atomic decay rates. Throughout, it is assumed that both atoms are identical, two-level systems with the transition frequency ω_0 for the transition $|2\rangle \to |1\rangle$.

Dipole-dipole interactions in the vicinity of a reflective interface generate modifications in the collective spontaneous emission rates [129–133]. As well as determining atomic lifetimes and atomic level shifts for these dipole-dipole systems, previous authors also consider how the arrangement of the atoms affect these phenomena, i.e. place one atom above the other or placing the atoms next to one another. However, none of these studies investigate the effect of separating the two atoms with a reflective interface, i.e. placing a thin semi-transparent mirror between the two atoms (see Fig. 7.1). Previous authors consider dipole-dipole systems in the presence of a dispersing or absorbing medium [134], as well as examining other interesting effects due to the immediate surroundings, e.g. atoms in accelerating reference frames, atoms in curved spacetime or coupling atomic systems to optical waveguides, see Refs. [135–138].

In addition, searching for a long-range interaction between two dipoles should not be too surprising as it has been shown that if one confines the electromagnetic field to propagate in one-dimension only, then one should be able to observe infinite-range interactions between dipoles [1]. Moreover, this has been experimentally verified recently using Rubidium atoms placed near an optical fibre [139], where the fibre restricts the propagation of the field. This effect is even demonstrated when two dipoles are separated by a distance of one hundred wavelengths or more - a drastic improvement on what would be achievable in free space. The same group also demonstrated a Purcell effect using a similar method [140].

---

[1]Removing the semi-transparent mirror means the dipole-dipole interaction takes the form of that presented in Chapter 4. In addition, removing one atom from the setup, then one obtains the results predicted in Chapter 6.
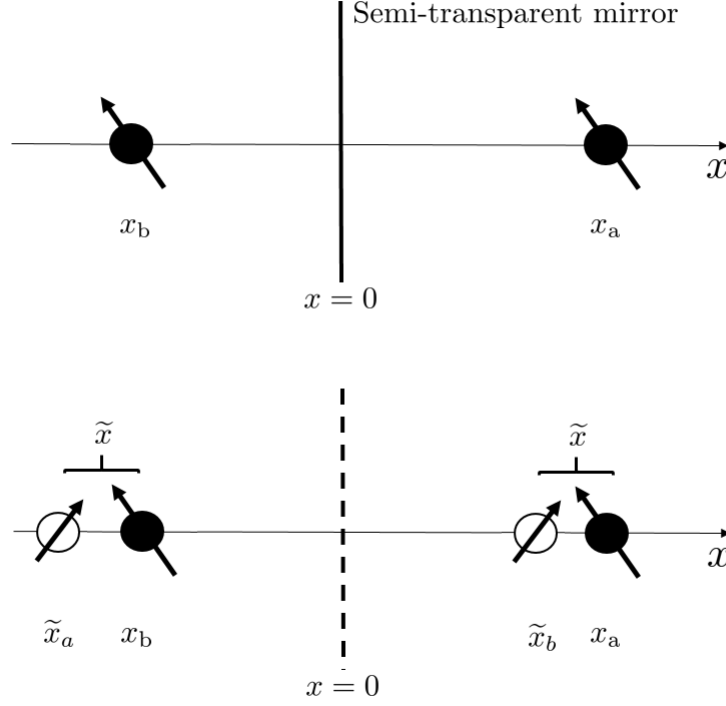
Figure 7.1: Schematic view of two dipoles separated by a thin, two-sided semi-transparent mirror and an equivalent scenario illustrated below through the mirror-image perspective. In the standard scenario, there is a thin mirror surface placed at $x = 0$, however one can ignore the mirror surface in this setup by introducing a mirror-image atom for each real atom. The mirror-image atom is placed on the opposite side of the setup i.e. one can see that if atom one is placed at some position $x > 0$, the corresponding mirror-image is placed at some position $x < 0$. Doing so for both atoms demonstrates that the two pictures are equivalent. Therefore, when using this interpretation it will be as if the mirror-image of one atom is sitting in close proximity to the other atom. This separation is denoted $\widetilde{x}$ and provided this is of the same order of magnitude as the wavelength of the emitted radiation λ_0 then the atoms can exchange excitations over relatively-large distances. Finally, the position of the mirror-image atoms are given by $\widetilde{x}_a$ and $\widetilde{x}_b$.

The work in this chapter has been adapted from Ref. [2] which predicts a long-range dipole-dipole interaction mediated by a two-sided semi-transparent

mirror. This allows one to treat photons as they are in free space and determine analytical expressions for the spontaneous emission rates, which are denoted by $\widetilde{\Gamma}_{\pm}$ (cf. Fig. 7.2). Successfully modelling the long-range dipole-dipole interaction shown in Fig. 7.1 would provide various applications in quantum optics and quantum information processing, particularly quantum sensing. The work outlined in this chapter provides theoretical groundwork for Professor Gin Jose's engineering group at the University of Leeds, whom are designing state of the art medical devices using a novel laser-based technique to measure blood glucose. The group use ultrafast laser plasma doping to fabricate thin glass films (or thin film sensors) using rare earth ions, namely Erbium (Er^{3+}) [141–144]. These structures can then be implemented to provide painless and non-invasive glucose-sensing technology which should allow the user to continuously monitor glucose and provide improved diabetic management [145]. This state of the art device uses the mechanism illustrated in Fig. 7.1, i.e. the presence of atoms above the laser-doped glass (when a patient places their finger on the device containing the thin film structure) effectively projects atoms within the patients finger into the device, and vice versa due to boundary conditions. One is able to laser drive the atoms doped within the glass structures allowing excitations to be exchanged between the doped atoms and the atoms projected from the patients finger, allowing one to measure atomic lifetimes through the induced dipole-dipole interaction.

7.1 Overview

In Chapter 4, it was demonstrated that a pair of interacting dipoles in free space can be modelled as a single four-level system consisting of a ground, excited, symmetric and anti-symmetric state denoted $|g\rangle, |e\rangle, |s\rangle$ and $|a\rangle$, respectively. However, the results derived here will differ from those in Chapter 4 as the time-dependent interaction picture Hamiltonian $\hat{H}_{\mathrm{SBI}}(t)$ now takes a different form than that in Eq. (4.9).
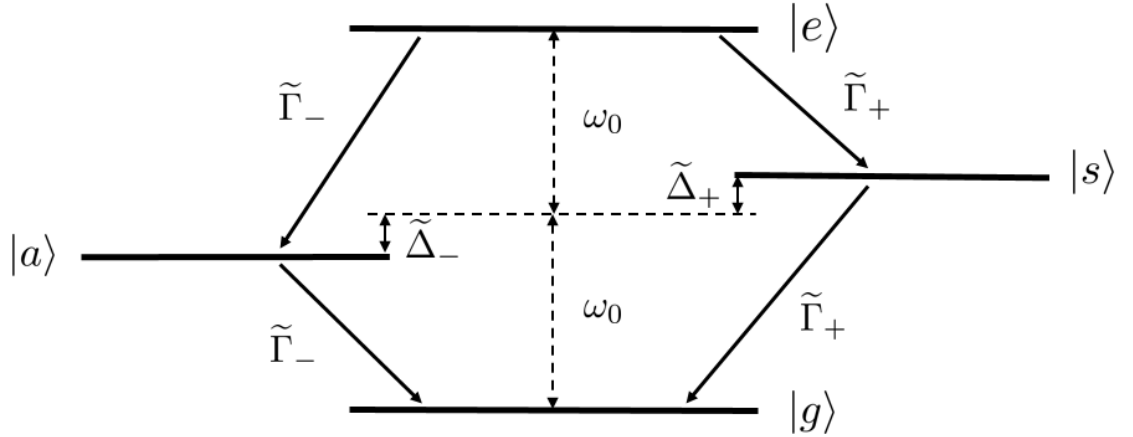
Figure 7.2: Level scheme for a dipole-dipole interaction between a pair of two-level atoms separated by a thin semi-transparent mirror. As with the dipole-dipole interaction in free space (cf. Fig. 4.2, this scenario is also described as a four-level system where each arrow denotes a one-photon transition and the free-space Dicke states; $|e\rangle$, $|g\rangle$, $|s\rangle$ and $|a\rangle$ are given in Eq. (4.1). However, the spontaneous emission rates $\widetilde{\Gamma}_{\pm}$ and atomic level shifts $\widetilde{\Delta}_{\pm}$ now take a different form those presented in Eqs. (4.33) and (4.34) due to the presence of the semi-transparent mirror.

7.2 Master equation for long-range dipole-dipole interaction

In this section a master equation description for two interacting dipoles separated by a thin, two-sided semi-transparent mirror is presented, where analytical expressions for the spontaneous emission rates $\widetilde{\Gamma}_{\pm}$ are obtained.

7.2.1 The relevant Hamiltonians

As in Chapter 4, the starting point is the Hamiltonian, which is again the sum of three contributions,

$$\hat{H} \;=\; \hat{H}_{\text{atom a}} + \hat{H}_{\text{atom b}} + \hat{H}_{\text{field}} + \hat{H}_{\text{SB}}. \tag{7.2}$$

These incorporate the non-interacting contributions from both atoms, the energy of the electromagnetic field and atom-field interactions. As before, the next step is to move the Hamiltonian into the interaction picture with respect to the free Hamiltonian

$$\hat{H}_0 = \hat{H}_{\text{atom a}} + \hat{H}_{\text{atom b}} + \hat{H}_{\text{field}} \tag{7.3}$$

(cf. Eq. (4.3)). The interaction Hamiltonian $\hat{H}_{\text{SB}}$ can again be defined through the dipole approximation in the following way

$$\hat{H}_{\text{SB}} = e \sum_{i=a,b} \hat{\mathbf{D}}_{12}^{(i)} \cdot \hat{\mathbf{E}}_{\text{mirr}}(\mathbf{r}_i), \tag{7.4}$$

where $\hat{\mathbf{E}}_{\text{mirr}}(\mathbf{r}_i)$ represents the electric field observable at the position of atom i. In front of a two-sided semi-transparent mirror, this observable equals $\hat{\mathbf{E}}_{\text{mirr}}(\mathbf{r}_i)$ (cf. Eq. (5.27)). Assuming that atom a sits on the right-hand side ($x > 0$) and atom b sits on the left-hand side of the mirror ($x < 0$), this allows the above interaction Hamiltonian to be expressed as

$$\hat{H}_{\text{SB}} = e \left[\hat{\mathbf{D}}_{12}^{(a)} \hat{\sigma}_a^- + \hat{\mathbf{D}}_{12}^{(a)*} \hat{\sigma}_a^+ \right] \cdot \hat{\mathbf{E}}_{\text{mirr}}(\mathbf{r}_a) + e \left[\hat{\mathbf{D}}_{12}^{(b)} \hat{\sigma}_b^- + \hat{\mathbf{D}}_{12}^{(b)*} \hat{\sigma}_b^+ \right] \cdot \hat{\mathbf{E}}_{\text{mirr}}(\mathbf{r}_b). \tag{7.5}$$

As before, one can write the dipole moments $\hat{\mathbf{D}}_{12}^{(i)}$ without restrictions in the following way

$$\frac{\hat{\mathbf{D}}_{12}^{(a)}}{\|\mathbf{D}_{12}\|} = \begin{pmatrix} d_1^{(a)} \\ 0 \\ d_3^{(a)} \end{pmatrix}, \quad \frac{\hat{\mathbf{D}}_{12}^{(b)}}{\|\mathbf{D}_{12}\|} = \begin{pmatrix} d_1^{(b)} \\ d_2^{(b)} \\ d_3^{(b)} \end{pmatrix} \tag{7.6}$$

with

$$|d_1^{(i)}|^2 + |d_2^{(i)}|^2 + |d_3^{(i)}|^2 = 1. \tag{7.7}$$
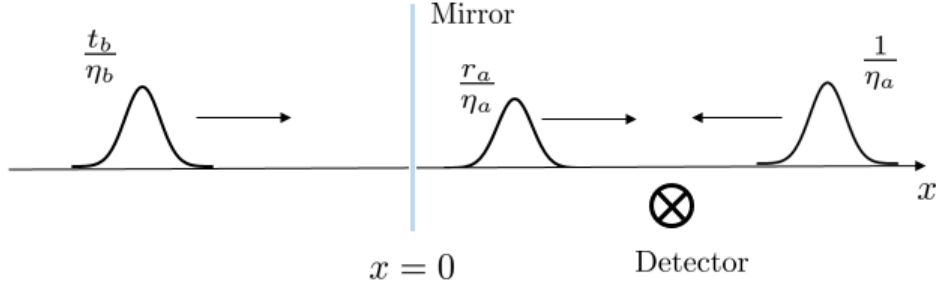
Figure 7.3: Schematic view of a semi-transparent mirror with light incident from both sides. Depending on the origin of the incoming light, we denote the transmission and reflection rates of the mirror t_a, t_b, r_a and r_b, respectively. The possible absorption of light in the mirror surface is explicitly taken into account and for simplicity we assume that the medium on both sides of the mirror is the same, free space.
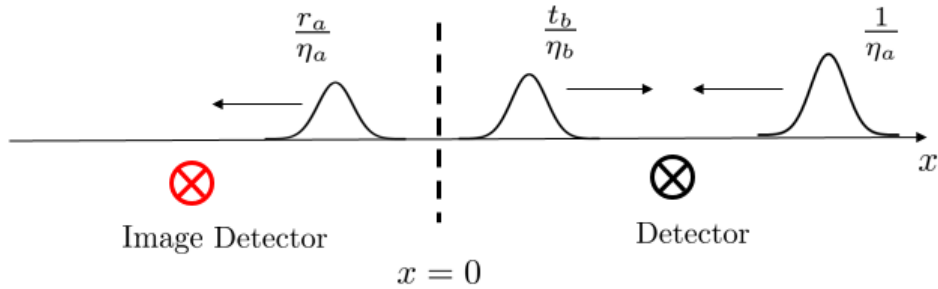
Figure 7.4: Schematic view of a semi-transparent mirror with light incident from both sides using the image-detector method. This figure demonstrates the different electric field amplitudes measured by the real and mirror-image detector. As in the above figure, depending on the origin of the incoming light, we denote the transmission and reflection rates of the mirror t_a, t_b, r_a and r_b, respectively. Moreover, the possible absorption of light in the mirror surface is explicitly taken into account and for simplicity we assume that the medium on both sides of the mirror is the same, free space.

Substituting the electric field observable from Eq. (5.27) into the above inter-
action Hamiltonian $\hat{H}_{\text{SB}}$, one now obtains the interaction Hamiltonian

$$
\begin{aligned}
\hat{H}_{\text{SB}} &= \frac{e}{\eta_a}\, \mathbf{D}_{12}^{(a)} \cdot \hat{\mathbf{E}}_{\text{free}}^{(a)}(\mathbf{r}_a) + e\, \mathbf{D}_{12}^{(a)} \cdot \left[\frac{r_a}{\eta_a}\, \hat{\tilde{\mathbf{E}}}_{\text{free}}^{(a)}(\widetilde{\mathbf{r}}_a, \varphi_1) + \frac{t_b}{\eta_b}\, \hat{\mathbf{E}}_{\text{free}}^{(b)}(\mathbf{r}_a, \varphi_2) \right] \\
&\quad + \frac{e}{\eta_b}\, \mathbf{D}_{12}^{(b)} \cdot \hat{\mathbf{E}}_{\text{free}}^{(b)}(\mathbf{r}_b) + e\, \mathbf{D}_{12}^{(b)} \cdot \left[\frac{r_b}{\eta_b}\, \hat{\tilde{\mathbf{E}}}_{\text{free}}^{(b)}(\widetilde{\mathbf{r}}_b, \varphi_3) + \frac{t_a}{\eta_a}\, \hat{\mathbf{E}}_{\text{free}}^{(a)}(\mathbf{r}_b, \varphi_4) \right] . \quad (7.8)
\end{aligned}
$$

The six terms in this equation are exactly the terms that one would expect,
when looking at Fig. 7.4. The first terms on lines one and two of Eq. (7.8)
describe the independent interaction of two atoms with two different free radiation
fields. The terms which scale with r_a and r_b, respectively, describe the coupling
of atoms to light modes which have been reflected by the mirror. The mirror
reflection introduces phase factors such that directly emitted and reflected light
interferes as one would expect also classically and energy is conserved. Moreover,
in case of non-zero transmission of light through the mirror surface, the atoms
see electromagnetic field modes originating from the opposite side of the mirror.
The normalisation factors η_a and η_b characterise the medium on either side of the
mirror and are later chosen such that a single excited atom at a relatively large
distance from the mirror surface has the spontaneous emission rate as it would
in free space.

Transferring H_{SB} in Eq. (7.8) into the interaction picture with respect to the
free Hamiltonian $\hat{H}_0$, one finds that

$$
\begin{aligned}
\hat{H}_{\text{SB I}}(t) &= \frac{\mathrm{i}e}{4\pi} \sum_{i=a,b} \sum_{\lambda=1,2} \int_{\mathbb{R}^3} \mathrm{d}^3\mathbf{k}\, \sqrt{\frac{\hbar\omega}{\pi\varepsilon}} \times \left[\mathrm{e}^{\mathrm{i}(\omega+\omega_0)t} \left(\hat{\mathbf{D}}_{12}^{(i)} \cdot \hat{\mathbf{e}}_{\mathbf{k}\lambda} \right) \hat{\sigma}_i^- \right. \\
&\qquad\qquad \left. + \mathrm{e}^{-\mathrm{i}(\omega-\omega_0)t} \left(\hat{\mathbf{D}}_{12}^{(i)*} \cdot \hat{\mathbf{e}}_{\mathbf{k}\lambda} \right) \hat{\sigma}_i^+ \right] \hat{s}_{\mathbf{k}\lambda}^{(i)}(\mathbf{r}_i) + \text{H.c.}
\end{aligned}
$$

$$(7.9)$$

Finally, one applies the rotating wave approximation to sift out any non-energy
conserving terms which yields the interaction Hamiltonian

$$
\hat{H}_{\text{SB I}}(t) = \frac{\mathrm{i}e}{4\pi} \sum_{i=a,b} \sum_{\lambda=1,2} \int_{\mathbb{R}^3} \mathrm{d}^3\mathbf{k}\, \sqrt{\frac{\hbar\omega}{\pi\varepsilon}}\, \mathrm{e}^{-\mathrm{i}(\omega-\omega_0)t} \left(\mathbf{D}_{12}^{(i)*} \cdot \hat{\mathbf{e}}_{\mathbf{k}\lambda} \right) \hat{\sigma}_i^+ \hat{s}_{\mathbf{k}\lambda}^{(i)}(\mathbf{r}_i) + \text{H.c.}
$$

$$(7.10)$$

with

$$\hat{s}_{\mathbf{k}\lambda}^{(a)}(\mathbf{r}_a) = \frac{1}{\eta_a} \left[e^{i\mathbf{k}\cdot\mathbf{r}_a} + r_a\, e^{i(\mathbf{k}\cdot\widetilde{\mathbf{r}}_a+\varphi_1)} \right] \hat{a}_{\mathbf{k}\lambda} + \frac{t_b}{\eta_b}\, e^{i(\mathbf{k}\cdot\mathbf{r}_a+\varphi_2)}\, \hat{b}_{\mathbf{k}\lambda}$$

$$\hat{s}_{\mathbf{k}\lambda}^{(b)}(\mathbf{r}_b) = \frac{1}{\eta_b} \left[e^{i\mathbf{k}\cdot\mathbf{r}_b} + r_b\, e^{i(\mathbf{k}\cdot\widetilde{\mathbf{r}}_b+\varphi_3)} \right] \hat{b}_{\mathbf{k}\lambda} + \frac{t_a}{\eta_a}\, e^{i(\mathbf{k}\cdot\mathbf{r}_b+\varphi_4)}\, \hat{a}_{\mathbf{k}\lambda} \,. \qquad (7.11)$$

This Hamiltonian has many similarities with the Hamiltonian in Eq. (4.9) of two atoms at positions $\mathbf{r}_a$ and $\mathbf{r}_b$ in free space but instead of coupling to the same set of $(\mathbf{k}, \lambda)$ photon modes, the atoms now couple to two different sets of modes. Notice that the annihilation operators in Eq. (7.11) are in general incorrectly normalised and do not obey bosonic commutator relations. Moreover, in general, the two atoms do not interact with pairwise orthogonal photons modes. For example, one can show that

$$\left[\hat{s}_{\mathbf{k}\lambda}^{(a)}(\mathbf{r}_a), \hat{s}_{\mathbf{k}\lambda}^{(b)}(\mathbf{r}_b)^{\dagger} \right]$$

$$= \frac{t_a}{\eta_a^2} \left[e^{i\mathbf{k}\cdot\mathbf{r}_a} + r_a\, e^{i(\mathbf{k}\cdot\widetilde{\mathbf{r}}_a+\varphi_1)} \right] e^{-i(\mathbf{k}\cdot\mathbf{r}_b+\varphi_4)} + \frac{t_b}{\eta_b^2}\, e^{i(\mathbf{k}\cdot\mathbf{r}_a+\varphi_2)} \left[e^{-i\mathbf{k}\cdot\mathbf{r}_b} + r_b\, e^{-i(\mathbf{k}\cdot\widetilde{\mathbf{r}}_b+\varphi_3)} \right]$$

$$(7.12)$$

which is in general different from zero. As we shall see below, as a result, the spontaneous emission of photons from both atoms becomes strongly correlated. Due to interference effects, it becomes impossible to distinguish if a photon has been emitted by atom a or by atom b. As a result, spontaneous emission rates change and atomic level shifts occur.

7.2.2 Master equation

Implementing the image-detector method from Chapter 5 allows one to map the situation of two atoms separated by thin semi-transparent mirror onto two analogous free space scenarios (cf. Fig. 7.1). Therefore, one should expect the long-range dipole-dipole interaction to take a similar form to the free-space dipole-dipole interaction described in Chapter 4. However, the long-range dipole-dipole interaction will now have an explicit dependence on the optical properties of the mirror, i.e. the mirror's transmission and reflection rates. For simplicity, in the following it is assumed that the absolute distance x of the atoms is much larger

than the atomic transition wavelength λ_0, meaning a direct interaction between both atoms will become negligible. On the other hand, the distance $\widetilde{x}$ between atoms and mirror-images can be relatively small (cf. Eq. (7.1)). Proceeding as described in App. E and keeping all terms which depend on $\widetilde{x}$, one obtains the conditional Hamiltonian,

$$
\hat{H}_{\text{cond I}}(t) = -\frac{\mathrm{i}\hbar}{2} \left[\Gamma_{\text{mirr}}^{(aa)} \hat{\sigma}_a^+ \hat{\sigma}_a^- + \widetilde{C}(\widetilde{x}) \hat{\sigma}_a^+ \hat{\sigma}_b^- + \widetilde{C}^*(\widetilde{x}) \hat{\sigma}_b^+ \hat{\sigma}_a^- + \Gamma_{\text{mirr}}^{(bb)} \hat{\sigma}_b^+ \hat{\sigma}_b^- \right],
\tag{7.13}
$$

and the following reset operator

$$
\begin{aligned}
\mathcal{L}(\hat{\rho}_{\text{S I}}(t)) &= \Gamma_{\text{mirr}}^{(aa)} \hat{\sigma}_a^- \hat{\rho}_{\text{S I}}(t) \hat{\sigma}_a^+ + \text{Re}(\widetilde{C}(\widetilde{x}) \hat{\sigma}_a^- \hat{\rho}_{\text{S I}}(t) \hat{\sigma}_b^+ \\
&\quad + \text{Re}(\widetilde{C}(\widetilde{x}) \hat{\sigma}_b^- \hat{\rho}_{\text{S I}}(t) \hat{\sigma}_a^+ + \Gamma_{\text{mirr}}^{(bb)} \hat{\sigma}_b^- \hat{\rho}_{\text{S I}}(t) \hat{\sigma}_b^+ ,
\end{aligned}
\tag{7.14}
$$

where the form of $\Gamma_{\text{mirr}}^{(aa)}$ and $\Gamma_{\text{mirr}}^{(bb)}$ are given in Eqs. (E.17) and (E.20). In addition, the full form of the distance-dependent dipole-coupling constant $\widetilde{C}(\widetilde{x})$ is given in Eq. (E.22).

Assuming the semi-transparent mirror is symmetric and lossless allows one to simplify the conditional Hamiltonian given in Eq. (7.13) such that[1]

$$
\hat{H}_{\text{cond I}}(t) = -\frac{\mathrm{i}\hbar}{2} \left[\widetilde{\Gamma}_{\text{mirr}} \left(\hat{\sigma}_a^+ \hat{\sigma}_a^- + \hat{\sigma}_b^+ \hat{\sigma}_b^- \right) + \text{Re}(\widetilde{C}(\widetilde{x})) \left(\hat{\sigma}_a^+ \hat{\sigma}_b^- + \hat{\sigma}_b^+ \hat{\sigma}_a^- \right) \right],
\tag{7.15}
$$

and similarly, the reset operator given in Eq. (7.14) can be simplified such that

$$
\begin{aligned}
\mathcal{L}(\hat{\rho}_{\text{S I}}(t)) &= \widetilde{\Gamma}_{\text{mirr}} \left(\hat{\sigma}_a^- \hat{\rho}_{\text{S I}}(t) \hat{\sigma}_a^+ + \hat{\sigma}_b^- \hat{\rho}_{\text{S I}}(t) \hat{\sigma}_b^+ \right) \\
&\quad + \text{Re}(\widetilde{C}(\widetilde{x})) \left(\hat{\sigma}_b^- \hat{\rho}_{\text{S I}}(t) \hat{\sigma}_a^+ + \hat{\sigma}_a^- \hat{\rho}_{\text{S I}}(t) \hat{\sigma}_b^+ \right) ,
\end{aligned}
\tag{7.16}
$$

---

[1]This is because the real part of the conditional Hamiltonian contributes to the atomic level shifts and the imaginary part contributes to the spontaneous emission rates. Therefore, by treating $\widetilde{C}(\widetilde{x}) \equiv \widetilde{C}^*(\widetilde{x})$ one can accurately calculate spontaneous emission rates as the real part of $\widetilde{C}(\widetilde{x})$ is equivalent to the real part of $\widetilde{C}^*(\widetilde{x})$. Therefore, $\widetilde{C}(\widetilde{x})$ and $\widetilde{C}^*(\widetilde{x})$ will now be replaced by $\text{Re}(\widetilde{C}(\widetilde{x}))$. This is important as it allows one to obtain the spontaneous emission rates of the system and this is what will be measured. In addition, the semi-transparent mirror is considered to be very thin, therefore it will assumed both sides of the mirror have the same optical properties, i.e. $r_a = r_b = r$, $t_a = t_b = t$ and therefore, $\eta_a^2 \equiv \eta_b^2$ and $\widetilde{\Gamma}_{\text{mirr}} \equiv \Gamma_{\text{mirr}}^{(aa)} \equiv \Gamma_{\text{mirr}}^{(bb)}$.

where the expressions for $\widetilde{\Gamma}_{\mathrm{mirr}}$ and $\mathrm{Re}(\widetilde{C}(\widetilde{x}))$ are given later (see Eqs. (7.21) and (7.22)).

Finally, in analogy to Eqs. (4.27) and (4.30), one is able to re-express these equations such that

$$\hat{H}_{\mathrm{cond\,I}}(t) \;\; = \;\; -\frac{\mathrm{i}\hbar}{2}\left[\left(\widetilde{\Gamma}_{\mathrm{mirr}}+\mathrm{Re}(\widetilde{C}(\widetilde{x}))\right)\hat{L}_+^\dagger\hat{L}_+ + \left(\widetilde{\Gamma}_{\mathrm{mirr}}-\mathrm{Re}(\widetilde{C}(\widetilde{x}))\right)\hat{L}_-^\dagger\hat{L}_-\right], \tag{7.17}$$

and

$$\mathcal{L}(\hat{\rho}_{\mathrm{S\,I}}(t)) \;\; = \;\; \left[\widetilde{\Gamma}_{\mathrm{mirr}}+\mathrm{Re}(\widetilde{C}(\widetilde{x}))\right]\hat{L}_+\hat{\rho}_{\mathrm{S\,I}}(t)\hat{L}_+^\dagger$$
$$+\left[\widetilde{\Gamma}_{\mathrm{mirr}}-\mathrm{Re}(\widetilde{C}(\widetilde{x}))\right]\hat{L}_-\hat{\rho}_{\mathrm{S\,I}}(t)\hat{L}_-^\dagger. \tag{7.18}$$

where the operators $\hat{L}_\pm$ and $\hat{L}_\pm^\dagger$ are defined in Eq. (4.26) through the Dicke states (cf. Eq. (4.22)). In order to obtain the final form of master equation, one must substitute the expressions for the conditional Hamiltonian and the reset operator from Eqs. (7.17) and (7.18) respectively, into the quantum jump master equation given in Eq. (3.24). This generates the following master equation

$$\dot{\hat{\rho}}_{\mathrm{S\,I}}(t) \;\; = \;\; \widetilde{\Gamma}_+\left(\hat{L}_+\,\hat{\rho}_{\mathrm{S\,I}}(t)\,\hat{L}_+^\dagger - \frac{1}{2}\left[\hat{L}_+^\dagger\hat{L}_+,\hat{\rho}_{\mathrm{S\,I}}(t)\right]_+\right)$$
$$+\widetilde{\Gamma}_-\left(\hat{L}_-\,\hat{\rho}_{\mathrm{S\,I}}(t)\,\hat{L}_-^\dagger - \frac{1}{2}\left[\hat{L}_-^\dagger\hat{L}_-,\hat{\rho}_{\mathrm{S\,I}}(t)\right]_+\right), \tag{7.19}$$

where the spontaneous emission rates $\widetilde{\Gamma}_\pm = \widetilde{\Gamma}_{\mathrm{mirr}} \pm \mathrm{Re}(\widetilde{C}(\widetilde{x}))$ are analogous to those in Eq. (4.32) for interacting dipole in free space. One should expected these results to be similar as the image-detector method maps onto analogous free-space scenarios.

7.2.3 Spontaneous emission rates

From the expressions from Eqs. (7.17) and (7.18), one can determine analytical expressions for the spontaneous emission rates for the long-range dipole-dipole interaction mediated by a symmetric and lossless semi-transparent mirror. In analogy to Eq. (4.32), the spontaneous emission rates of two interacting dipoles separated by a symmetric and lossless semi-transparent mirror are given by

$$\widetilde{\Gamma}_{\pm} \;=\; \widetilde{\Gamma}_{\text{mirr}} \pm \text{Re}(\widetilde{C}(\widetilde{x})) \,, \tag{7.20}$$

where the solution with the positive sign corresponds to the spontaneous emission rate when the dipole-dipole system is prepared in a symmetric state and the solution with the negative sign corresponds to the spontaneous emission rate when the dipole-dipole system is prepared in an anti-symmetric state. Assuming a symmetric and lossless semi-transparent mirror then one can simplify and combine $\Gamma_{\text{mirr}}^{(aa)}$ and $\Gamma_{\text{mirr}}^{(bb)}$ from Eqs. (E.17) and (E.20) to give

$$\widetilde{\Gamma}_{\text{mirr}} \;=\; \frac{1}{\eta_a^2} \left[1 + r^2 + t^2 + 2t \, \cos(\varphi_2) \right] \Gamma_{\text{free}} \,. \tag{7.21}$$

As it was shown in Chapter 6, the normalisation constants $\eta_a^2 = \eta_b^2 = 2$ for a symmetric and lossless mirror. In analogy to Eq. (4.12), one finds that the real part of the distance-dependent dipole coupling constant for a lossless, symmetric mirror takes the form

$$
\begin{aligned}
\widetilde{C}(\widetilde{x}) \;=\;& \frac{3r}{2\eta_a^2} \, \cos(\varphi_1) \\
& \times \left[\frac{\sin(k_0\widetilde{x})}{k_0\widetilde{x}} \, \widetilde{c}_1 + \left(\frac{\cos(k_0\widetilde{x})}{(k_0\widetilde{x})^2} - \frac{\sin(k_0\widetilde{x})}{(k_0\widetilde{x})^3} \right) \widetilde{c}_2 \right] \Gamma_{\text{free}} \,,
\end{aligned}
\tag{7.22}
$$

where $\widetilde{x}$ is defined in Eq. (7.1) and in analogy to Eq. (4.14), the constants $\widetilde{c}_1$ and $\widetilde{c}_2$ are given by

$$
\begin{aligned}
\widetilde{c}_1 \;&=\; \left(\hat{\mathbf{D}}_{12}^{(a)} \cdot \hat{\widetilde{\mathbf{D}}}_{12}^{(b)} \right) - \left(\hat{\mathbf{D}}_{12}^{(a)} \cdot \hat{\mathbf{x}} \right) \left(\hat{\widetilde{\mathbf{D}}}_{12}^{(b)} \cdot \hat{\mathbf{x}} \right) \,, \\
\widetilde{c}_2 \;&=\; \left(\hat{\mathbf{D}}_{12}^{(a)} \cdot \hat{\widetilde{\mathbf{D}}}_{12}^{(b)} \right) - 3 \left(\hat{\mathbf{D}}_{12}^{(a)} \cdot \hat{\mathbf{x}} \right) \left(\hat{\widetilde{\mathbf{D}}}_{12}^{(b)} \cdot \hat{\mathbf{x}} \right) \,.
\end{aligned}
\tag{7.23}
$$

Using Eq. (7.20) combined with Eqs. (7.21) – (7.23), one finds the spontaneous emission rates for the long-range dipole-dipole interaction mediated by a symmetric and lossless semi-transparent mirror take the form

$$
\widetilde{\Gamma}_\pm = \left[\frac{1}{\eta_a^2} \left[1 + t \, \cos(\varphi_2) \right] \pm \frac{3r}{2\eta_a^2} \, \cos(\varphi_1) \right.
$$
$$
\left. \times \left[\frac{\sin(k_0 \widetilde{x})}{k_0 \widetilde{x}} \, \widetilde{c}_1 + \left(\frac{\cos(k_0 \widetilde{x})}{(k_0 \widetilde{x})^2} - \frac{\sin(k_0 \widetilde{x})}{(k_0 \widetilde{x})^3} \right) \widetilde{c}_2 \right] \right] \Gamma_{\text{free}} \,, \quad (7.24)
$$

where η_a^2 is given in Eq. (6.12). Moreover, if one assumes both atoms have the same dipole moment, i.e. $\hat{\mathbf{D}}_{12}^{(a)} = \hat{\mathbf{D}}_{12}^{(b)}$ then one finds $\widetilde{c}_1 = 1 - \mu$ and $\widetilde{c}_2 = 1 + \mu$, as predicted by Eq. (7.23) and the definition of the atomic dipole moment μ can be found in Eq. (4.15).

Fig. 7.5 demonstrates the spontaneous emission rates for the symmetric (Fig. 7.5 (a)) and anti-symmetric (Fig. 7.5 (b)) rate of a long-range dipole-dipole interaction, mediated by a symmetric and lossless 50:50 beamsplitter. This figures illustrates the dependence of $\widetilde{\Gamma}_\pm$ on the atomic separation $\widetilde{x}$ and the atomic dipole moment μ. On the other hand, Fig. 7.6 illustrates the spontaneous emission rates for the symmetric and anti-symmetric rate of a long-range dipole-dipole interaction, mediated by a thin, lossless mirror of varying reflectivity. By considering the two extreme examples for the dipole orientation ($\mu = 0$ and $\mu = 1$), one can see how the symmetric states of the interaction are affected when the mirror's reflectivity is changed (cf. Fig. 7.6 (a) & (c)) and similarly, how the anti-symmetric states are affected (cf. Fig. 7.6 (b) & (d)). For both these states, $\widetilde{\Gamma}_\pm \to \Gamma_{\text{free}}$ when the mirror is removed (free space where $r = 0$) or when a perfectly-reflective mirror separates the atoms. However, in the case of free space, provided one atom is excited then a photon can be exchanged between the two atoms and this interaction would affect the spontaneous decay rates in the same way as described in Chapter 4, i.e. it is only the long-range interaction that vanishes when the mirror is removed or made perfectly-reflective, as one would expect.

7.2.4   Limiting Cases

To gain more intuition for the spontaneous emission rates in Eq. (7.20), let us have a closer look at some limiting cases and concrete scenarios.
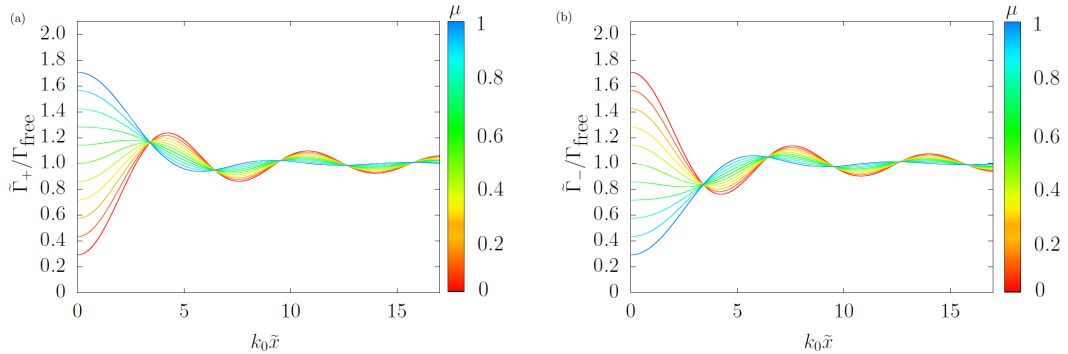
Figure 7.5: [Colour online] The spontaneous emission rates $\widetilde{\Gamma}_{\pm}$ for the (a) symmetric and (b) anti-symmetric states of a long-range, mirror-mediated dipole-dipole interaction as a function of the separation $\widetilde{x}$ for different orientations of the atomic dipole moment, where $\hat{\mathbf{D}}_{12}^{(a)} = \hat{\mathbf{D}}_{12}^{(b)}$. For distances $\widetilde{x}$ of the same order of magnitude as the wavelength λ_0 of the emitted light, the last few terms in Eq. (7.22) are no longer negligible and $\Gamma_{\pm}$ depend strongly on $\widetilde{x}$ and μ. Moreover, for $k_0\widetilde{x} \gg 1$, we have $\widetilde{\Gamma}_{\pm} = \Gamma_{\text{free}}$, as it should. For simplicity it is assumed the mirror is a symmetric, lossless 50:50 beamsplitter, i.e. $r = r_a = r_b = 1/\sqrt{2}$.

Perfect mirrors

Looking at the case of a perfect mirror requires setting the reflection coefficient $r_a = r_b = 1$ and the transmission coefficient $t_a = t_b = 0$. Due to the nature of this surface, one also finds the phase factors $\varphi_1 = \varphi_3 = \pi$. From Eqs. (7.22) and (7.24), it is not immediately obvious what happens to the long-range interaction when the atoms are separated by a perfect mirror. From Fig. 7.1, one can see the long-range interaction manifests itself as an interaction between a 'mirror-image' atom and a real atom. Therefore, when a perfect mirror is placed between the atoms, neither atom is aware of the other as they live in distinctly separate Hilbert spaces. This means the interference effect which generates the long-range
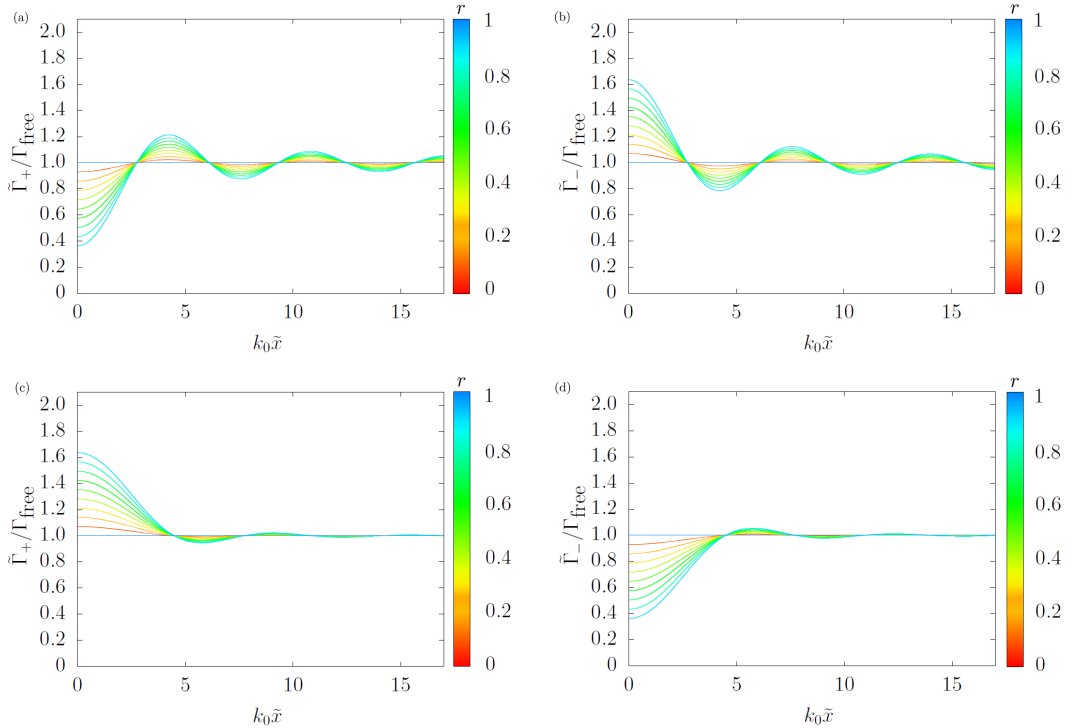
Figure 7.6: [Colour online] The spontaneous emission rates $\widetilde{\Gamma}_{\pm}$ for the symmetric and anti-symmetric states of a long-range dipole-dipole interaction mediated by a mirror of varying reflectivity, where $\hat{\mathbf{D}}_{12}^{(a)} = \hat{\mathbf{D}}_{12}^{(b)}$. Plots (a) and (b) demonstrate how the reflectivity of the mirror affects the spontaneous emission rates for the symmetric and anti-symmetric states, when the dipoles have the orientation $\mu = 0$. Similarly, plots (c) and (d) demonstrate how the reflectivity of the mirror affects the spontaneous emission rates for the symmetric and anti-symmetric states, when the dipoles have the orientation $\mu = 1$. These figures demonstrate the interaction is mirror-mediated. As the effect of the mirror is removed ($r = 0$) or in the case a perfectly-reflective mirror is placed between the atoms ($r = 1$), then the long-range interaction is no longer present. For simplicity the mirror is assumed to be symmetric and lossless, i.e. $r^2 + t^2 = 1$ always holds.

interaction is never able to happen, i.e. $\text{Re}(\widetilde{C}(\widetilde{x})) = 0$ as the mirror does not transmit light. As a result, both atoms decay independently of each other and as one would expect in front of a perfect mirror, i.e. the decay rates $\widetilde{\Gamma}_{\pm}$ take the form of $\widetilde{\Gamma}_{\text{mirr}}^{(aa)}$ and $\widetilde{\Gamma}_{\text{mirr}}^{(bb)}$ in App. E (cf. Eqs. (E.17) and (E.20)).

Free space

For the case of free space one finds that $r_a = r_b = 0$ and $t_a = t_b = 1$. This means $\mathrm{Re}(\widetilde{C}(\widetilde{x})) = 0$, which one would expect as the mirror, which mediates the long-range interaction, has now been removed. This results in the spontaneous decay rates to take the form

$$\widetilde{\Gamma}_{\pm} = \widetilde{\Gamma}_{\mathrm{mirr}}, \tag{7.25}$$

where $\widetilde{\Gamma}_{\mathrm{mirr}}$ is given in Eq. (7.21). Substituting in the necessary conditions for free space ($\varphi_2 = 0$, $r = 0$ and $t = 1$) and using Eq. (6.12), one finds

$$\widetilde{\Gamma}_{\pm} = \frac{4}{\eta_a^2} \Gamma_{\mathrm{free}} = 2\,\Gamma_{\mathrm{free}}, \tag{7.26}$$

which is the result one would predict provided the separation of the atoms is comparable to wavelength of emitted radiation and one of the atoms is in its excited state. In other words, by removing the mirror one obtains a dipole-dipole interaction as described in Chapter 4.

Behaviour for large atomic separation

Next, let us consider the physical behaviour of the system when a real atom and a mirror-image are separated over large distances. In other words, the case where $\widetilde{x} \to \infty$, then one finds that $\mathrm{Re}(\widetilde{C}(\widetilde{x})) \to 0$ yielding

$$\widetilde{\Gamma}_{\pm} = \Gamma_{\mathrm{free}}, \tag{7.27}$$

Strictly, the separation cannot be taken to infinity as this would violate the Markovian approximation used earlier. This atomic separation $\widetilde{x}$ can be taken to approximately $0.03cm$ provided the time period under consideration Δt is approximately $10^{-13}s$.

Behaviour for small atomic separation

Finally, let us consider the physical behaviour of the system when a real atom and a mirror-image are separated over very small distances. Assuming both atoms have the same atomic dipole moment i.e. the case where $\widetilde{x} \to 0$, and. As a result,

$$\mathrm{Re}(\widetilde{C}(\widetilde{x})) \to \frac{3r}{2}\,\cos(\varphi_1)\left[(1 - \mu) - \frac{1}{3}(1 + \mu)\right]\Gamma_{\mathrm{free}}, \tag{7.28}$$

(cf. Eq. (7.22)). This results in the indistinguishability of two nearby emitters. Using Eqs. (7.20), (7.24) and (7.21), one finds the spontaneous decay rates reduce to

$$\widetilde{\Gamma}_\pm = \left[\frac{2}{\eta_a^2} \left[1 + t \, \cos(\varphi_2) \right] \pm \frac{3r}{\eta_a^2} \left[(1 - \mu) - \frac{1}{3}(1 + \mu) \right] \, \cos(\varphi_1) \right] \Gamma_{\text{free}} \, . \quad (7.29)$$

Therefore, for a symmetric and lossless semi-transparent mirror, the spontaneous emission rates take the form

$$\widetilde{\Gamma}_\pm = \left[\frac{2}{\eta_a^2} \left[1 + t \, \cos(\varphi_2) \right] \pm \frac{2r}{\eta_a^2} \, \cos(\varphi_1) \right] \Gamma_{\text{free}} \, . \quad (7.30)$$

7.3 Summary

In this chapter, the image-detector method is used to present a master equation description for mirror-mediated long-range dipole-dipole interactions. This description allows one to determine analytical expressions for the spontaneous emission rates $\widetilde{\Gamma}_\pm$ (cf. Eqs. (7.20) – (7.22)). The spontaneous emission rates take a similar form as those presented in Chapter 4 as the image-detector method maps onto analogous free space scenarios. However, due to the atoms being separated by a semi-transparent mirror, the spontaneous emission rates now depend on the optical properties of the mirror. From Fig. 7.1, it is shown that an atom on one side of a mirror is able to detect the presence of another atom on the other side, even if the other atom is large distance from the mirror surface. This interaction changes the spontaneous emission rates of both atoms leading to potential uses in quantum technologies and sensing applications, such as the non-invasive glucose-sensing technology discussed at the beginning of Chapter 7. Finally, one could also investigate this scenario a step further and consider how to obtain analytical expressions for the atomic level shifts for this system.

Chapter 8

A continuous-mode model for optical cavities

In Chapter 5, a continuous-mode model approach to quantising the electromagnetic field in the presence of a two-sided semi-transparent mirror was presented. Here, the aim is to extend the continuous-mode model for single interfaces to describe the behaviour of light within an optical cavity, ultimately aiming to reproduce results consistent with those found in Refs. [2, 14]. Successfully modelling these scenarios will pave the way for the modelling of more complex systems. Moreover, it will also hopefully give more insight into non-intuitive phenomenon such as the Casimir effect.

8.1 Overview

While quantising the electromagnetic field inside an optical cavity with perfect mirrors is straight forward [146], modelling more realistic cavities with finite transmission and reflection rates remains challenging [2]. There exists a range of approaches which are sufficient for modelling optical cavities in a wide range of experiments. The input-output formalism provides a phenomenological approach, where the modes inside and outside of the cavity are related through a linear coupling and the mirrors impose vanishing boundary conditions on electric field amplitudes [3–5], in such a way that is consistent with Maxwell's equations [6, 7].

Another approach is the modes-of-the-universe description [7, 10–13]. These approaches describe the electromagnetic field in terms of the modes of a much larger cavity - the universe. Refs. [7, 10] obtain a quasi-mode representation of the electromagnetic field, where the non-orthogonal modes allow for leakage of photons through the cavity mirrors. Alternatively, Barlow *et al.* [2] proposed a master equation description for a two-sided optical cavity, which describes the correct spontaneous photon emission from an optical cavity, while providing consistency with classical electrodynamics. Moreover, it is assumed there exists a continuum of modes within the cavity. However, this approach is unable to describe a single interfaces. In addition, the consistency between current models is not obvious [112]. Designing a continuous-mode model for optical cavities could provide insight into a wide range of experiments and generate motivation to consider the physical consequences of quantising the electromagnetic field between two mirrors e.g. the Casimir effect.
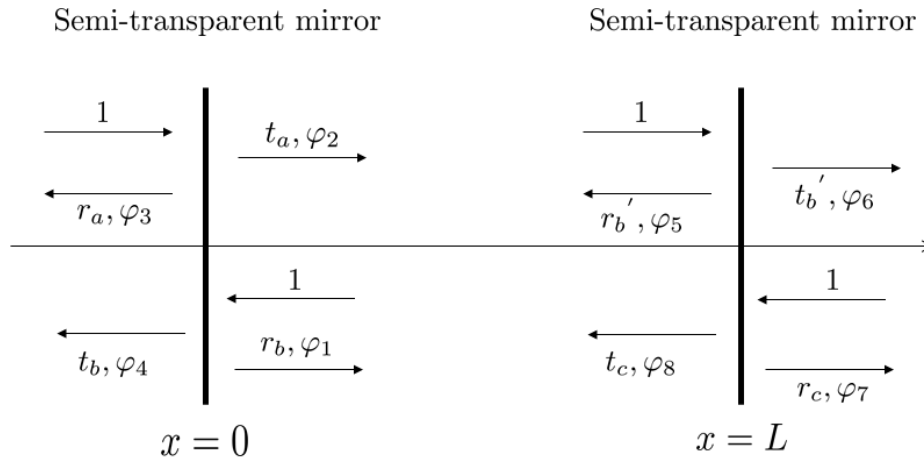
Figure 8.1: Schematic view of an optical cavity with semi-transparent mirrors as the boundaries, with finite transmission and reflection rates. Depending on the direction of the incoming light and which mirror surface it sees, we denote these rates t_a, r_a, t_b, r_b, t_b', r_b', t_c and r_c. To maintain generality, each side of the mirror surfaces have different phase factors, φ. For simplicity we assume that the medium on both sides of the each mirror is the same - free space. The possible absorption of light in the mirror surface is explicitly taken into account.

The work in this chapter aims to develop a continuous-mode field quantisation within an optical cavity (see Fig. 5.1) by extending the quantisation scheme outlined in Chapter 5 to a two mirror setup. Throughout, photons are characterised as in free space and the electromagnetic field between two semi-transparent mirrors with finite transmission and reflection rates is quantised through the image-detector method. As in Chapter 5, the possible dissipation of light by the mirror surface is taken into account, meaning

$$
\begin{aligned}
t_a{}^2 + r_a{}^2 \leq 1 \quad &\text{and} \quad t_b{}^2 + r_b{}^2 \leq 1 \,, \\
t_b'{}^2 + r_b'{}^2 \leq 1 \quad &\text{and} \quad t_c{}^2 + r_c{}^2 \leq 1 \,.
\end{aligned}
\tag{8.1}
$$

Again, it is assumed that the mirror surface does not alter the coherent properties of the incoming light - it only reduces the amplitude of incoming wave packets. As it will be demonstrated later, the mapping results in the electric field contributions forming an infinite geometric series.

8.2 A continuous-mode field quantisation for optical cavities

In the following section a continuous-mode model description of the quantised electromagnetic field between two thin semi-transparent mirrors is presented. To maintain generality different transmission and reflection rates are assigned to each side of both mirrors, as well as corresponding phase factors φ (cf. Fig. 8.1). First, a discussion of how to implement the image-detector method for the two mirror scenario is presented, which outlines how to generate expressions for the one-dimensional electromagnetic field observables $\hat{E}_{\text{cav}}(x)$ and $\hat{B}_{\text{cav}}(x)$. Extending this description to three dimensions allows one to obtain the relevant electromagnetic field observables $\hat{\mathbf{E}}_{\text{free}}(\mathbf{r})$ and $\hat{\mathbf{B}}_{\text{free}}(\mathbf{r})$.

8.2.1   General idea

First let us consider the single mirror case. For this one-mirror setup it is only ever necessary to consider a single image detector and this is always placed at some arbitrary position $-x$. The general solution obtained through the image-detector method is then a linear superposition of the electric field amplitudes measured by both detectors (cf. Chapter 5). However, for the two mirror scenario light is reflected multiple times between the two mirrors. Putting this in the perspective of the image-detector approach, it would require an infinite number of image-detectors to measure the electric field within the cavity setup for some position x, when compared to the single mirror setup. The infinite number of image-detectors allows one to replicate the effect of a wave packet traversing the cavity multiple times. Therefore, both the electric and magnetic field observables becomes an infinite sum of free-field solutions to Maxwell's equations. In order to keep track of all contributions, the overall Hilbert space $\mathcal{H}$ is divided into three subspaces. Previously, for the single mirror case, the overall Hilbert space is divided into two subspaces such that, $\mathcal{H} = \mathcal{H}^{(a)} \otimes \mathcal{H}^{(b)}$, which allowed one to specify which subspace the wave packet was in at time $t = 0$. For the scenario illustrated in Fig. 8.1, one divides the overall Hilbert space such that

$$\mathcal{H} \;=\; \mathcal{H}^{(a)} \otimes \mathcal{H}^{(b)} \otimes \mathcal{H}^{(c)} \;, \tag{8.2}$$

where $\mathcal{H}^{(a)}$, $\mathcal{H}^{(b)}$ and $\mathcal{H}^{(c)}$ denote the sub-spaces for $x < 0$, $0 \leq x \leq L$ and $x > L$, respectively.

Now, by considering a simple example, one can derive the form of the electromagnetic field between the two mirrors. To do so, one first introduces a wave packet into the cavity and also places an electric-field detector at some arbitrary position, x. Suppose the wave packet is completely right-travelling and initially exists in the subspace $\mathcal{H}^{(b)}$ (cf. Fig. 8.2). Looking at the possible electric field amplitudes the detector could measure; the initial measurement would correspond to the electric field amplitude, $\hat{E}^{(b)}_{\text{free}}(x)$ and at some later time t in this evolution, the next possible measurements one could make would correspond to the wave packet after undergoing reflection(s) by either the mirror placed at $x = 0$ or $x = L$. From Fig. 8.2, one can see the corresponding electric field
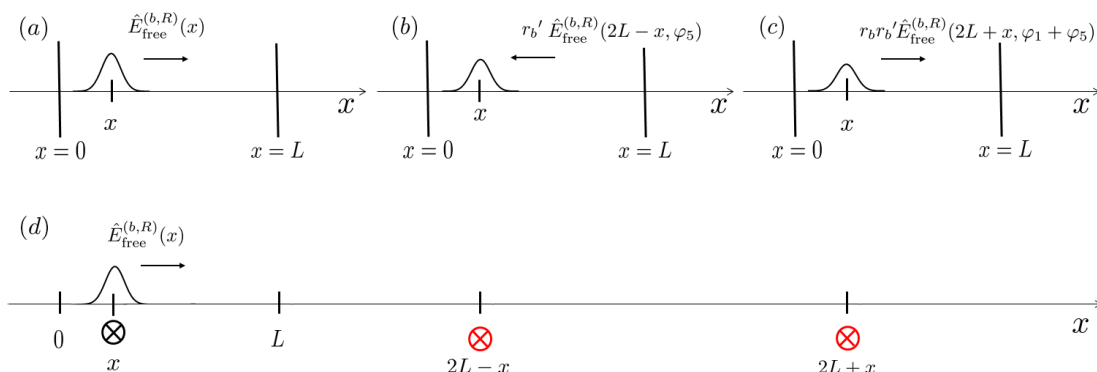
Figure 8.2: An illustration of how to construct the one-dimensional electric field observable for the cavity, $\hat{E}_{\text{cav}}^{(b,R)}(x)$ using the image-detector method. A thought experiment is used to compare the expected evolution of light (plots (a)–(c)) with a free-space alternative (plot (d)). Plots (a)–(c) show how an initially right-travelling wave packet interacts with the walls of the cavity. The plots show how the wave packet evolves over time where all these contributions can be measured by the detector at x. Plot (d) uses the image-detector method to map plots (a)–(c) onto an analogous free space scenario, where the mirrors are replaced with appropriately weighted image-detectors. By summing over all electric field amplitudes measured by both real and image-detectors allows one to obtain expressions for the electric field observable. Here, contributions that initially existed outside the cavity have been ignored.

amplitudes for the evolution of the wave packet. From here, one can follow this thought experiment to obtain the form of all subsequent electric field amplitudes. The image-detector method allows one to describe the behaviour of light within the cavity by mapping the problem onto an analogous free-space scenario where non-physical image-detectors are introduced and wave packets propagate freely (c.f. Fig. 8.2). Figs. 8.2 (a)–(c) illustrates a right-travelling wave packet traversing an optical cavity and Fig. 8.2 (d) illustrates how the packet evolves in this thought experiment using the image-detector method. The detector (shown in black) in Figs. 8.2 (a)–(c) is used to measure electric field amplitudes at the position x. Fig. 8.2 (d) illustrates the evolution of Figs. 8.2 (a)–(c) using an analogous free space scenario and the detector (black) corresponds to the initial measurement

of the field. The subsequent measurements are represented by image-detectors (shown in red), which are placed along the propagation axis corresponding to the evolution of the wave packet. In Fig. 8.2, the first image-detector is placed at $2L - x$ as the wave packet travelled a distance of $x + 2(L - x)$ between Figs. 8.2 (a) and (b). Similarly, the second image-detector is placed at $2L + x$ as the wave packet travelled a distance $x + 2(L - x) + 2x$ between Figs. 8.2 (b) and (c). Moreover, it is important to note direction of propagation in order to determine the positions of the image-detectors correctly, i.e. right-travelling wave packets are travelling in the positive x-direction and left-travelling ones travel in negative x-direction. Using the above thought experiment and the details shown in Fig. 8.2, one uses the image-detector method to sum over all detectors giving

$$
\begin{aligned}
\hat{E}_{\text{cav}}^{(R)}(x) \;=\; \frac{1}{\eta_b} \Bigg[& \hat{E}_{\text{free}}^{(b,R)}(x) + r_b' \, \hat{E}_{\text{free}}^{(b,R)}(2L - x, \varphi_5) \\
& + r_b \, r_b' \, \hat{E}_{\text{free}}^{(b,R)}(2L + x, \varphi_1 + \varphi_5) + ... \Bigg],
\end{aligned}
\tag{8.3}
$$

where superscript R denotes a right-travelling amplitude and η_b is a normalisation constant to be determined later. Similarly, one can use a left-travelling wave packet in the above example which yields

$$
\begin{aligned}
\hat{E}_{\text{cav}}^{(L)}(x) \;=\; \frac{1}{\eta_b} \Bigg[& \hat{E}_{\text{free}}^{(b,L)}(x) + r_b \, \hat{E}_{\text{free}}^{(b,L)}(-x, \varphi_1) \\
& + r_b \, r_b' \, \hat{E}_{\text{free}}^{(b,L)}(x - 2L, \varphi_1 + \varphi_5) + ... \Bigg],
\end{aligned}
\tag{8.4}
$$

8.2.2 One-dimensional cavity model

One can use this thought experiment and by combining Eqs. (8.3) and (8.4), one can describe the electric field between two semi-transparent mirrors. Notice these expressions take the form of an infinite geometric series, therefore, one can make use of the identity [147]

$$
\sum_{n=0}^{\infty} a k^n = \frac{a}{1 - k} \;\;, \;\; \text{for } |k| < 1 \;.
\tag{8.5}
$$

This yields the following expression

$$\hat{E}_{\text{cav}}(x) \;=\; \frac{1}{\eta_b}\left[\frac{\hat{E}_{\text{free}}^{(b,L)}(x) + r_b\,\hat{E}_{\text{free}}^{(b,L)}(-x,\varphi_1)}{1 + r_b\,r_b'\,\mathrm{e}^{-2\mathrm{i}kL}\,\mathrm{e}^{\mathrm{i}(\varphi_1+\varphi_5)}}\right.$$
$$\left.+\;\frac{\hat{E}_{\text{free}}^{(b,R)}(x) + r_b'\,\hat{E}_{\text{free}}^{(b,R)}(2L-x,\varphi_5)}{1 + r_b\,r_b'\,\mathrm{e}^{2\mathrm{i}kL}\,\mathrm{e}^{\mathrm{i}(\varphi_1+\varphi_5)}}\right]. \tag{8.6}$$

In Eq. (8.6), one must split the contributions into two parts; left- and right-travelling components as it is important to state which mirror does the wave packet see first. Therefore, one must specify the direction of propagation of the wave packet in order to model the field correctly. From this splitting, one finds

$$\hat{E}_{\text{free}}^{(b)}(x) \;=\; \hat{E}_{\text{free}}^{(b,L)}(x) + \hat{E}_{\text{free}}^{(b,R)}(x)$$
$$= \mathrm{i} \int_{-\infty}^{\infty} \mathrm{d}k \sqrt{\frac{\hbar\omega}{4\pi\varepsilon_0 A}}\,\mathrm{e}^{\mathrm{i}kx}\,b_k + \text{H.c.}, \tag{8.7}$$

which arises from left- and right-travelling wave packets being assigned negative and positive wavenumbers k, respectively. In addition, one can deduce the form of the magnetic field between the two mirrors

$$\hat{B}_{\text{cav}}(x) \;=\; \frac{1}{\eta_b}\left[\frac{\hat{B}_{\text{free}}^{(b,L)}(x) + r_b\,\hat{B}_{\text{free}}^{(b,L)}(-x)}{1 - r_b\,r_b'\,\mathrm{e}^{-2\mathrm{i}kL}}\right.$$
$$\left.+\;\frac{\hat{B}_{\text{free}}^{(b,R)}(x) + r_b'\,\hat{B}_{\text{free}}^{(b,R)}(2L-x)}{1 - r_b\,r_b'\,\mathrm{e}^{2\mathrm{i}kL}}\right]. \tag{8.8}$$

In analogy to Eq. (8.7), one also obtains the following expression for the magnetic field, $B_{\text{free}}(x)$

$$\hat{B}_{\text{free}}^{(b)}(x) \;=\; \hat{B}_{\text{free}}^{(b,L)}(x) + \hat{B}_{\text{free}}^{(b,R)}(x)$$
$$= -\mathrm{i}\sqrt{\varepsilon_0\mu_0} \int_{-\infty}^{\infty} \mathrm{d}k \sqrt{\frac{\hbar\omega}{4\pi\varepsilon_0 A}}\,\mathrm{e}^{\mathrm{i}kx}\,b_k\,\text{sign}(k) + \text{H.c.}. \tag{8.9}$$

Finally, one finds the system Hamiltonian $\hat{H}_{\text{sys}}$ describing the two semi-transparent mirrors and electromagnetic field takes the form

$$\hat{H}_{\text{sys}} \;=\; \int_{\infty}^{\infty} \mathrm{d}k\,\hbar\omega \left[a_k^{\dagger}a_k + b_k^{\dagger}b_k + c_k^{\dagger}c_k\right], \tag{8.10}$$

as photons are characterised as they are in free space.

8.2.3   Three-dimensional cavity model

Finally, let us generalise this quantisation scheme to three dimensions. To do so, one follows the same process as in the previous subsection, however, now one must use the three-dimensional free-space electric- and magnetic-field observables defined in Eq. (2.77).

To obtain the observable $\hat{\mathbf{E}}_{\mathrm{cav}}(\mathbf{r})$ of the electric field at position $\mathbf{r}$, one again makes use of the quantum image-detector method introduced above. More concretely, it is assumed in the following that a detector at a position $\mathbf{r} = (x, y, z)$ observes light arriving directly at the detector which originates either from the same or from the other side of the mirror. In addition, the detector measures the electric field amplitude at a position $\widetilde{\mathbf{r}}$ with $\widetilde{\mathbf{r}} = (x, y, z)$ as well as measuring periodically thereafter i.e. every $2L$ from $\widetilde{\mathbf{r}}$. These different field contributions need to be weighted by the appropriate transmission and reflection rates. Moreover, it is the y- and z- components that are affected by the mirror, while the x-component of the electric field remains the same. Taking this into account, one obtains the three-dimensional electric field observable

$$
\hat{\mathbf{E}}_{\mathrm{cav}}(\mathbf{r}) = \frac{1}{\eta_b}\left[\frac{\hat{\mathbf{E}}^{(b,L)}_{\mathrm{free}}(\mathbf{r}) + r_b \widetilde{\hat{\mathbf{E}}}^{(b,L)}_{\mathrm{free}}(\widetilde{\mathbf{r}}, \varphi_1)}{1 + r_b r'_b\, \mathrm{e}^{-2ikL}\,\mathrm{e}^{i(\varphi_1 + \varphi_5)}}\right.
$$
$$
\left. + \frac{\hat{\mathbf{E}}^{(b,R)}_{\mathrm{free}}(\mathbf{r}) + r'_b \widetilde{\hat{\mathbf{E}}}^{(b,R)}_{\mathrm{free}}(2L + \widetilde{\mathbf{r}}, \varphi_5)}{1 + r_b r'_b\, \mathrm{e}^{2ikL}\,\mathrm{e}^{i(\varphi_1 + \varphi_5)}}\right]\Theta(L - x),
$$

$$(8.11)$$

which generalises Eq.(8.6) to field propagation in three dimensions. In Eq. (8.11), $\widetilde{\hat{\mathbf{E}}}^{(s)}_{\mathrm{free}}(\widetilde{\mathbf{r}})$[1] is defined such that it differs from $\hat{\mathbf{E}}^{(s)}_{\mathrm{free}}(\widetilde{\mathbf{r}})$ only by the sign of their x-component. Similarly, in analogy to Eq. (8.8), one can obtain the three-dimensional magnetic field observable

$$
\hat{\mathbf{B}}_{\mathrm{cav}}(\mathbf{r}) = \frac{1}{\eta_b}\left[\frac{\hat{\mathbf{B}}^{(b,L)}_{\mathrm{free}}(\mathbf{r}) + r_b \widetilde{\hat{\mathbf{B}}}^{(b,L)}_{\mathrm{free}}(\widetilde{\mathbf{r}})}{1 - r_b r'_b \mathrm{e}^{-2ikL}}\right.
$$
$$
\left. + \frac{\hat{\mathbf{B}}^{(b,R)}_{\mathrm{free}}(\mathbf{r}) + r'_b \widetilde{\hat{\mathbf{B}}}^{(b,R)}_{\mathrm{free}}(2L + \widetilde{\mathbf{r}})}{1 + r_b r'_b \mathrm{e}^{2ikL}}\right]\Theta(L - x)\ ,
$$

$$(8.12)$$

[1] $s = a, b, c.$

Finally, in analogy to Eq. (8.10), one finds that in three-dimensions the system Hamiltonian $\hat{H}_{\text{sys}}$ takes the form

$$\hat{H}_{\text{sys}} = \int_{\infty}^{\infty} \mathrm{d}^3\mathbf{k}\, \hbar\omega \left[a_{\mathbf{k}}^\dagger a_{\mathbf{k}} + b_{\mathbf{k}}^\dagger b_{\mathbf{k}} + c_{\mathbf{k}}^\dagger c_{\mathbf{k}} \right] . \tag{8.13}$$

8.2.4 Limiting cases

In this section limiting cases of the continuous-mode model for optical cavities are presented. First the free space case is considered where the influence of the mirrors is removed and then the case of perfectly-reflective mirrors is examined.

Cavity with perfectly-transmissive mirrors

For the free space case, one must remove the influence of the mirrors and assign the transmission rates $t_b = t_b' = 1$ as well as the reflection rates $r_b = r_b = 0$. Making the substitution into the electromagnetic field observable from Eq. (8.6), one can readily confirm the cavity fields given in Eqs. (8.6), (8.8), (8.12) and (8.11) reduce to their respective free-field expressions for the electric- and magnetic-field observables (cf. Eqs. (2.75) and (2.77)).

Cavity with perfectly-reflective mirrors

If one considers the limit of perfectly-reflective mirrors, then one must assign the reflection rates $r_b = r_b' = 1$ as well as the transmission rates $t_b = t_b' = 0$. In addition, the associated phase factors take the following value $\varphi_1 = \varphi_5 = \pi$. Looking at Eqs. (8.5) and (8.11), one can see that imposing such conditions no longer allows the field to be approximated as an infinite geometric series.

8.3 Summary

In this chapter the image-detector method is used to present a continuous-mode model for optical cavities by building from the work presented in Chapter 5. The proposed model allows one to determine expressions for the electromagnetic field observables as a function of the optical properties of the mirrors. Expressions for the one-dimensional electromagnetic field observables for an optical cavity,

$\hat{E}_{\mathrm{cav}}(x)$ and $\hat{B}_{\mathrm{cav}}(x)$ are given in Eqs. (8.6) and (8.8), respectively. In addition, expressions for the three-dimensional electromagnetic field observables for an optical cavity, $\hat{\mathbf{E}}_{\mathrm{cav}}(\mathbf{r})$ and $\hat{\mathbf{B}}_{\mathrm{cav}}(\mathbf{r})$ are given in Eqs. (8.11) and (8.12), respectively. In both scenarios, one finds the system Hamiltonian $\hat{H}_{\mathrm{sys}}$, which describes the electromagnetic field and mirrors, takes the same form as the harmonic oscillator Hamiltonian (cf. Eqs. (8.10) and (8.13)). These results are expected to help model various scenarios such as coherent cavity networks [148] and quantum metrology schemes [149].

Chapter 9

Conclusions & future work

In this chapter the concluding remarks are presented first, followed by a discussion of potential future work.

Conclusions

This thesis has presented a novel approach to understanding how to impose boundary conditions, ultimately providing the image-detector method to describe the electromagnetic field in the presence of two-sided semi-transparent mirrors and within optical cavities, as well as potential applications in designing quantum technologies.

In Chapter 2 a theoretical background on classical electrodynamics was presented, followed by introducing the basic tools of quantum mechanics and how one quantises the electromagnetic field in free space. In Chapter 3 open quantum systems are discussed and a general derivation of a quantum optical master equation is presented. Applying a master equation description allows one to determine the spontaneous emission rate of a two-level atom in free space, Γ_{free}. Finally, Chapter 4 concludes the background section by presenting the well-known example of a dipole-dipole interaction in free space and analytical expressions for the collective spontaneous emission rates $\Gamma_\pm$ are determined.

Using the ideas outlined in the previous chapters, a novel approach to understanding how to impose boundary conditions is presented in Chapter 5. The image-detector method describes the electromagnetic field in the presence of a

two-sided semi-transparent mirror by mapping onto an analogous free space scenario and correctly models the long term behaviour of wave packets in the presence of a two-sided semi-transparent mirror. In Chapter 6 the image-detector method was applied to a radiating atom in the presence of a two-sided semi-transparent mirror, where analytical expressions for the spontaneous emission rate Γ_{mirr} were determined. In Chapter 7 the image-detector method was used to describe the mirror-mediated long-range dipole-dipole interaction, where analytical expressions for the collective spontaneous emission rates $\widetilde{\Gamma}_{\pm}$ are determined. Finally, in Chapter 8 the image-detector method is extended to describe an optical cavity.

The summary table shown in Fig. 9.1 compiles the quantum optical master equations and the associated spontaneous emission rates for each scenario discussed in the thesis. From above one can see the master equations for the various scenarios all take the same Lindblad form, which was the general form of a quantum optical master equation describing the interaction between a system and an external bath (discussed in Chapter 3). The master equations on row's one and three describe single atom systems, as the Lindblad operators $\hat{L}$ and $\hat{L}^{\dagger}$ take the form of the atomic lowering and raising operators $\hat{\sigma}^{-}$ and $\hat{\sigma}^{+}$. Row one describes the spontaneous emission of a single two-level atom (Chapter 3) and row three describes a radiating atom in the presence of a semi-transparent mirror (Chapter 6). On the other hand, the master equations on row's two and four describe two atom systems, where the Lindblad operators $\hat{L}$ and $\hat{L}^{\dagger}$ take the form of linear superpositions of the atomic lowering and raising operators $\hat{\sigma}^{-}$ and $\hat{\sigma}^{+}$ leading to interference effects. Row two describes the free space dipole-dipole interaction (Chapter 4) and row four describes the mirror-mediated dipole-dipole interaction (Chapter 7). The constants c_1 and c_2 shown in the spontaneous emission rates $\Gamma_{\pm}$ (row two) take the form $c_1 = 1 - \mu$ and $c_2 = 1 - 3\mu$ when both atoms have the same dipole moment $\hat{\mathbf{D}}_{12}^{(a)} = \hat{\mathbf{D}}_{12}^{(b)} = \hat{\mathbf{D}}_{12}$ where $\mu = \|\hat{\mathbf{D}}_{12} \cdot \hat{x}\|^2$ (cf. Eq. (4.15)). Similarly, the constants $\widetilde{c}_1$ and $\widetilde{c}_2$ shown in the spontaneous emission rates $\widetilde{\Gamma}_{\pm}$ (row four) take the form $\widetilde{c}_1 = 1 - \mu$ and $\widetilde{c}_2 = 1 + \mu$. Although the master equations remain of a similar form, the spontaneous emission rates for the systems change due to the atom(s) coupling to different surroundings, i.e. free electromagnetic field or the free electromagnetic field in the presence of a two-sided

Master Equation	Spontaneous Emission Rate
$\dot{\hat{\rho}}_{S1}(t) = \Gamma_{\text{free}}\left(\hat{\sigma}^-\hat{\rho}_{S1}(t)\hat{\sigma}^+ - \frac{1}{2}[\hat{\sigma}^+\hat{\sigma}^-,\hat{\rho}_{S1}(t)]_+\right)$	$\Gamma_{\text{free}} = \frac{e^2\|\mathbf{D}_{12}\|^2\omega_0^3}{3\pi\varepsilon_0 c^3\hbar}$
$\dot{\hat{\rho}}_{S1}(t) = \Gamma_\pm\left(\hat{L}\hat{\rho}_{S1}(t)\hat{L}^\dagger - \frac{1}{2}[\hat{L}^\dagger\hat{L},\hat{\rho}_{S1}(t)]_+\right)$	$\Gamma_\pm = \left[1 \pm \frac{3}{2}\left[c_1\frac{\sin(k_0 x)}{k_0 x} + c_2\left(\frac{\cos(k_0 x)}{(k_0 x)^2} - \frac{\sin(k_0 x)}{(k_0 x)^3}\right)\right]\right]\Gamma_{\text{free}}$
$\dot{\hat{\rho}}_{S1}(t) = \Gamma_{\text{mirr}}\left(\hat{\sigma}^-\hat{\rho}_{S1}(t)\hat{\sigma}^+ - \frac{1}{2}\frac{1}{2}[\hat{\sigma}^+\hat{\sigma}^-,\hat{\rho}_{S1}(t)]_+\right)$	$\Gamma_{\text{mirr}} = \left[\left[\frac{1+r_a^2}{\eta_a^2}\right] + \frac{3r_a}{\eta_a^2}\cos(\varphi_1)\left[\frac{\sin(2k_0 x)}{2k_0 x}(1-\mu) + \left(\frac{\cos(2k_0 x)}{(2k_0 x)^2} - \frac{\sin(2k_0 x)}{(2k_0 x)^3}\right)(1+\mu)\right]\right]\Gamma_{\text{free}}$
$\dot{\hat{\rho}}_{S1}(t) = \widetilde{\Gamma}_\pm\left(\hat{L}\hat{\rho}_{S1}(t)\hat{L}^\dagger - \frac{1}{2}[\hat{L}^\dagger\hat{L},\hat{\rho}_{S1}(t)]_+\right)$	$\widetilde{\Gamma}_\pm = \left[\frac{1}{\eta_a^2}[1 + t\cos(\varphi_2)] \pm \frac{3r}{2\eta_a^2}\cos(\varphi_1)\left[\frac{\sin(k_0\widetilde{x})}{k_0\widetilde{x}}\widetilde{c}_1 + \left(\frac{\cos(k_0\widetilde{x})}{(k_0\widetilde{x})^2} - \frac{\sin(k_0\widetilde{x})}{(k_0\widetilde{x})^3}\right)\widetilde{c}_2\right]\right]\Gamma_{\text{free}}$

Figure 9.1: A summary table showing the Lindblad master equations and the associated spontaneous emission rates for different scenarios. The first row describes the interaction of an atom and the free electromagnetic field generating a finite probability of a photon emission Γ_{free} (Chapter 3) and the second row describes the free-space dipole-dipole interaction with the associated rates $\Gamma_\pm$ (Chapter 4). In addition, the third row describes the scenario of a radiating atom in the presence of a two-sided semi-transparent mirror, where the spontaneous emission rate Γ_{mirr} is applicable to an atom placed at some position $x > 0$ (Chapter 6). Finally, the fourth row describes the mirror-mediated long-range dipole-dipole interaction with spontaneous emission rates $\widetilde{\Gamma}_\pm$ (Chapter 7). The master equations all take a similar form, i.e. a quantum system coupled to external bath (cf. Eq. (3.2)). However, the spontaneous emission rates change as the atomic systems couple to different external baths e.g. free electromagnetic field or free electromagnetic field and a two-sided semi-transparent mirror.

semi-transparent mirror. Particularly in the case of a semi-transparent mirror, the mirror surface affects how and where electric field amplitudes can be measured - a key idea behind the image-detector method. The spontaneous emission rates for these systems, particularly those for the long-range dipole-dipole interaction (row four of summary table) should provide insight into the functionality of a non-invasive glucose sensing quantum technology being designed in the Chemical Engineering department at the University of Leeds [141–144].

Future work

Dipole interaction coupled to a thermal bath

An extension of the work presented in Chapter 7 could consider the mirror-mediated dipole interaction where the electromagnetic field resides in a thermal state, rather than the vacuum state. This would allow both atoms to acquire excitations from the bath, which could lead to further enhancements to the spontaneous emission rates $\widetilde{\Gamma}_\pm$ (cf. Eq. (7.24)).

Transmission rate of a Fabry-Pérot cavity

An extension of the work presented in Chapter 8 could model a laser-driven Fabry-Pérot cavity and compare the results with Fig. 1.1. Using Fig. 8.1 and laser driving the cavity from the left-hand side at its resonant frequency ω_0, one can then examine what leaves the cavity on the right-hand side of the setup. The transmission rate of the optical cavity is then given by the ratio of the modulus of the two field amplitudes; the transmitted field and the incident field (see Ref. [2]).

Casimir effect

In reality, the dipole interactions considered in this thesis are all part of a much larger picture, intermolecular forces which are more commonly known as van der Waals forces or London dispersion forces (which are effective dipole-dipole interactions). These dispersion forces attract two atoms or molecules together when separated by a distance d. In the non-retarded regime this force is proportional

to d^{-3} for the short-range separation and proportional to d^{-6} for the long-range separation, which is also consistent with classical dipole interactions. By explicitly considering the role of retardation (light travels at a finite speed meaning the interaction does not happen instantaneously) in these interactions, then one finds the interaction varies as d^{-7} [150]. This scenario was first investigated by Casimir and Polder using two neural atoms, which was extended to study the interaction between a neutral atom and a solid boundary. The atom and solid boundary scenario has since been revisited more recently [151–155].

The above scenario also links into the Casimir effect which was predicted in 1948 and has since developed into a large field of research in its own right. The Casimir effect manifests itself as an attractive force between two flat and neutrally-charged conducting plates [156]. The Casimir force is proportional to d^{-4}, where d is the plate separation. Previously, authors have attributed this effect to fluctuations in the electromagnetic vacuum, which in some cases has been attributed to a consequence of the canonical quantisation [150] (the electromagnetic field is treated as a collection of harmonic oscillators each with a zero-point energy of $\frac{1}{2}\hbar\omega$). For more in-depth reviews and interpretations of these topics, see Refs. [84, 157–160]. Although the existence of the Casimir effect is said to have been experimentally verified [161, 162], some authors still debate whether the effect exists or whether such an effect is too small to measure [163].

As a scope for future work, one could implement the cavity quantisation scheme outlined in Chapter 8 in an attempt to predict the correct scaling of the zero-temperature Casimir force and attribute the effect to a dipole-dipole interaction between atoms sitting on the mirror surfaces or opposing mirrors.

Appendix A

Master equation for dipole-dipole interaction in free space

In this supplementary chapter I present some of the details and calculations required to derive a master equation for the dipole-dipole interaction between a pair of atoms coupled to the free-electromagnetic field. First I will outline the steps required to obtain the conditional Hamiltonian $\hat{H}_{\mathrm{cond\,I}}(t)$ and then the reset operator $\mathcal{L}(\hat{\rho}_{\mathrm{S\,I}}(t))$.

A.1 $\hat{H}_{\mathrm{cond\,I}}(t)$ for dipole-dipole interaction in free space

The first step requires substituting the interaction picture Hamiltonian $\hat{H}_{\mathrm{I}}(t)$ from Eq. (4.9) into the expression derived for the conditional Hamiltonian $\hat{H}_{\mathrm{cond\,I}}(t)$ in Eq. (3.25). Doing so, one finds that the conditional Hamiltonian $\hat{H}_{\mathrm{cond\,I}}(t)$ of an atom in free space equals

$$
\begin{aligned}
\hat{H}_{\mathrm{cond\,I}}(t) \;=\; & -\frac{\mathrm{i}\hbar}{\Delta t} \int\limits_{t}^{t+\Delta t} \mathrm{d}t' \int\limits_{t}^{t'} \mathrm{d}t'' \sum_{i,j=a,b} \sum_{\lambda=1,2} \int_{\mathbb{R}^3} \mathrm{d}^3\mathbf{k}\, \frac{e^2\omega}{16\pi^3\varepsilon_0\hbar}\, \mathrm{e}^{-\mathrm{i}(\omega-\omega_0)(t'-t'')} \\
& \times \left(\hat{\mathbf{D}}_{12}^{(i)*}\cdot\hat{\mathbf{e}}_{\mathbf{k}\lambda}\right)\left(\hat{\mathbf{D}}_{12}^{(j)}\cdot\hat{\mathbf{e}}_{\mathbf{k}\lambda}\right) \mathrm{e}^{\mathrm{i}\mathbf{k}\cdot(\mathbf{r_i}-\mathbf{r_j})}\, \hat{\sigma}_i^+\hat{\sigma}_j^- \qquad (\mathrm{A.1})
\end{aligned}
$$

Again making use of Eqs. (3.45) – (3.47) as well as the atomic dipole moments defined in Eq. (7.6), one finds that

$$
\hat{H}_{\text{cond I}}(t) = -\frac{\mathrm{i}\hbar}{\Delta t} \int\limits_{t}^{t+\Delta t} \mathrm{d}t' \int\limits_{t}^{t'} \mathrm{d}t'' \int_0^\infty \mathrm{d}\omega \int_0^\pi \mathrm{d}\vartheta \, \sin(\vartheta) \int_0^{2\pi} \mathrm{d}\phi \, \frac{e^2 \left\| \mathbf{D}_{12} \right\|^2 \omega^3}{16\pi^3 \varepsilon_0 c^3 \hbar}
$$

$$
\times \mathrm{e}^{-\mathrm{i}(\omega-\omega_0)(t'-t'')} \left\{ \left[|d_1^{(a)}|^2 \left(1 - \cos^2(\vartheta)\right) + |d_3^{(a)}|^2 \left(1 - \sin^2(\vartheta)\sin^2(\phi)\right) \right. \right.
$$

$$
\left. + \left(d_1^{(a)*} d_3^{(a)} + d_3^{(a)*} d_1^{(a)} \right) \sin(\vartheta) \cos(\vartheta) \sin(\phi) \right] \hat{\sigma}_a^+ \hat{\sigma}_a^-
$$

$$
+ \, \mathrm{e}^{-\mathrm{i}\mathbf{k}\cdot(\mathbf{r}_a-\mathbf{r}_b)} \times \left[d_1^{(a)*} d_1^{(b)} \left(1 - \cos^2(\vartheta)\right) + d_3^{(a)*} d_3^{(b)} \left(1 - \sin^2(\vartheta)\sin^2(\phi)\right) \right.
$$

$$
+ d_1^{(a)*} d_2^{(b)} \sin(\vartheta) \cos(\vartheta) \cos(\phi) + d_1^{(a)*} d_3^{(b)} \sin(\vartheta) \cos(\vartheta) \sin(\phi)
$$

$$
+ d_3^{(a)*} d_1^{(b)} \sin(\vartheta) \cos(\vartheta) \sin(\phi) + d_3^{(a)*} d_2^{(b)} \sin^2(\vartheta) \sin(\phi) \cos(\phi) \right] \hat{\sigma}_a^+ \hat{\sigma}_b^-
$$

$$
+ \, \mathrm{e}^{\mathrm{i}\mathbf{k}\cdot(\mathbf{r}_a-\mathbf{r}_b)} \times \left[d_1^{(b)*} d_1^{(a)} \left(1 - \cos^2(\vartheta)\right) + d_3^{(b)*} d_3^{(a)} \left(1 - \sin^2(\vartheta)\sin^2(\phi)\right) \right.
$$

$$
+ d_1^{(b)*} d_3^{(a)} \sin(\vartheta) \cos(\vartheta) \sin(\phi) + d_3^{(b)*} d_1^{(a)} \sin(\vartheta) \cos(\vartheta) \sin(\phi)
$$

$$
+ d_3^{(b)*} d_2^{(a)} \sin^2(\vartheta) \sin(\phi) \cos(\phi) \right] \hat{\sigma}_b^+ \hat{\sigma}_a^-
$$

$$
+ \left[|d_1^{(b)}|^2 \left(1 - \cos^2(\vartheta)\right) + |d_2^{(b)}|^2 \left(1 - \sin^2(\vartheta)\cos^2(\phi)\right) \right.
$$

$$
+ |d_3^{(b)}|^2 \left(1 - \sin^2(\vartheta)\sin^2(\phi)\right) + d_1^{(b)*} d_2^{(b)} \sin(\vartheta) \cos(\vartheta) \cos(\phi)
$$

$$
+ d_1^{(b)*} d_3^{(b)} \sin(\vartheta) \cos(\vartheta) \sin(\phi) + d_2^{(b)*} d_1^{(b)} \sin(\vartheta) \cos(\vartheta) \cos(\phi)
$$

$$
+ d_2^{(b)*} d_3^{(b)} \sin^2(\vartheta) \sin(\phi) \cos(\phi) + d_3^{(b)*} d_1^{(b)} \sin(\vartheta) \cos(\vartheta) \sin(\phi)
$$

$$
\left. \left. + d_3^{(b)*} d_2^{(b)} \sin^2(\vartheta) \sin(\phi) \cos(\phi) \right] \hat{\sigma}_b^+ \hat{\sigma}_b^- \right\}. \tag{A.2}
$$

The exponential terms in the above equation can be simplified using the definition of the wave vector $\mathbf{k}$ and Fig. 4.3. In other words, the atoms are aligned

along the x-axis such that

$$\mathbf{r}_a - \mathbf{r}_b = \begin{pmatrix} x_a - x_b \\ 0 \\ 0 \end{pmatrix} = \begin{pmatrix} x \\ 0 \\ 0 \end{pmatrix}. \tag{A.3}$$

In the following, $x \equiv |x_a - x_b| \equiv |x_b - x_a|$ denotes the distance between the two atoms (see Eq. (4.13)). Therefore, one can re-express the exponential terms in the following way

$$e^{i\mathbf{k}\cdot(\mathbf{r}_a - \mathbf{r}_b)} = e^{ik\cos(\vartheta)x}. \tag{A.4}$$

The atomic separation x is of the same order of magnitude as the wavelength of the emitted radiation λ_0. Taking this into account and performing the ϕ-integration, whilst introducing the new variable $s = \cos(\vartheta)$, yields

$$\hat{H}_{\text{cond I}}(t) = -\frac{i\hbar}{\Delta t} \int\limits_t^{t+\Delta t} dt' \int\limits_t^{t'} dt'' \int_0^\infty d\omega \int_{-1}^1 ds \frac{e^2 \|\mathbf{D}_{12}\|^2 \omega^3}{8\pi^2 \varepsilon_0 c^3 \hbar} e^{-i(\omega - \omega_0)(t' - t'')}$$

$$\times \Bigg\{ \left[|d_1^{(a)}|^2 (1 - s^2) + \frac{1}{2} |d_3^{(a)}|^2 (1 + s^2) \right] \hat{\sigma}_a^+ \hat{\sigma}_a^-$$

$$+ e^{ikxs} \times \left[d_1^{(a)*} d_1^{(b)} (1 - s^2) + \frac{1}{2} d_3^{(a)*} d_3^{(b)} (1 + s^2) \right] \hat{\sigma}_a^+ \hat{\sigma}_b^-$$

$$+ e^{ikxs} \times \left[d_1^{(b)*} d_1^{(a)} (1 - s^2) + \frac{1}{2} d_3^{(b)*} d_3^{(a)} (1 + s^2) \right] \hat{\sigma}_b^+ \hat{\sigma}_a^-$$

$$+ \left[|d_1^{(b)}|^2 (1 - s^2) + \frac{1}{2} |d_2^{(b)}|^2 (1 + s^2) + \frac{1}{2} |d_3^{(b)}|^2 (1 + s^2) \right] \hat{\sigma}_b^+ \hat{\sigma}_b^- \Bigg\}. \tag{A.5}$$

Evaluating the s-integration, one obtains the following conditional Hamiltonian

$$\hat{H}_{\text{cond I}}(t) = -\frac{i\hbar}{2} \frac{1}{\Delta t} \frac{\Gamma_{\text{free}}}{\pi \omega_0^3} \int\limits_t^{t+\Delta t} dt' \int\limits_t^{t'} dt'' \int_0^\infty d\omega\, \omega^3\, e^{-i(\omega - \omega_0)(t' - t'')}$$

$$\times \Bigg\{ \hat{\sigma}_a^+ \hat{\sigma}_a^- + \frac{3}{2} \left[\frac{\sin(kx)}{kx} c_1 + \left(\frac{\cos(kx)}{(kx)^2} - \frac{\sin(kx)}{(kx)^3} \right) c_2 \right] \hat{\sigma}_a^+ \hat{\sigma}_b^-$$

$$+ \frac{3}{2} \left[\frac{\sin(kx)}{kx} c_1^* + \left(\frac{\cos(kx)}{(kx)^2} - \frac{\sin(kx)}{(kx)^3} \right) c_2^* \right] \hat{\sigma}_b^+ \hat{\sigma}_a^- + \hat{\sigma}_b^+ \hat{\sigma}_b^- \Bigg\}, \tag{A.6}$$

where the constants c_1 and c_2 are consistent with Eq. (4.14). Therefore, one obtains the conditional Hamiltonian

$$
\hat{H}_{\text{cond I}}(t) = \hbar \left[C_{\text{a-a}} \, \hat{\sigma}_a^+ \hat{\sigma}_a^- + C_{\text{a-b}}(x) \, \hat{\sigma}_a^+ \hat{\sigma}_b^- + C_{\text{b-a}}(x) \, \hat{\sigma}_b^+ \hat{\sigma}_a^- + C_{\text{b-b}} \, \hat{\sigma}_b^+ \hat{\sigma}_b^- \right].
$$
(A.7)

In order to obtain real dipole moments, one requires both atoms to have the same dipole moment such that $\hat{\mathbf{D}}_{12}^{(a)} = \hat{\mathbf{D}}_{12}^{(b)}$ in Eq. (7.6) [1]. Moreover, this means that $C_{a-b}(x) = C_{b-a}(x) = C(x)$. In addition, it will also be demonstrated that both constants C_{a-a} and C_{b-b} coincide such that $C_{a-a} = C_{b-b} = A$, where A is some constant. This means one can simplify Eq. (A.7) into the compact form

$$
\hat{H}_{\text{cond I}}(t) = \hbar \left[A \left(\hat{\sigma}_a^+ \hat{\sigma}_a^- + \hat{\sigma}_b^+ \hat{\sigma}_b^- \right) + C(x) \left(\hat{\sigma}_a^+ \hat{\sigma}_b^- + \hat{\sigma}_b^+ \hat{\sigma}_a^- \right) \right].
$$
(A.8)

Isolating the two constants from the above equation separately and comparing with the expression in Eq. (A.6), one finds that

$$
A = -\frac{i}{2\pi} \frac{\Gamma_{\text{free}}}{\omega_0^3} \frac{1}{\Delta t} \int_t^{t+\Delta t} dt' \int_t^{t'} dt'' \int_0^\infty d\omega \, \omega^3 \, e^{-i(\omega - \omega_0)(t' - t'')}, \quad \text{(A.9)}
$$

where the free-space spontaneous decay rate Γ_{free} is defined as in Eq. (3.62). Similarly, one finds that

$$
\begin{aligned}
C(x) = &-\frac{i}{2\pi} \frac{\Gamma_{\text{free}}}{\omega_0^3} \frac{1}{\Delta t} \int_t^{t+\Delta t} dt' \int_t^{t'} dt'' \int_0^\infty d\omega \, \omega^3 \, e^{-i(\omega - \omega_0)(t' - t'')} \\
&\times \frac{3}{2} \left\{ \frac{\sin(kx)}{kx} c_1 + \left(\frac{\cos(kx)}{(kx)^2} - \frac{\sin(kx)}{(kx)^3} \right) c_2 \right\}.
\end{aligned}
$$
(A.10)

In order to evaluate the remaining integrals in Eqs. (A.11) and (A.12) one is required to making the substitution, $\widetilde{\omega} = \omega - \omega_0$. Doing so, one finds that Eq. (A.11) reduces to

$$
A = -\frac{i}{2\pi} \frac{\Gamma_{\text{free}}}{\omega_0^3} \frac{1}{\Delta t} \int_t^{t+\Delta t} dt' \int_t^{t'} dt'' \int_0^\infty d\omega \, \omega^3 \, e^{-i\widetilde{\omega}}, \quad \text{(A.11)}
$$

---

[1]If complex dipole moments were allowed this could potentially lead to extra damping on the spontaneous emission rate for the system

and Eq. (A.12) reduces to

$$
\begin{aligned}
C(x) &= -\frac{\mathrm{i}}{2\pi}\frac{\Gamma_{\mathrm{free}}}{\omega_0^3}\frac{1}{\Delta t}\int_t^{t+\Delta t}\mathrm{d}t'\int_t^{t'}\mathrm{d}t''\int_0^\infty \mathrm{d}\omega\,\omega^3\,\mathrm{e}^{-\mathrm{i}\tilde{\omega}(t'-t'')} \\
&\quad\times\frac{3}{2}\left\{\frac{\sin(kx)}{kx}c_1+\left(\frac{\cos(kx)}{(kx)^2}-\frac{\sin(kx)}{(kx)^3}\right)c_2\right\}.
\end{aligned}
\tag{A.12}
$$

The next step is to evaluate the remaining frequency and time integrations. To do so, $\sin(kx)$ and $\cos(kx)$ are decomposed into exponentials. Afterwards, one substitutes $k=\omega/c$ and $\tilde{\omega}=\omega-\omega_0$. Moreover, one considers time intervals Δt such that

$$
\omega_0 \gg 1/\Delta t\,,
\tag{A.13}
$$

which is physically well justified by the fact that spontaneous emissions in the optical regime obey exponential decay laws [48, 49]. This observation allows one to extend the lower limit of the $\tilde{\omega}$-integral to minus infinity, an approximation also made by previous authors. Infinitely large level shifts (i.e. free-space level shifts) can be absorbed into the definition of the atomic transition frequency ω_0 and one assumes that

$$
\begin{aligned}
\int_{-\infty}^\infty \mathrm{d}\tilde{\omega}\,\tilde{\omega}^2\,\mathrm{e}^{-\mathrm{i}\tilde{\omega}(t'-t''-x/c)} &= -2\pi\,\delta''(t'-t''-x/c)\,, \\
\int_{-\infty}^\infty \mathrm{d}\tilde{\omega}\,\tilde{\omega}\,\mathrm{e}^{-\mathrm{i}\tilde{\omega}(t'-t''-x/c)} &= -2\mathrm{i}\pi\,\delta'(t'-t''-x/c)\,, \\
\int_{-\infty}^\infty \mathrm{d}\tilde{\omega}\,\mathrm{e}^{-\mathrm{i}\tilde{\omega}(t'-t''-x/c)} &= 2\pi\,\delta(t'-t''-x/c)\,,
\end{aligned}
\tag{A.14}
$$

where δ' and δ'' are the first and the second time derivative of the δ-function with respect to t'' and x/c denotes some constant. When introducing the exponential form of $\sin(kx)$ and $\cos(kx)$ into Eq. (A.12), one also finds terms proportional to to $\delta(t'-t''+x/c)$. These terms do not contribute to the integration as they do not exist within the time interval considered here [1]. The delta function $\delta(t'-t''-x/c)$ also does not contribute if the time period Δt is smaller than x/c. This means that

$$
\Delta t \gg x/c\,,
\tag{A.15}
$$

---

[1]The derivatives of the δ-function also do not contribute

which means that the chosen time period must be greater than the time it takes for light to travel the path between the atoms. In order to simplify the application, it is worthwhile to introduce a second approximation, namely to neglect any retardation contribution x/c. This makes sense if the atomic separation lies in the order of magnitude of the wavelength λ_0, as it has already been assumed that $\Delta t \gg 1/\omega_0$. Therefore, $\Delta t \gg 1/\omega_0 \approx x/c$ is then automatically fulfilled as well. Finally, performing the time integration, one must assume that the distance of the atoms is not so large that retardation effects need to be taking into account, i.e.

$$\Delta t \;\gg\; k_0 x\,. \tag{A.16}$$

Doing so, we eventually obtain the conditional Hamiltonian

$$\hat{H}_{\mathrm{cond\,I}}(t) \;=\; -\frac{\mathrm{i}\hbar}{2}\left[\Gamma_{\mathrm{free}}\hat{\sigma}_a^+\hat{\sigma}_a^- + C(x)\left(\hat{\sigma}_a^+\hat{\sigma}_b^- + \hat{\sigma}_b^+\hat{\sigma}_a^-\right) + \Gamma_{\mathrm{free}}\hat{\sigma}_b^+\hat{\sigma}_b^-\right], \tag{A.17}$$

where the dipole-coupling constant is given in Eq. (4.12).

A.2 $\mathcal{L}(\hat{\rho}_{\mathrm{S\,I}}(t))$ for dipole-dipole interaction in free space

To obtain an expression for the reset operator $\mathcal{L}(\hat{\rho}_{\mathrm{S\,I}}(t))$, one again makes use of the interaction picture Hamiltonian $\hat{H}_{\mathrm{SB\,I}}(t)$ from Eq. (4.9) and substitutes this into the reset operator expression in Eq. (3.26). Substituting in from Eq. (4.9), one finds

$$
\begin{aligned}
\mathcal{L}(\hat{\rho}_{\mathrm{S\,I}}(t)) \;=\; & \frac{1}{\Delta t}\int_t^{t+\Delta t}\mathrm{d}t'\int_t^{t+\Delta t}\mathrm{d}t''\sum_{i=a,b}\sum_{\lambda=1,2}\int_{\mathbb{R}^3}\mathrm{d}^3\mathbf{k}\,\frac{e^2\omega}{16\pi^3\varepsilon_0\hbar}\,\mathrm{e}^{\mathrm{i}(\omega-\omega_0)(t'-t'')} \\
& \times\left(\hat{\mathbf{D}}_{12}^{(i)*}\cdot\hat{\mathbf{e}}_{\mathbf{k}\lambda}\right)\left(\hat{\mathbf{D}}_{12}^{(j)}\cdot\hat{\mathbf{e}}_{\mathbf{k}\lambda}\right)\mathrm{e}^{-\mathrm{i}\mathbf{k}\cdot(\mathbf{r}_i-\mathbf{r}_j)} \\
& \times\langle 1_{\mathbf{k}\lambda}|\hat{a}_{\mathbf{k}\lambda}^\dagger|0_{\mathbf{k}\lambda}\rangle\hat{\sigma}_j^-\hat{\rho}_{\mathrm{S\,I}}(t)\hat{\sigma}_i^+\langle 0_{\mathbf{k}\lambda}|\hat{a}_{\mathbf{k}\lambda}|1_{\mathbf{k}\lambda}\rangle\,.
\end{aligned}
\tag{A.18}
$$

Following the same process as in the previous subsection and this time making use of

$$\int_{t'-(t+\Delta t)}^{t'-t}\mathrm{d}\xi\,\mathrm{e}^{\mathrm{i}(\omega-\omega_0)\xi} \;=\; \int_{-\infty}^\infty\mathrm{d}\xi\,\mathrm{e}^{\mathrm{i}(\omega-\omega_0)\xi} = 2\pi\delta(\omega-\omega_0)\,, \tag{A.19}$$

one finds this generates a reset operator of the from

$$
\begin{aligned}
\mathcal{L}(\hat{\rho}_{\mathrm{SI}}(t)) \;=\; & \Gamma_{\mathrm{free}} \left[\hat{\sigma}_a^- \hat{\rho}_{\mathrm{SI}}(t) \hat{\sigma}_a^+ + \hat{\sigma}_b^- \hat{\rho}_{\mathrm{SI}}(t) \hat{\sigma}_b^+ \right] \\
& + \mathrm{Re}(C(x)) \left[\hat{\sigma}_b^- \hat{\rho}_{\mathrm{SI}}(t) \hat{\sigma}_a^+ + \hat{\sigma}_a^- \hat{\rho}_{\mathrm{SI}}(t) \hat{\sigma}_b^+ \right] ,
\end{aligned}
\tag{A.20}
$$

with the dipole-coupling constant is given in Eq. (4.12).

Appendix B

Calculation of classical phase shifts for two-sided semi-transparent mirrors

The aim of this supplementary chapter is to derive a relation between the phase shifts of incoming and outgoing wave packets as they interact with a two-sided semi-transparent mirror. Here, I consider the specific case from 5.2.3 where light is incident on both sides of a semi-transparent mirror. Note that for the perfect mirror case when light incident from both sides, one does not need to worry about this problem as the wave packets live in separate Hilbert spaces and will therefore never meet.

Suppose two relatively well-localised wave packets approach a semi-transparent mirror from either side. Considering only one specific frequency contribution of these wave packets with positive wave number k and with

$$
\begin{aligned}
E_{\text{mirr}}^{(a)}(x,0) &= \left[E_0^{(a)} \, e^{i\xi_1} \, e^{-ikx} + \text{c.c.} \right] \Theta(x) \, , \\
E_{\text{mirr}}^{(b)}(x,0) &= \left[E_0^{(b)} \, e^{i\xi_2} \, e^{ikx} + \text{c.c.} \right] \Theta(-x) \, ,
\end{aligned}
\tag{B.1}
$$

where $E_0^{(a)}$ and $E_0^{(b)}$ denote real amplitudes and ξ_1 and ξ_2 specify initial phases. After a sufficiently long time, once both wave packets have seen the mirror, the

electric field $E_{\mathrm{mirr}}(x, t)$ is given by

$$
\begin{aligned}
E_{\mathrm{mirr}}(x, t) \;=\; & \left[r_a\, E_0^{(a)}\, \mathrm{e}^{\mathrm{i}(\xi_1 + \varphi_1)}\, \mathrm{e}^{\mathrm{i}(kx - \omega t)} \right. \\
& \left. + t_b\, E_0^{(b)}\, \mathrm{e}^{\mathrm{i}(\xi_2 + \varphi_2)}\, \mathrm{e}^{\mathrm{i}(kx - \omega t)} \right] \Theta(x)\,, \\
& + \left[r_b\, E_0^{(b)}\, \mathrm{e}^{\mathrm{i}(\xi_2 + \varphi_3)}\, \mathrm{e}^{-\mathrm{i}(kx + \omega t)} \right. \\
& \left. + t_a\, E_0^{(a)}\, \mathrm{e}^{\mathrm{i}(\xi_1 + \varphi_4)}\, \mathrm{e}^{-\mathrm{i}(kx + \omega t)} \right] \Theta(-x) \\
& + \mathrm{c.c.}\,,
\end{aligned}
\tag{B.2}
$$

which is in agreement with Eq. (5.9). Rearranging this equation, one finds that $E_{\mathrm{mirr}}(x, t)$ also equals

$$
\begin{aligned}
E_{\mathrm{mirr}}(x, t) \;=\; & \left[r_a\, E_0^{(a)} + t_b\, E_0^{(b)}\, \mathrm{e}^{\mathrm{i}(\xi_2 - \xi_1 + \varphi_2 - \varphi_1)} \right] \\
& \times \mathrm{e}^{\mathrm{i}(\xi_1 + \varphi_1)}\, \mathrm{e}^{\mathrm{i}(kx - \omega t)}\, \Theta(x)\,, \\
& + \left[t_a\, E_0^{(a)} + r_b\, E_0^{(b)}\, \mathrm{e}^{\mathrm{i}(\xi_2 - \xi_1 + \varphi_3 - \varphi_4)} \right] \\
& \times \mathrm{e}^{\mathrm{i}(\xi_1 + \varphi_4)}\, \mathrm{e}^{-\mathrm{i}(kx + \omega t)}\, \Theta(-x) + \mathrm{c.c.}
\end{aligned}
\tag{B.3}
$$

which shows that maximum interference of electric field amplitudes on one side of the mirror *always* implies minimum interference on the other side, when

$$
\mathrm{e}^{\mathrm{i}(\xi_2 - \xi_1 + \varphi_2 - \varphi_1)} \;=\; -\mathrm{e}^{\mathrm{i}(\xi_2 - \xi_1 + \varphi_3 - \varphi_4)}\,.
\tag{B.4}
$$

This equation yields

$$
\varphi_1 - \varphi_2 + \varphi_3 - \varphi_4 \;=\; \pm(2n + 1)\,\pi\,,
\tag{B.5}
$$

which is consistent with Eq. (5.11) in the main text. The same applies for the magnetic field amplitudes which interfere in the same way on the same side of the mirror, as the electric field amplitudes.

Appendix C

Calculation of field Hamiltonian for one-sided perfect mirror

In this supplementary chapter I derive an expression for the field Hamiltonian $\hat{H}_{\text{field}}$ for the one-sided perfect mirror scenario. To do so, one must substitute the electromagnetic field observables $\hat{E}_{\text{mirr}}(x)$ and $\hat{B}_{\text{mirr}}(x)$ from Eq. (5.18) into Eq. (2.62), which yields

$$
\begin{aligned}
\hat{H}_{\text{field}} \;=\; & \frac{A}{2} \int_0^\infty \mathrm{d}x \int_{-\infty}^\infty \mathrm{d}k \int_{-\infty}^\infty \mathrm{d}k' \, \frac{\hbar}{4\pi\varepsilon_0 A c} \sqrt{\omega\omega'} \\
& \times 2\varepsilon_0 c^2 \left[\left(\mathrm{e}^{\mathrm{i}kx}\hat{\xi}_k - \mathrm{e}^{-\mathrm{i}kx}\hat{\xi}_k^\dagger \right) \left(\mathrm{e}^{\mathrm{i}k'x}\hat{\xi}_{k'} - \mathrm{e}^{-\mathrm{i}k'x}\hat{\xi}_{k'}^\dagger \right) \right] \times \left[1 + \mathrm{sign}(kk') \right]
\end{aligned} \quad (C.1)
$$

Keeping the relevant terms, one finds that this field Hamiltonian can also be written as

$$
\begin{aligned}
\hat{H}_{\text{field}} \;=\; & -\frac{\hbar}{8\pi} \int_{-\infty}^0 \mathrm{d}x \int_{-\infty}^\infty \mathrm{d}k \int_{-\infty}^\infty \mathrm{d}k' \, \sqrt{\omega\omega'} \\
& \times \left(\mathrm{e}^{\mathrm{i}kx}\hat{\xi}_k - \mathrm{e}^{-\mathrm{i}kx}\hat{\xi}_k^\dagger \right) \left(\mathrm{e}^{\mathrm{i}k'x}\hat{\xi}_{k'} - \mathrm{e}^{-\mathrm{i}k'x}\hat{\xi}_{k'}^\dagger \right) \times \left[1 + \mathrm{sign}(kk') \right] . \quad (C.2)
\end{aligned}
$$

Finally, employing the relation

$$
\int_0^\infty \mathrm{d}x \, \mathrm{e}^{\pm \mathrm{i}k_0 x} \;=\; \pi \, \delta(k_0) , \qquad (C.3)
$$

where k_0 denotes a constant, to show that

$$
\hat{H}_{\text{field}} \;=\; \frac{1}{2} \int_{-\infty}^\infty \mathrm{d}k \, \hbar\omega \left[\hat{\xi}_k^\dagger \hat{\xi}_k + \hat{\xi}_k \hat{\xi}_k^\dagger \right] . \qquad (C.4)
$$

The above Hamiltonian can then be re-expressed in the standard harmonic oscillator form using the ξ-mode description. This yields the field Hamiltonian

$$\hat{H}_{\text{field}} \;\; = \;\; \int_{-\infty}^{\infty} \mathrm{d}k \, \hbar\omega \, \hat{\xi}_k^{\dagger} \hat{\xi}_k \, , \tag{C.5}$$

up to a constant summand. Therefore, Eqs. (C.4) and (C.5) differ by this constant summand, which is determined by the commutation relation of the operators $\hat{\xi}_k$ and $\hat{\xi}_k^{\dagger}$. However, as this constant is not necessary for any of the calculations performed here, one can neglect it and obtain the field Hamiltonian given in Eq. (C.5).

Appendix D

Calculation of master equation for a radiating atom in the presence of a two-sided semi-transparent mirror

In this supplementary chapter some of the details and calculations required to derive a master equation for a radiating atom in the presence of a two-sided semi-transparent mirror. First the steps required to obtain the conditional Hamiltonian $\hat{H}_{\mathrm{cond\,I}}(t)$ are outlined and then the reset operator $\mathcal{L}(\hat{\rho}_{\mathrm{S\,I}}(t))$.

D.1 $\hat{H}_{\mathrm{cond\,I}}(t)$ for an atom in the presence of a semi-transparent mirror

As before, one combines Eqs. (3.25) and (6.3) to find that the conditional Hamiltonian $H_{\mathrm{cond\,I}}(t)$ of a radiating atom near a semi-transparent mirror is equal to

$$
\begin{aligned}
\hat{H}_{\mathrm{cond\,I}}(t) &= -\frac{\mathrm{i}\hbar}{\Delta t} \int_{t}^{t+\Delta t} \mathrm{d}t' \int_{t}^{t'} \mathrm{d}t'' \sum_{\lambda=1,2} \int_{\mathbb{R}^3} \mathrm{d}^3\mathbf{k}\, \frac{e^2\omega}{16\pi^3\varepsilon_0\hbar} \\
&\quad \times \left[\frac{1}{\eta_a^2} \left| \left(\hat{\mathbf{D}}_{12}^* \, \mathrm{e}^{\mathrm{i}\mathbf{k}\cdot\mathbf{r}} - r_a \, \hat{\tilde{\mathbf{D}}}_{12}^* \, \mathrm{e}^{\mathrm{i}\mathbf{k}\cdot\tilde{\mathbf{r}}} \right) \cdot \hat{\mathbf{e}}_{\mathbf{k}\lambda} \right|^2 + \dots \right]
\end{aligned}
$$

D.1 $\hat{H}_{\text{cond I}}(t)$ for an atom in the presence of a semi-transparent mirror

$$+... \frac{t_b^2}{\eta_b^2}\left|\left(\hat{\mathbf{D}}_{12}^\star \cdot \hat{\mathbf{e}}_{\mathbf{k}\lambda}\right)\right|^2\right] \mathrm{e}^{-\mathrm{i}(\omega-\omega_0)(t'-t'')}\,\hat{\sigma}^+\hat{\sigma}^-. \tag{D.1}$$

Again, it is appropriate to express the atomic dipole moment $\hat{\mathbf{D}}_{12}$ as in Eq. (3.43), with $|d_1|^2 + |d_3|^2 = 1$. In addition, in this coordinate system, the dipole moment $\hat{\tilde{\mathbf{D}}}_{12}$ of the mirror image of the atom equals

$$\hat{\tilde{\mathbf{D}}}_{12} = \|\mathbf{D}_{12}\| \begin{pmatrix} -d_1 \\ 0 \\ d_3 \end{pmatrix}. \tag{D.2}$$

As in Chapter 3, one can make use of Eqs. (3.45) – (3.47) to simplify the integrals in Eq. (D.1). Implementing these relations and defining μ as in Eq. (6.8) implies $|d_1|^2 = \mu$ and $|d_3|^2 = 1 - \mu$. Taking this into account and performing the ϕ integration, whilst introducing two new variables $s = \cos(\vartheta)$ and $\xi = t' - t''$, which yields

$$\begin{aligned}
\hat{H}_{\text{cond I}}(t) &= -\frac{\mathrm{i}\hbar}{\Delta t} \int\limits_t^{t+\Delta t} \mathrm{d}t' \int\limits_0^{t'-t} \mathrm{d}\xi \int_0^\infty \mathrm{d}\omega \int_{-1}^1 \mathrm{d}s\, \frac{e^2\,\|\mathbf{D}_{12}\|^2\,\omega^3}{8\pi^2\varepsilon_0 c^3\hbar} \\
&\quad \times \left[\frac{1}{\eta_a^2}\left(1 + r_a^2 + 2r_a\cos\left(2kxs\right)\right)\left(1 - s^2\right)\mu \right. \\
&\qquad + \frac{1}{2\eta_a^2}\left(1 + r_a^2 - 2r_a\cos\left(2kxs\right)\right)\left(1 + s^2\right)\left(1 - \mu\right) \\
&\qquad \left. + \frac{t_b^2}{\eta_b^2}\left(1 - s^2\right)\mu + \frac{t_b^2}{2\eta_b^2}\left(1 + s^2\right)\left(1 - \mu\right)\right] \\
&\quad \times \mathrm{e}^{-\mathrm{i}(\omega-\omega_0)\xi}\,\hat{\sigma}^+\hat{\sigma}^- \tag{D.3}
\end{aligned}$$

with $k = \omega/c$. Next, one can perform the t'- and s-integration and re-express the ξ-integration such that

$$H_{\text{cond}} = \hbar C_{\text{mirr}}\,\hat{\sigma}^+\hat{\sigma}^- \tag{D.4}$$

with the constant C_{mirr} given by

$$C_{\text{mirr}} = -\frac{\mathrm{i}}{2\pi}\frac{\Gamma_{\text{free}}}{\omega_0^3}\int\limits_0^\infty \mathrm{d}\xi \int_0^\infty \mathrm{d}\omega\,\omega^3 \mathrm{e}^{-\mathrm{i}(\omega-\omega_0)\xi}$$

D.1 $\hat{H}_{\text{cond I}}(t)$ for an atom in the presence of a semi-transparent mirror

$$\times \left[\frac{1 + r_a^2}{\eta_a^2} + \frac{t_b^2}{\eta_b^2} - \frac{3r_a}{\eta_a^2} \frac{\sin(2kx)}{2kx}(1 - \mu) \right.$$
$$\left. - \frac{3r_a}{\eta_a^2} \left(\frac{\cos(2kx)}{(2kx)^2} - \frac{\sin(2kx)}{(2kx)^3} \right)(1 + \mu) \right] \quad \text{(D.5)}$$

Using the relation derived in Eq. (3.57) to evaluate the ξ-integration yields

$$
\begin{aligned}
C_{\text{mirr}} &= -\frac{\text{i}}{2} \left[\frac{1 + r_a^2}{\eta_a^2} + \frac{t_b^2}{\eta_b^2} \right] \Gamma_{\text{free}} + \frac{1}{2\pi} \left[\frac{1 + r_a^2}{\eta_a^2} + \frac{t_b^2}{\eta_b^2} \right] \int_0^\infty \text{d}\omega \, \frac{\omega^3}{\omega - \omega_0} \frac{\Gamma_{\text{free}}}{\omega_0^3} \\
&\quad - \frac{\text{i}}{2} \left(-\frac{3r_a}{\eta_a^2} \right) \left[\frac{\sin(2k_0 x)}{2k_0 x}(1 - \mu) \right. \\
&\quad \left. + \left(\frac{\cos(2k_0 x)}{(2k_0 x)^2} - \frac{\sin(2k_0 x)}{(2k_0 x)^3} \right)(1 + \mu) \right] \Gamma_{\text{free}} \\
&\quad - \frac{1}{2\pi} \frac{3r_a}{\eta_a^2} \int_0^\infty \text{d}\omega \, \frac{\omega^3}{\omega - \omega_0} \\
&\quad \times \left[\frac{\sin(2kx)}{2kx}(1 - \mu) - \left(\frac{\cos(2kx)}{(2kx)^2} - \frac{\sin(2kx)}{(2kx)^3} \right)(1 + \mu) \right] \frac{\Gamma_{\text{free}}}{\omega_0^3}.
\end{aligned}
$$
$$\text{(D.6)}$$

From the general form of the conditional Hamiltonian in Eq. (6.5) one can see that the imaginary part of this constant denotes a spontaneous decay rate, while its real part denotes an atomic level shift [48, 49]. More concretely, comparing Eqs. (6.5) and (D.4), one finds that

$$\Gamma_{\text{mirr}} = -2 \, \text{Im} \, C_{\text{mirr}} \, , \quad \Delta_{\text{mirr}} = \text{Re} \, C_{\text{mirr}} \, . \quad \text{(D.7)}$$

Demanding that Γ_{mirr} equals Γ_{free} for large values of x shows that the expressions in square brackets in Eq. (D.6) equals unity, c.f. Eq. (6.12). The last term therefore describes an atomic level shift which does not depend on the presence of the mirror. As usual, this level shift is absorbed into the definition of ω_0. The remaining level shift evaluated using standard quantum optical approximations. Doing so, one can show that

$$
\begin{aligned}
\Delta_{\text{mirr}} &= \frac{3r_a}{2\eta_a^2} \Gamma_{\text{free}} \\
&\quad \times \text{Im} \left[\frac{\text{i}}{2k_0 x} e^{2\text{i}k_0 x}(1 - \mu) - e^{2\text{i}k_0 x} \left(\frac{1}{(2k_0 x)^2} + \frac{\text{i}}{(2k_0 x)^3} \right)(1 + \mu) \right] .
\end{aligned}
$$
$$\text{(D.8)}$$

which equals Δ_{mirr} in Eq. (6.7).

D.2 $\mathcal{L}(\hat{\rho}_{\mathrm{SI}}(t))$ for an atom in the presence of a semi-transparent mirror

To obtain an expression for the reset operator $\mathcal{L}(\hat{\rho}_{\mathrm{SI}}(t))$, one again makes use of the interaction picture Hamiltonian $\hat{H}_{\mathrm{SBI}}(t)$ from Eq. (6.3) and substitutes this into the reset operator expression in Eq. (3.26). Following the process outlined above and making use of

$$\int_{t'-(t+\Delta t)}^{t'-t} \mathrm{d}\xi\, \mathrm{e}^{\mathrm{i}(\omega-\omega_0)\xi} \;=\; \int_{-\infty}^{\infty} \mathrm{d}\xi\, \mathrm{e}^{\mathrm{i}(\omega-\omega_0)\xi} = 2\pi\,\delta(\omega-\omega_0)\,, \qquad \text{(D.9)}$$

one finds that

$$\mathcal{L}(\hat{\rho}_{\mathrm{SI}}(t)) \;=\; \Gamma_{\mathrm{mirr}}\,\hat{\sigma}^-\,\hat{\rho}_{\mathrm{SI}}(t)\,\hat{\sigma}^+ \qquad \text{(D.10)}$$

with Γ_{mirr} given in Eq. (6.7).

Appendix E

Calculation of master equation for long-range dipole-dipole interaction mediated by a two-sided semi-transparent mirror

In this supplementary chapter some of the details and calculations required to derive a master equation for the dipole-dipole interaction between a pair of atoms which are separated by a thin two-sided semi-transparent mirror are presented. First the steps required to obtain the conditional Hamiltonian $\hat{H}_{\mathrm{cond\,I}}(t)$ are outlined and then the reset operator $\mathcal{L}(\hat{\rho}_{\mathrm{S\,I}}(t))$.

E.1 $\hat{H}_{\mathrm{cond\,I}}(t)$ for two atoms separated by a semi-transparent mirror

Following the same procedure as in previous appendices, one must first substitute the interaction picture Hamiltonian $\hat{H}_{\mathrm{I}}(t)$ from Eq. (7.10) into the expression derived for the conditional Hamiltonian $\hat{H}_{\mathrm{cond\,I}}(t)$ in Eq. (3.25). This substitution

E.1 $\hat{H}_{\mathrm{cond\,I}}(t)$ for two atoms separated by a semi-transparent mirror

yields

$$\hat{H}_{\mathrm{cond\,I}}(t) \;=\; \hbar\left[C_{aa}\,\hat{\sigma}_a^+\hat{\sigma}_a^- + C_{ab}\,\hat{\sigma}_a^+\hat{\sigma}_b^- + C_{ba}\,\hat{\sigma}_b^+\hat{\sigma}_a^- + C_{bb}\,\hat{\sigma}_b^+\hat{\sigma}_b^-\right]. \quad \text{(E.1)}$$

The constants C_{aa} and C_{bb} in the above equation can be expressed in the following way

$$
\begin{aligned}
C_{aa} \;=\;& -\frac{\mathrm{i}}{\Delta t}\sum_{\lambda=1,2}\int_t^{t+\Delta t}\mathrm{d}t'\int_t^{t'}\mathrm{d}t''\int_{\mathbb{R}^3}\mathrm{d}^3\mathbf{k}\,\frac{e^2\omega}{16\pi^3\varepsilon_0\hbar}\,\mathrm{e}^{-\mathrm{i}(\omega-\omega_0)(t'-t'')} \\
&\times\left[\left(\frac{1}{\eta_a^2}+\frac{t_b^2}{\eta_b^2}+\frac{2t_b}{\eta_a\eta_b}\,\cos(\varphi_2)\right)\|\hat{\mathbf{D}}_{12}^{(a)}\cdot\hat{\mathbf{e}}_{\mathbf{k}\lambda}\|^2 + \frac{r_a^2}{\eta_a^2}\,\|\hat{\widetilde{\mathbf{D}}}_{12}^{(a)*}\cdot\hat{\mathbf{e}}_{\mathbf{k}\lambda}\|^2\right. \\
&\left.+\left(\frac{2r_a}{\eta_a^2}\,\cos(\mathbf{k}\cdot(\mathbf{r}_a-\widetilde{\mathbf{r}}_a)-\varphi_1)+\frac{2r_a t_b}{\eta_a\eta_b}\,\cos(\mathbf{k}\cdot(\mathbf{r}_a-\widetilde{\mathbf{r}}_a)+(\varphi_2-\varphi_1))\right)\right. \\
&\left.\times\left(\hat{\mathbf{D}}_{12}^{(a)*}\cdot\hat{\mathbf{e}}_{\mathbf{k}\lambda}\right)\left(\hat{\widetilde{\mathbf{D}}}_{12}^{(a)}\cdot\hat{\mathbf{e}}_{\mathbf{k}\lambda}\right)\right],
\end{aligned} \quad \text{(E.2)}
$$

and

$$
\begin{aligned}
C_{bb} \;=\;& -\frac{\mathrm{i}}{\Delta t}\sum_{\lambda=1,2}\int_t^{t+\Delta t}\mathrm{d}t'\int_t^{t'}\mathrm{d}t''\int_{\mathbb{R}^3}\mathrm{d}^3\mathbf{k}\,\frac{e^2\omega}{16\pi^3\varepsilon_0\hbar}\,\mathrm{e}^{-\mathrm{i}(\omega-\omega_0)(t'-t'')} \\
&\times\left[\left(\frac{1}{\eta_b^2}+\frac{t_a^2}{\eta_a^2}+\frac{2t_a}{\eta_a\eta_b}\,\cos(\varphi_4)\right)\|\hat{\mathbf{D}}_{12}^{(b)}\cdot\hat{\mathbf{e}}_{\mathbf{k}\lambda}\|^2 + \frac{r_b^2}{\eta_b^2}\,\|\hat{\widetilde{\mathbf{D}}}_{12}^{(b)}\cdot\hat{\mathbf{e}}_{\mathbf{k}\lambda}\|^2\right. \\
&\left.+\left(\frac{2r_b}{\eta_b^2}\,\cos(\mathbf{k}\cdot(\mathbf{r}_b-\widetilde{\mathbf{r}}_b)-\varphi_3)+\frac{2t_a r_b}{\eta_a\eta_b}\,\cos(\mathbf{k}\cdot(\mathbf{r}_b-\widetilde{\mathbf{r}}_b)+(\varphi_4-\varphi_3))\right)\right. \\
&\left.\times\left(\hat{\mathbf{D}}_{12}^{(b)*}\cdot\hat{\mathbf{e}}_{\mathbf{k}\lambda}\right)\left(\hat{\widetilde{\mathbf{D}}}_{12}^{(b)}\cdot\hat{\mathbf{e}}_{\mathbf{k}\lambda}\right)\right],
\end{aligned} \quad \text{(E.3)}
$$

In addition, one can define the remaining two constants such that

$$C_{ab} \;=\; -\frac{\mathrm{i}}{\Delta t}\sum_{\lambda=1,2}\int_t^{t+\Delta t}\mathrm{d}t'\int_t^{t'}\mathrm{d}t''\int_{\mathbb{R}^3}\mathrm{d}^3\mathbf{k}\,\frac{e^2\omega}{16\pi^3\varepsilon_0\hbar}\,\mathrm{e}^{-\mathrm{i}(\omega-\omega_0)(t'-t'')}\times F,$$

$$\text{(E.4)}$$

and

$$C_{ba} \;=\; -\frac{\mathrm{i}}{\Delta t}\sum_{\lambda=1,2}\int_t^{t+\Delta t}\mathrm{d}t'\int_t^{t'}\mathrm{d}t''\int_{\mathbb{R}^3}\mathrm{d}^3\mathbf{k}\,\frac{e^2\omega}{16\pi^3\varepsilon_0\hbar}\,\mathrm{e}^{-\mathrm{i}(\omega-\omega_0)(t'-t'')}\times F^*.$$

$$\text{(E.5)}$$

The function F is defined in the following way

$$
F = \left[\left(\frac{r_a t_a}{\eta_a^2} + \frac{r_a}{\eta_a \eta_b} \right) \mathrm{e}^{\mathrm{i}\varphi_1} + \frac{r_a t_a}{\eta_a^2} \mathrm{e}^{-\mathrm{i}\varphi_4} \right] \times \mathrm{e}^{\mathrm{i}\mathbf{k}\cdot(\widetilde{\mathbf{r}}_a - \mathbf{r}_b)} \left(\hat{\widetilde{\mathbf{D}}}_{12}^{(a)*} \cdot \hat{\mathbf{e}}_{\mathbf{k}\lambda} \right) \left(\hat{\mathbf{D}}_{12}^{(b)} \cdot \hat{\mathbf{e}}_{\mathbf{k}\lambda} \right)
$$
$$
+ \left[\left(\frac{r_b}{\eta_a \eta_b} + \frac{r_b t_b}{\eta_b^2} \right) \mathrm{e}^{-\mathrm{i}\varphi_3} + \frac{r_b t_b}{\eta_b^2} \mathrm{e}^{\mathrm{i}\varphi_2} \right] \times \mathrm{e}^{\mathrm{i}\mathbf{k}\cdot(\mathbf{r}_a - \widetilde{\mathbf{r}}_b)} \left(\hat{\mathbf{D}}_{12}^{(a)*} \cdot \hat{\mathbf{e}}_{\mathbf{k}\lambda} \right) \left(\hat{\widetilde{\mathbf{D}}}_{12}^{(b)} \cdot \hat{\mathbf{e}}_{\mathbf{k}\lambda} \right),
\tag{E.6}
$$

where some terms have been omitted in order to isolate the contributions of F which arise due to the presence of the mirror i.e. the source of the long-range dipole-dipole interaction[1].

As in previous appendices, one can make use of Eqs. $(3.45) - (3.47)$ to simplify the integrals in Eqs. $(E.1) - (E.6)$. One must also assume that both atoms have real dipole moments such that $\hat{\mathbf{D}}_{12}^{(a,b)} = \hat{\mathbf{D}}_{12}^{(a,b)*}$ and one can define the dipole orientation using the relation

$$
\mu^{(a,b)} = \|\hat{\mathbf{D}}_{12}^{(a,b)} \cdot \hat{\mathbf{x}}\|^2,
\tag{E.7}
$$

where these denote the normalised vector expressions. Taking this into account and performing the ϕ integration in Eqs. $(E.2) - (E.5)$, whilst introducing the new variables $s = \cos(\vartheta)$, yields the following expressions for the constants,

$$
C_{aa} = -\frac{\mathrm{i}}{\Delta t} \frac{3\Gamma_{\mathrm{free}}}{8\pi\omega_0^3} \int_t^{t+\Delta t} \mathrm{d}t' \int_t^{t'} \mathrm{d}t'' \int_0^\infty \mathrm{d}\omega \int_{-1}^1 \mathrm{d}s\, \omega^3 \mathrm{e}^{-\mathrm{i}(\omega-\omega_0)(t'-t'')}
$$
$$
\times \left[\left(\frac{1+r_a^2}{\eta_a^2} + \frac{t_b^2}{\eta_b^2} + \frac{2t_b}{\eta_a \eta_b} \cos(\varphi_2) \right) \times \left(\mu^{(a)}(1-s^2) + (1-\mu^{(a)})\frac{1}{2}(1+s^2) \right) \right.
$$
$$
+ \left(\frac{2r_a}{\eta_a^2} \cos(2kx_a s - \varphi_1) + \frac{2r_a t_b}{\eta_a \eta_b} \cos(2kx_a s + (\varphi_2 - \varphi_1)) \right)
$$
$$
\left. \times \left(-\mu^{(a)}(1-s^2) + (1-\mu^{(a)})\frac{1}{2}(1+s^2) \right) \right],
\tag{E.8}
$$

---

[1] For reference, the two omitted terms take the form

$$
(O1) = \left[\left(\frac{t_a}{\eta_a^2} + \frac{t_a t_b}{\eta_a \eta_b} \right) \mathrm{e}^{-\mathrm{i}\varphi_4} + \left(\frac{t_b}{\eta_b^2} + \frac{t_a t_b}{\eta_a \eta_b} \right) \mathrm{e}^{\mathrm{i}\varphi_2} + \frac{1}{\eta_a \eta_b} \right] \times \mathrm{e}^{\mathrm{i}\mathbf{k}\cdot(\mathbf{r}_a - \mathbf{r}_b)} \left(\hat{\mathbf{D}}_{12}^{(a)*} \cdot \hat{\mathbf{e}}_{\mathbf{k}\lambda} \right) \left(\hat{\mathbf{D}}_{12}^{(b)} \cdot \hat{\mathbf{e}}_{\mathbf{k}\lambda} \right)
$$
$$
(O2) = \frac{r_a r_b}{\eta_a \eta_b} \mathrm{e}^{\mathrm{i}\mathbf{k}\cdot(\widetilde{\mathbf{r}}_a - \widetilde{\mathbf{r}}_b)} \left(\hat{\widetilde{\mathbf{D}}}_{12}^{(a)*} \cdot \hat{\mathbf{e}}_{\mathbf{k}\lambda} \right) \left(\hat{\widetilde{\mathbf{D}}}_{12}^{(b)} \cdot \hat{\mathbf{e}}_{\mathbf{k}\lambda} \right).
$$

Note that these terms will not dominate as the long-range interaction requires the condition that one real atom sits in the immediate vicinity of a mirror-image atom i.e. this separation is on the order of the wavelength of the emitted radiation λ_0.

and

$$
\begin{aligned}
C_{bb} &= -\frac{\text{i}}{\Delta t} \frac{3\Gamma_{\text{free}}}{8\pi\omega_0^3} \int_t^{t+\Delta t} \text{d}t' \int_t^{t'} \text{d}t'' \int_0^\infty \text{d}\omega \int_{-1}^1 \text{d}s\, \omega^3 \text{e}^{-\text{i}(\omega-\omega_0)(t'-t'')} \\
&\quad \times \left[\left(\frac{1+r_b^2}{\eta_b^2} + \frac{t_a^2}{\eta_a^2} + \frac{2t_a}{\eta_a\eta_b} \cos(\varphi_4) \right) \times \left(\mu^{(b)}(1-s^2) + (1-\mu^{(b)})\frac{1}{2}(1+s^2) \right) \right. \\
&\quad + \left(\frac{2r_b}{\eta_b^2} \cos(2kx_b s - \varphi_3) + \frac{2r_b t_a}{\eta_a\eta_b} \cos(2kx_b s + (\varphi_4 - \varphi_3)) \right) \\
&\quad \left. \times \left(-\mu^{(b)}|^2(1-s^2) + (1-\mu^{(b)})\frac{1}{2}(1+s^2) \right) \right]
\end{aligned}
\tag{E.9}
$$

In addition, one can define the remaining constants such that

$$
\begin{aligned}
C_{ab} &= -\frac{\text{i}}{\Delta t} \frac{3\Gamma_{\text{free}}}{8\pi\omega_0^3} \int_t^{t+\Delta t} \text{d}t' \int_t^{t'} \text{d}t'' \int_0^\infty \text{d}\omega \int_{-1}^1 \text{d}s\, \omega^3 \text{e}^{-\text{i}(\omega-\omega_0)(t'-t'')} \\
&\quad \times \left[\left(\frac{r_a t_a}{\eta_a^2} \text{e}^{\text{i}(\varphi_1-\varphi_4)} + \frac{r_b t_b}{\eta_b^2} \text{e}^{\text{i}(\varphi_2-\varphi_3)} + \frac{1}{\eta_a\eta_b} \left(r_a \text{e}^{\text{i}\varphi_1} + r_b \text{e}^{-\text{i}\varphi_3} \right) \right) \right. \\
&\quad \left. \times \text{e}^{\text{i}k\widetilde{x}s} \left(-d_1^{(a)} d_1^{(b)}(1-s^2) + d_3^{(a)} d_3^{(b)}\frac{1}{2}(1+s^2) \right) \right],
\end{aligned}
\tag{E.10}
$$

where $|\widetilde{\mathbf{r}}_a - \mathbf{r}_b| \equiv |\mathbf{r}_a - \widetilde{\mathbf{r}}_b| = \widetilde{x}$. This denotes the distance between an atom and the mirror-image of another atom. Therefore, provided that this separation is of the same order of magnitude as the wavelength of the emitted radiation λ_0, it should be possible to observe oscillations in atomic lifetimes for fairly large atom-mirror distances. The next step requires evaluating the s-integration in Eqs. (E.8) – (E.10), which yields the constants

$$
\begin{aligned}
C_{aa} &= -\frac{\text{i}}{2} \frac{1}{\Delta t} \frac{\Gamma_{\text{free}}}{\pi\omega_0^3} \int_t^{t+\Delta t} \text{d}t' \int_t^{t'} \text{d}t'' \int_0^\infty \text{d}\omega\, \omega^3 \text{e}^{-\text{i}(\omega-\omega_0)(t'-t'')} \\
&\quad \times \left[\left(\frac{1+r_a^2}{\eta_a^2} + \frac{t_b^2}{\eta_b^2} + \frac{2t_b}{\eta_a\eta_b} \cos(\varphi_2) \right) + \left(\frac{3r_a}{\eta_a^2} \cos(\varphi_1) + \frac{3r_a t_b}{\eta_a\eta_b} \cos(\varphi_2 - \varphi_1) \right) \right. \\
&\quad \left. \times \left[\frac{\sin(2kx_a)}{(2kx_a)}(1-\mu^{(a)}) + \left(\frac{\cos(2kx_a)}{(2kx_a)^2} - \frac{\sin(2kx_a)}{(2kx_a)^3} \right)(1+\mu^{(a)}) \right] \right],
\end{aligned}
\tag{E.11}
$$

E.1 $\hat{H}_{\mathrm{cond\,I}}(t)$ for two atoms separated by a semi-transparent mirror

with,

$$
\begin{aligned}
C_{bb} \;=\; &-\frac{\mathrm{i}}{2}\frac{1}{\Delta t}\frac{\Gamma_{\mathrm{free}}}{\pi\omega_0^3}\int_t^{t+\Delta t}\mathrm{d}t'\int_t^{t'}\mathrm{d}t''\int_0^\infty\mathrm{d}\omega\,\omega^3\mathrm{e}^{-\mathrm{i}(\omega-\omega_0)(t'-t'')}\\
&\times\left[\left(\frac{1+r_b^2}{\eta_b^2}+\frac{t_a^2}{\eta_a^2}+\frac{2t_a}{\eta_a\eta_b}\cos(\varphi_4)\right)+\left(\frac{3r_b}{\eta_b^2}\cos(\varphi_3)+\frac{3r_bt_a}{\eta_a\eta_b}\cos(\varphi_4-\varphi_3)\right)\right.\\
&\left.\times\left[\frac{\sin(2kx_b)}{(2kx_b)}(1-\mu^{(b)})+\left(\frac{\cos(2kx_b)}{(2kx_b)^2}-\frac{\sin(2kx_b)}{(2kx_b)^3}\right)(1+\mu^{(b)})\right]\right].
\end{aligned}
\tag{E.12}
$$

The other two constants C_{ab} and C_{ba} can be expressed in the following way

$$
\begin{aligned}
C_{ab} \;=\; &-\frac{\mathrm{i}}{2}\frac{1}{\Delta t}\frac{3\Gamma_{\mathrm{free}}}{2\pi\omega_0^3}\int_t^{t+\Delta t}\mathrm{d}t'\int_t^{t'}\mathrm{d}t''\int_0^\infty\mathrm{d}\omega\,\omega^3\mathrm{e}^{-\mathrm{i}(\omega-\omega_0)(t'-t'')}\\
&\times\left[\frac{\sin(k\widetilde{x})}{(k\widetilde{x})}\widetilde{c}_1+\left(\frac{\cos(k\widetilde{x})}{(k\widetilde{x})^2}-\frac{\sin(k\widetilde{x})}{(k\widetilde{x})^3}\right)\widetilde{c}_2\right]\\
&\times\left(\frac{r_at_a}{\eta_a^2}\mathrm{e}^{\mathrm{i}(\varphi_1-\varphi_4)}+\frac{r_bt_b}{\eta_b^2}\mathrm{e}^{\mathrm{i}(\varphi_2-\varphi_3)}+\frac{1}{\eta_a\eta_b}\left(r_a\mathrm{e}^{\mathrm{i}\varphi_1}+r_b\mathrm{e}^{-\mathrm{i}\varphi_3}\right)\right),
\end{aligned}
\tag{E.13}
$$

and

$$
\begin{aligned}
C_{ba} \;=\; &-\frac{\mathrm{i}}{2}\frac{1}{\Delta t}\frac{3\Gamma_{\mathrm{free}}}{2\pi\omega_0^3}\int_t^{t+\Delta t}\mathrm{d}t'\int_t^{t'}\mathrm{d}t''\int_0^\infty\mathrm{d}\omega\,\omega^3\mathrm{e}^{-\mathrm{i}(\omega-\omega_0)(t'-t'')}\\
&\times\left[\frac{\sin(k\widetilde{x})}{(k\widetilde{x})}\widetilde{c}_1^*+\left(\frac{\cos(k\widetilde{x})}{(k\widetilde{x})^2}-\frac{\sin(k\widetilde{x})}{(k\widetilde{x})^3}\right)\widetilde{c}_2^*\right]\\
&\times\left(\frac{r_at_a}{\eta_a^2}\mathrm{e}^{\mathrm{i}(\varphi_1-\varphi_4)}+\frac{r_bt_b}{\eta_b^2}\mathrm{e}^{\mathrm{i}(\varphi_2-\varphi_3)}+\frac{1}{\eta_a\eta_b}\left(r_a\mathrm{e}^{\mathrm{i}\varphi_1}+r_b\mathrm{e}^{-\mathrm{i}\varphi_3}\right)\right),
\end{aligned}
\tag{E.14}
$$

where $\widetilde{x}$ denotes the separation of a real atom and a mirror-image atom and in analogy to Eq. (4.14), $\widetilde{c}_1$ and $\widetilde{c}_2$ can be defined in the following way

$$
\begin{aligned}
\widetilde{c}_1 \;&=\; \left(\hat{\mathbf{D}}_{12}^{(a)}\cdot\hat{\widetilde{\mathbf{D}}}_{12}^{(b)}\right)-\left(\hat{\mathbf{D}}_{12}^{(a)}\cdot\hat{\mathbf{x}}\right)\left(\hat{\widetilde{\mathbf{D}}}_{12}^{(b)}\cdot\hat{\mathbf{x}}\right),\\
\widetilde{c}_2 \;&=\; \left(\hat{\mathbf{D}}_{12}^{(a)}\cdot\hat{\widetilde{\mathbf{D}}}_{12}^{(b)}\right)-3\left(\hat{\mathbf{D}}_{12}^{(a)}\cdot\hat{\mathbf{x}}\right)\left(\hat{\widetilde{\mathbf{D}}}_{12}^{(b)}\cdot\hat{\mathbf{x}}\right),
\end{aligned}
\tag{E.15}
$$

where $\hat{\mathbf{x}}$ and $\hat{\mathbf{D}}_{12}^{(i)}$ denote the unit vectors.

Finally, one can solve the remaining integrals in Eqs. (E.11) – (E.14) by making use of the relation in Eq. (3.57). First, lets consider the constant C_{aa} and

E.1 $\hat{H}_{\text{cond I}}(t)$ for two atoms separated by a semi-transparent mirror

evaluating the remaining integrals through the given relation. Doing so and ignoring level shifts, one finds that

$$C_{aa} = -\frac{\mathrm{i}}{2}\Gamma_{\text{mirr}}^{(aa)}, \tag{E.16}$$

where,

$$
\begin{aligned}
\Gamma_{\text{mirr}}^{(aa)} &= \left(\frac{1+r_a^2}{\eta_a^2} + \frac{t_b^2}{\eta_b^2} + \frac{2t_b}{\eta_a\eta_b}\cos(\varphi_2)\right) + \left(\frac{3r_a}{\eta_a^2}\cos(\varphi_1) + \frac{3r_a t_b}{\eta_a\eta_b}\cos(\varphi_2 - \varphi_1)\right) \\
&\quad \times \left[\frac{\sin(2kx_a)}{(2kx_a)}(1-\mu^{(a)}) + \left(\frac{\cos(2kx_a)}{(2kx_a)^2} - \frac{\sin(2kx_a)}{(2kx_a)^3}\right)(1+\mu^{(a)})\right].
\end{aligned} \tag{E.17}
$$

Similarly for the constant C_{bb}, one finds that

$$C_{bb} = -\frac{\mathrm{i}}{2}\Gamma_{\text{mirr}}^{(bb)}, \tag{E.18}$$

where,

$$
\begin{aligned}
\Gamma_{\text{mirr}}^{(bb)} &= \left(\frac{1+r_b^2}{\eta_b^2} + \frac{t_a^2}{\eta_a^2} + \frac{2t_a}{\eta_a\eta_b}\cos(\varphi_4)\right) + \left(\frac{3r_a}{\eta_a^2}\cos(\varphi_3) + \frac{3r_a t_b}{\eta_a\eta_b}\cos(\varphi_4 - \varphi_3)\right) \\
&\quad \times \left[\frac{\sin(2kx_b)}{(2kx_b)}(1-\mu^{(b)}) + \left(\frac{\cos(2kx_b)}{(2kx_b)^2} - \frac{\sin(2kx_b)}{(2kx_b)^3}\right)(1+\mu^{(b)})\right].
\end{aligned} \tag{E.19}
$$

The remaining integrals in Eqs. (E.13) and (E.14) can be solved similarly. Following this procedure, one finds that

$$C_{ab} = -\frac{\mathrm{i}}{2}\widetilde{C}(\widetilde{x}), \tag{E.20}$$

and similarly,

$$C_{ba} = -\frac{\mathrm{i}}{2}\widetilde{C}^*(\widetilde{x}). \tag{E.21}$$

Moreover, one can define the distance-dependent constant $\widetilde{C}(\widetilde{x})$ in the following way

$$
\begin{aligned}
\widetilde{C}(\widetilde{x}) &= \frac{3}{2}\left[\frac{\sin(k_0\widetilde{x})}{k_0\widetilde{x}}\widetilde{c}_1 + \left(\frac{\cos(k_0\widetilde{x})}{(k_0\widetilde{x})^2} - \frac{\sin(k_0\widetilde{x})}{(k_0\widetilde{x})^3}\right)\widetilde{c}_2\right]\Gamma_{\text{free}} \\
&\quad \times \left(\frac{r_a t_a}{\eta_a^2}\mathrm{e}^{\mathrm{i}(\varphi_1 - \varphi_4)} + \frac{r_b t_b}{\eta_b^2}\mathrm{e}^{\mathrm{i}(\varphi_2 - \varphi_3)} + \frac{1}{\eta_a\eta_b}\left(r_a\mathrm{e}^{\mathrm{i}\varphi_1} + r_b\mathrm{e}^{-\mathrm{i}\varphi_3}\right)\right),
\end{aligned}
$$
$$\tag{E.22}$$

where the above equation denotes the real part of the contribution. This part is responsible for the spontaneous emission rate of the system, where as the imaginary part contributes to the atomic level shifts. Noting the form of the long-range dipole-coupling constant $\widetilde{C}(\widetilde{x})$, one can observe a strong analogy between this and the form of the dipole-coupling constant for two interacting atoms in free space (c.f. Eq. (4.12)).

Combining the above results with the conditional Hamiltonian outlined earlier in Eq. (E.1), one obtains the expression

$$\hat{H}_{\mathrm{cond\,I}}(t) \;\; = \;\; -\frac{\mathrm{i}\hbar}{2} \left[\Gamma_{\mathrm{mirr}}^{(aa)} \hat{\sigma}_a^+ \hat{\sigma}_a^- + \widetilde{C}(\widetilde{x})\, \hat{\sigma}_a^+ \hat{\sigma}_b^- + \widetilde{C}^*(\widetilde{x})\, \hat{\sigma}_b^+ \hat{\sigma}_a^- + \Gamma_{\mathrm{mirr}}^{(bb)} \hat{\sigma}_b^+ \hat{\sigma}_b^- \right].$$

(E.23)

E.2 $\mathcal{L}(\hat{\rho}_{\mathrm{S\,I}}(t))$ for two atoms separated by a semi-transparent mirror

In order to obtain an expression for the reset operator $\mathcal{L}(\hat{\rho}_{\mathrm{S\,I}}(t))$, one again makes use of the interaction picture Hamiltonian $\hat{H}_{\mathrm{SB\,I}}(t)$ from Eq. (7.10) and substitutes this into the reset operator expression in Eq. (3.26). Following the same procedure as above and making use of

$$\int_{t'-(t+\Delta t)}^{t'-t} \mathrm{d}\xi\, \mathrm{e}^{\mathrm{i}(\omega-\omega_0)\xi} \;\; = \;\; \int_{-\infty}^{\infty} \mathrm{d}\xi\, \mathrm{e}^{\mathrm{i}(\omega-\omega_0)\xi} = 2\pi\, \delta(\omega-\omega_0)\,, \qquad \text{(E.24)}$$

one finds this generates a reset operator of the form

$$\begin{aligned} \mathcal{L}(\hat{\rho}_{\mathrm{S\,I}}(t)) \;\; = \;\; & \Gamma_{\mathrm{mirr}}^{(aa)} \hat{\sigma}_a^- \hat{\rho}_{\mathrm{S\,I}}(t)\hat{\sigma}_a^+ + \Gamma_{\mathrm{mirr}}^{(bb)} \hat{\sigma}_b^- \hat{\rho}_{\mathrm{S\,I}}(t)\hat{\sigma}_b^+ \\ & + \mathrm{Re}(\widetilde{C}(\widetilde{x}))\hat{\sigma}_b^- \hat{\rho}_{\mathrm{S\,I}}(t)\hat{\sigma}_a^+ + \mathrm{Re}(\widetilde{C}(\widetilde{x})^*)\hat{\sigma}_a^- \hat{\rho}_{\mathrm{S\,I}}(t)\hat{\sigma}_b^+\,. \quad \text{(E.25)} \end{aligned}$$

References

[1] H. J. Kimble. The quantum internet. *Nature*, 453:1023–30, 2008. 1, 93

[2] T. M. Barlow, R. Bennett, and A. Beige. A master equation for a two-sided optical cavity. *J. Mod. Opt.*, 62:S11, 2015. 1, 2, 3, 65, 109, 110, 122

[3] M. J. Collett and C. W. Gardiner. Squeezing of intracavity and travelling-wave light fields produced in parametric amplification. *Phys. Rev. A*, 30: 1386, 1984. 2, 65, 109

[4] C. W. Gardiner and M. J. Collett. Input and output in damped quantum systems: Quantum stochastic differential equations and the master equation. *Phys. Rev. A*, 31:3761, 1985.

[5] S. Fan, S. E. Kocabaş, and J. T. Shen. Input-output formalism for few-photon transport in one-dimensional nanophotonic waveguides coupled to a qubit. *Phys. Rev. A*, 82:063821, 2010. 2, 65, 109

[6] D. F. Walls and G. J. Milburn. *Quantum optics*. Springer-Verlag Berlin Heidelberg, 1994. 2, 109

[7] S. M. Barnett, C. R. Claire, B. Huttner, and N. Imoto. Field commutation relations in optical cavities. *Phys. Rev. Lett.*, 77:1739, 1996. 2, 109, 110

[8] B. J. Dalton, E. S. Guerra, and P. L. Knight. Field quantization in dielectric media and the generalized multipolar hamiltonian. *Phys. Rev. A*, 54:2292, 1996. 2, 65

[9] B. J. Dalton, S. M. Barnett, and P. L. Knight. Quasi mode theory of macroscopic canonical quantization in quantum optics and cavity quantum electrodynamics. *J. Mod. Opt.*, 46:1315, 1999.

[10] S. M. Dutra and G. Nienhuis. Quantized mode of a leaky cavity. *Phys. Rev. A*, 62:063805, 2000. 2, 65, 110

[11] R. Lang, M. O. Scully, and W. E. Lamb Jr. Why is the laser line so narrow? A theory of single-quasimode laser operation. *Phys. Rev. A*, 7:1788, 1973.

[12] K. Ujihara. Quantum theory of a one-dimensional optical cavity with output coupling field quantization. *Phys. Rev. A*, 12:148, 1975.

[13] J. Geo-Benacloche, N. Lu, L. M. Pedrotti, S. Prassad, M. O. Scully, and K. Wodkiewicz. Treatment of the spectrum of squeezing based on the modes of the universe. I. Theory and a physical picture. *Phys. Rev. A*, 41: 369, 1990. 2, 110

[14] D. Geskus N. Ismail, C. C. Kores and M. Pollnau. Fabry-pérot resonator: spectral line shapes, generic and related airy distributions, linewidths, finesses and performance at low or frequency-dependent reflectivity. *Opt. Exp.*, 24, 2016. 3, 109

[15] G. Lindblad. On the generators of quantum dynamical semigroups. *Comm. Math. Phys.*, 48:119, 1976. 5, 31

[16] J. C. Maxwell. A dynamical theory of the electromagnetic field. *Phil. Trans. R. Soc.*, 155:459512, 1865. 8

[17] J. D. Jackson. *Classical Electrodynamics*. John Wiley & Sons, 3rd edition edition, 1998. 11, 13, 66, 68

[18] J.H. Jeans M.A. XI. On the partition of energy between matter and ether. *The London, Edinburgh, and Dublin Philosophical Magazine and Journal of Science*, 10:91–98, 1905. 13

[19] M. Planck. On the theory of the energy distribution law of the normal spectrum. *Ann. Phys. (Leipzig)*, 309:553–563, 1901. 13

[20] John Von Neumann. *Mathematical Foundations of Quantum Mechanics.* Princeton University Press, 1996. 14

[21] J. M. Jauch. *Foundations of Quantum Mechanics.* Addison-Wesley Educational Publishers, 1968. 14

[22] N. Bohr. Über die serienspektra der elemente. *Z. Phys.*, 2:423–69, 1920. 15

[23] N. Bohr. Über die anwendung der quantentheorie auf den atombau: I. grundpostulate der quantentheorie. *Z. Phys.*, 13:117–65, 1923.

[24] N. Bohr. The structure of the atom. *Nature*, 112:29–41, 1923. 15

[25] P. A. M. Dirac. The fundamental equations of quantum mechanics. *Proc. R. Soc. A*, 109:642–653, 1925. 16, 20

[26] P. A. M. Dirac. *The principles of Quantum Mechanics.* Claredon Press (Oxford), 1958. 16

[27] J. D. Jackson. From lorenz to coulomb and the other explicit gauge transformations. *Am. J. Phys.*, 70:917–28, 2002. 20

[28] R. Bennett, T. M. Barlow, and A. Beige. A physically-motivated quantisation of the electromagnetic field. *Eur. J. Phys.*, 37:014001, 2015. 23, 24, 27, 28, 66

[29] M. D. Eisaman, J. Fan, A. Migdall, and S. V. Polyakov. Invited review article: single-photon sources and detectors. *Rev. Sci. Instrum.*, 82:071101, 2011. 23

[30] F. Marsili et al. Detecting single infrared photons with 93% system efficiency. *Nat. Photon*, 7:210, 2013.

[31] A. Kuhn, M. Hennrich, , and G. Rempe. Deterministic single-photon source for distributed quantum networking. *Phys. Rev. Lett.*, 89:067901, 2002.

[32] S. Scheel. Single-photon sources - an introduction. *J. Mod. Opt.*, 56:141, 2009.

[33] H. C. Bennett and G. Brassard. Quantum cryptography: public key distribution and coin tossing. *Proc. IEEE Int. Conf. on Computers, Systems and Signal Processing*, page 175, 1984.

[34] A. Ekert. Quantum cryptography based on bell's theorem. *Phys. Rev. Lett.*, 67:661, 1991.

[35] N. Gisin, G. G. Ribordy, W. Tittel, and H. Zbinden. Quantum cryptography. *Rev. Mod. Phys.*, 74:145, 2002.

[36] E. Knill, R. Laflamme, and G. J. Milburn. A scheme for efficient quantum computation with linear optics. *Nature*, 409:46, 2001.

[37] P. Kok, W. J. Munro, K. Nemoto, T. C. Ralph, J. P. Dowling, and G. J. Milburn. Linear optical quantum computing with photonic qubits. *Rev. Mod. Phys.*, 79:135, 2007.

[38] D. L. Andrews. Physicality of the photon. *J. Phys. Chem.*, 4:3878, 2013. 23

[39] D. V. Schroeder and M. E. Peskin. *An Introduction To Quantum Field Theory*. CRC Press, 1995. 28, 36

[40] A. Messiah. *Quantum mechanics*. Dover publications (New York), 1999.

[41] M. O. Scully and M. S. Zubairy. *Quantum optics*. Cambridge university press, 1997.

[42] R. Loudon. *The quantum theory of light*. Oxford University Press, 2000. 28, 34

[43] P. A. M. Dirac. The quantum theory of the emission and absorption of radiation. *Proc. R. Soc. A*, 114:243–265, 1927. 30

[44] R. P. Feynman. *Quantum Electrodynamics (Frontiers in Physics)*. Perseus, 1998. 30

[45] J. Schwinger. *Selected papers on quantum electrodynamics*. Courier Corporation, 1958. 30

[46] E. Fermi. *Nuclear physics.* University of Chicago press, 1950. 31

[47] G. S. Agarwal. *Springer Tracts in Modern Physics; Quantum Optics.* Springer Verlag Berlin, 1974. 31

[48] G. C. Hegerfeldt. How to reset an atom after a photon detection; applications to photon counting processes. *Phys. Rev. A*, 47(449), 1993. 38, 86, 128, 137

[49] A. Stokes, A. Kurcz, T. P. Spiller, and A. Beige. Extending the validity range of quantum optical master equations. *Phys. Rev. A*, 85(053805), 2012. 31, 34, 40, 49, 62, 87, 128, 137

[50] W. H. Zurek. Decoherence, einselection, and the quantum origins of the classical. *Rev. Mod. Phys.*, 75(715), 2003. 34

[51] C. Schön and A. Beige. Analysis of a two-atom double-slit experiment based on environment-induced measurements. *Phys. Rev. A*, 64(023806), 2001. 34

[52] J. Dalibard, Y. Castin, and K. Mølmer. Wave-function approach to dissipative processes in quantum optics. *Phys. Rev. Lett.*, 68(580), 1992. 38

[53] H. Carmichael. *An Open Systems Approach to Quantum Optics*, volume 18 of *Lecture Notes in Physics.* Springer-Verlag, 1993. 38

[54] Ram P. Kanwal. *Linear Integral Equations: theory and technique.* Birkhäuser, 1996. 46

[55] G. K. Brennen, C. M. Caves, P. S. Jessen, and I. H. Deutsch. Quantum logic gates in optical lattices. *Phys. Rev. Lett.*, 82(1060), 1999. 50

[56] D. Jaksch, J. I. Cirac, P. Zoller, S. L. Rolston, R. Cote, and M. D. Lukin. Fast quantum gates for neutral atoms. *Phys. Rev. Lett.*, 85(2208), 2000.

[57] G. K. Brennen, I. H. Deutsch, and P. S. Jessen. Entangling dipole-dipole interactions for quantum logic with neutral atoms. *Phys. Rev. A*, 61(062309), 2000. 50

[58] T. F. Gallagher and P. Pillet. Dipole-dipole interactions of rydberg atoms. *Adv. in Atomic, Mol. and Opt. Phys.*, 56, 2008.

[59] V. Zhelyazkova and S. D. Hogan. Probing interactions between rydberg atoms with large electric dipole moments in amplitude modulated electric fields. *Phys. Rev. A*, 92(011402), 2015. 50

[60] R. Tanas and Z. Ficek. Entangled states and collective nonclassical effects in two-atom systems. *Phys. Rep.*, 372, 2002. 50

[61] Z. Ficek and R. Tanas. Entanglement induced by spontaneous emission in spatially extended two-atom systems. *J. Mod. Opt.*, 50(18), 2003. 50

[62] E. Shahmoon and G. Kurizki. Nonradiative interaction and entanglement between distant atoms. *Phys. Rev. A*, 87(033831), 2013.

[63] G. Menezes. Vacuum fluctuations and radiation reaction in radiative processes of entangled states. *Phys. Rev. A*, 92(062131), 2015.

[64] G. Araneda, D. B. Higginbottom, L. Slodicka, Y. Colombe, and R. Blatt. Interference of single photons emitted by entangled atoms in free space. *Phys. Rev. Lett.*, 120(193603), 2018.

[65] M. Tavakoli and E. Amooghorban. Entanglement of two two-level atoms mediated by a cylindrical optical black hole. *J. Opt. Soc. Am. B*, 35, 2018. 50

[66] R. J. Bettles. *Cooperative Interactions in Lattices of Atomic Dipoles*. PhD thesis, Faculty of Science - Department of Physics, Durham University, Department of Physics, South Rd, Durham DH1 3LE, 2016. 50

[67] E. Munro, A. Asenjo-Garcia, Y. Lin, L. C. Kwek, C. A. Regal, and D. E. Chang. Population mixing due to dipole-dipole interactions in a 1d array of multi-level atoms. *hys. Rev. A*, 98(033815), 2017. 50

[68] F. Damanet and J. Martin. Competition between finite-size effects and dipole-dipole interactions in few-atom systems. *J. Phys B: At. Mol. Opt. Phys.*, 49(225501), 2016. 50

[69] I. C. Khoo. Two-atom interaction in the dynamical operator treatment. *Opt. Comm.*, 20, 1977. 50

[70] A. Beige and G. C. Hegerfeldt. Transition from antibunching to bunching for two dipole-interacting atoms. *Phys. Rev. A*, 58(4133), 1998. 50, 84, 88, 92

[71] A. Beige and G. C. Hegerfeldt. Cooperative effects in the light and dark periods of two dipole-interacting atoms. *Phys. Rev. A*, 59(2385), 1999.

[72] C. Schon and A. Beige. An analysis of a two-atom double-slit experiment based on environment-induced measurements. *Phys. Rev. A*, 64(023806), 2001. 50

[73] A. Stokes and A. Nazir. A gauge-invariant master equation approach for strongly interacting dipoles. *New J. Phys.*, 20(043022), 2018. 50

[74] R. H. Dicke. Coherence in spontaneous radiation processes. *Phys. Rev.*, 93, 1945. 51

[75] R. H. Lehmberg. Radiation from an n-atom system. I. General formalism. *Phys. Rev. A*, 2(883), 1970. 51

[76] R. H. Lehmberg. Radiation from an n-atom system. II. Spontaneous emission from a pair of atoms. *Phys. Rev. A*, 2(889), 1970.

[77] G. S. Agarwal. *Quantum optics*, volume 70 of *Springer Tracts of Modern Physics*. Springer-Verlag, Berlin, 1974.

[78] H. Blank, M. Blank K. Blum, and A. Faridani. Cooperative effects in the spontaneous decay of few atoms. *Phys. Lett.*, 105A(1), 1984.

[79] Z. Ficek, R. Tanas, and S. Kielich. Photon antibunching and squeezing in resonance fluorescence of two interacting atoms. *Phys. Rev. A*, 29(4), 1984.

[80] Z. Ficek and B. C. Sanders. Quantum beats in two-atom resonance fluorescence. *Phys. Rev. A*, 41(359), 1990.

[81] T. Rudolph and Z. Ficek. Interference pattern with a dark center from two atoms driven by a coherent laser field. *Phys. Rev. A*, 58(748), 1998.

[82] M. Kiffner, H. Park, W. Li, and T. F. Gallagher. Dipole-dipole-coupled double-Rydberg molecules. *Phys. Rev. A*, 86(031401), 2012. 51

[83] P. W. Milonni and P. L. Knight. Retardation in the resonant interaction of two identical atoms. *Phys. Rev. A*, 1974. 51

[84] P. W. Milonni and S. M. H. Rafsanjani. Distance-dependence of two-atom dipole interactions with one atom in an excited state. *Phys. Rev. A*, 92 (062711), 2015. 51, 123

[85] A. Sommerfeld. Propagation of waves in wireless telegraphy. *Ann. Phys. (Leipzig)*, 309(553), 1909. 64

[86] C. K. Carniglia and L. Mandel. Quantization of evanescent electromagnetic waves. *Phys. Rev. D*, 3(280), 1971. 64, 66, 67, 73, 81

[87] S. T. Wu and C. Eberlein. Quantum electrodynamics of an atom in front of a nondispersive dielectric halfspace. *Proc R. Soc. A*, 455(2487), 1999. 65

[88] W. Zakowicz and A. Bledowski. Spontaneous emission in the presence of a dielectric slab. *Phys. Rev. A*, 52(1640), 1995.

[89] H. Hammer. Orthogonality relations for triple modes at dielectric boundary surfaces. *J. Mod. Opt.*, 50(207), 2003.

[90] A. M. Contreras Reyes and C. Eberlein. Casimir-polder interaction between an atom and a dielectric slab. *Phys. Rev. A*, 80(032901), 2009.

[91] R. Bennett and C. Eberlein. Quantum electrodynamics of a free particle near dispersive dielectric or conducting boundaries. *Phys. Rev. A*, 86 (062505), 2012. 65, 66, 81

[92] G. S. Agarwal. Coherence in spontaneous emission in the presence of a dielectric. *Phys. Rev. Lett.*, 32(703), 1974. 65

[93] G. Barton. Frequency shifts near an interface: inadequacy of two-level atomic models. *J. Phys. B*, 7(16), 1974. 65

[94] G. S. Agarwal. Quantum electrodynamics in the presence of dielectrics and conductors. I. Electromagnetic-field response functions and black-body fluctuations in finite geometries. *Phys. Rev. A*, 11(230), 1975. 65

[95] G. S. Agarwal. Quantum electrodynamics in the presence of dielectrics and conductors. II. Theory of dispersion forces. *Phys. Rev. A*, 11(243), 1975.

[96] G. S. Agarwal. Quantum electrodynamics in the presence of dielectrics and conductors. III. Relations among one-photon transition probabilities in stationary and nonstationary fields, density of states, the field-correlation functions, and surface-dependent response functions. *Phys. Rev. A*, 11(253), 1975.

[97] G. S. Agarwal. Quantum electrodynamics in the presence of dielectrics and conductors. IV. General theory for spontaneous emission in finite geometries. *Phys. Rev. A*, 12(1475), 1975.

[98] G. S. Agarwal. Quantum electrodynamics in the presence of dielectrics and conductors. V. The extinction and moment theorems for correlation functions and relativistic aspects of blackbody fluctuations. *Phys. Rev. A*, 12(1974), 1975.

[99] G. S. Agarwal. Quantum electrodynamics in the presence of dielectrics and conductors. VI. Theory of Lippmann fringes. *Phys. Rev. A*, 12(1987), 1975. 65

[100] S. Y. Buhmann and D. G. Welsch. Dispersion forces in macroscopic quantum electrodynamics. *Progress in Quantum Electronics*, 31(51), 2007. 65

[101] S. Scheel and S. Y. Buhmann. Macroscopic quantum electrodynamics: Concept and applications. *Acta Phys. Slov.*, 58(675), 2008. 65, 67

[102] M. Hillery and L. D. Mlodinow. Quantization of electrodynamics in nonlinear dielectric media. *Phys. Rev. A*, 30(1860), 1984. 65

[103] W. Vogel L. Knöll and D.-G. Welsch. Action of passive, lossless optical systems in quantum optics. *Phys. Rev. A*, 36(3803), 1987.

[104] P. D. Drummond. Electromagnetic quantization in dispersive inhomogeneous nonlinear dielectrics. *Phys. Rev. A*, 42(6845), 1990.

[105] R. J. Glauber and M. Lewenstein. Quantum optics of dielectric media. *Phys. Rev. A*, 43(467), 1991.

[106] B. Huttner and S. M. Barnett. Quantization of the electromagnetic field in dielectrics. *Phys. Rev. A*, 46(4306), 1992.

[107] L. G. Suttorp and M. Wubs. Field quantization in inhomogeneous absorptive dielectrics. *Phys. Rev. A*, 70(013816), 2004.

[108] T. G. Philbin. Canonical quantization of macroscopic electromagnetism. *New J. Phys.*, 12(123008), 2010.

[109] C. Eberlein and R. Zietal. Quantum electrodynamics near a dispersive and absorbing dielectric. *Phys. Rev. A*, 86(022111), 2012. 65

[110] M. Liscidini, L. G. Helt, and J. E. Sipe. Asymptotic fields for a Hamiltonian treatment of nonlinear electromagnetic phenomena. *Phys. Rev. A*, 85 (013833), 2012. 65

[111] Y. L. Lim and A. Beige. Multiphoton entanglement through a Bell-multiport beam splitter. *Phys. Rev. A*, 71(062311), 2005. 65, 67

[112] M. Khanbekyan, L. Knöll, D.-G. Welsch, A. A. Semenov, and W. Vogel. QED of lossy cavities: Operator and quantum-state input-output relations. *Phys. Rev. A*, 72(053813), 2005. 65, 110

[113] V. Degiorgio. Phase shift between the transmitted and the reflected optical fields of a semireflecting lossless mirror is $\pi/2$. *Am. J. Phys.*, 48(81), 1980. 73

[114] F. Henault. The nature of light: What are photons? vi. *SPIE Proc.*, 9670 (95700Q), 2015. 73

[115] H. Morawitz. Self-coupling of a two-level system by a mirror. *Phys. Rev.*, 187(1792), 1969. 77, 83, 91

[116] K. E. Drabe, G. Cnossen, and D. A. Wiersma. Localization of spontaneous emission in front of a mirror. *Opt. Comm.*, 73(91), 1989.

[117] D. Meschede, W. Jhe, and E. A. Hinds. Radiative properties of atoms near a conducting plane: An old problem in a new light. *Phys. Rev. A*, 41(1587), 1990.

[118] R. Matloob. Radiative properties of an atom in the vicinity of a mirror. *Phys. Rev. A*, 62(022113), 2000.

[119] U. Dorner and P. Zoller. Laser-driven atoms in half-cavities. *Phys. Rev. A*, 66(023816), 2002. 84

[120] A. Beige, J. K. Pachos, and H. Walther. Spontaneous emission of an atom in front of a mirror. *Phys. Rev. A*, 66(063801), 2002. 77

[121] P. Stehle. Atomic radiation in a cavity. *Phys. Rev. A*, 2(102), 1970.

[122] P. W. Milonni and P. L. Knight. Spontaneous emission between mirrors. *Opt. Comm.*, 9(113), 1973.

[123] D. Kleppner. Inhibited spontaneous emission. *Phys. Rev. Lett.*, 47(233), 1981.

[124] J. M. Wylie and J. E. Sipe. Quantum electrodynamics near an interface. *Phys. Rev. A*, 30(1185), 1984.

[125] H. F. Arnoldus and T. F. George. Correlations between photons in resonance fluorescence emitted by an atom near a metal surface. *Phys. Rev. A*, 37(770), 1988. 83, 91

[126] K. H. Drexhage. Influence of a dielectric interface on fluorescence decay time. *JOL*, 1(693), 1970. 83, 91

[127] J. Eschner, C. Raab, F. Schmidt-Kaler, and R. Blatt. Light interference from single atoms and their mirror images. *Nature*, 413(495), 2001.

[128] I.-C. Hoi, A. F. Kockum, L. Tornberg, A. Pourkabirian, G. Johansson, P. Delsing, and C. M. Wilson. Probing the quantum vacuum with an artificial atom in front of a mirror. *Nat. Phys.*, 11(1045), 2015. 83, 91

[129] E. Arias, J. G. Duenas, G. Menezes, and N. F. Svaiter. Boundary effects on radiative processes of two engtangled atoms. *J. Hi. En. Phys.*, 2016(7), 2016. 93

[130] L. M. Zhou, P. J. Yao, N. Zhao, and F. W. Sun. Enhanced and tunable electric dipole-dipole interactions near a planar metal film. *J. Phys. B: At. Mol. Opt. Phys.*, 50(165501), 2017.

[131] W. Zhou, L. Rizzuto, and R. Passante. Vacuum fluctuations and radiation reaction contributions to the resonance dipole-dipole interaction between two atoms near a reflecting boundary. *Phys. Rev. A*, 97(042503), 2018.

[132] R. Palacino, R. Passante, L. Rizzuto, P. Barcellona, and S. Y. Buhmann. Tuning the collective decay of two entangled emitters by means of a nearby surface. *J. Phys. B: At. Mol. Opt. Phys.*, 50(154001), 2017.

[133] R. Jones, J. A. Needham, I. Leasnovsky, F. Intravaia, and B. Olmos. Modified dipole-dipole interaction and dissipation in an atomic ensemble near surfaces. *Phys. Rev. A*, 97(053841), 2018. 93

[134] H. T. Dung, L. Knöll, and D. G. Welsch. Resonant dipole-dipole interaction in the presence of dispersing and absorbing surroundings. *Phys. Rev. A*, 66 (063810), 2002. 93

[135] J. Audretsch and R. Mueller. Spontaneous excitation of an accelerated atom: The contributions of vacuum fluctuations and radiation reaction. *Phys. Rev. A*, 50(2), 1994. 93

[136] W. Zhou, R. Passante, and L. Rizzuto. Resonance dipole-dipole interaction between two accelerated atoms in the presence of a reflecting plane boundary. *Symmetry*, 20, 2018.

[137] G. Menezes and N. F. Svaiter. Radiative processes of uniformly accelerated entangled atoms. *Phys. Rev. A*, 93(052117), 2016.

[138] J. Kumlin, S. Hofferberth, and H. P. Bulcher. Emergent universal dynamics for an atomic cloud coupled to an optical wave-guide. *Phys. Rev. Lett.*, 121 (013601), 2018. 93

[139] P. Solano, P. Barberis-Blostein, F. K. Fatemi, L. A. Orozco, and S. L. Rolston. Super- and sub-radiance reveal infinite-range interactions through a nanofiber. *Nat. Comm.*, 8(1857), 2018. 93

[140] P. Solano, J. A. Grover, Y. Xu, P. Barberis-Blostein, N. Munday, L. A. Orozco, W. D. Phillips, and S. L. Rolston. Alignment-dependent decay rate of an atomic dipole near an optical nanofiber. *Phys. Rev. A*, 99(013822), 2019. 93

[141] Tarun Kakkar. *Ultrafast pulsed laser plasma fabrication of erbium doped thin film sensors*. PhD thesis, School of Chemical and Process Engineering (Leeds), 2018. 95, 122

[142] *Glass Thin Films for Planar Optical Components Fabricated using Ultrafast Laser Plasma Doping*, 2018. 20th International Conference on Transparent Optical Networks (ICTON).

[143] T. Mann, R. Mathieson, M. Murray, B. D. O. Richards, and Gin Jose. Femtosecond laser ablation properties of Er^{3+} ion doped zinc-sodium tellurite glass. *J. App. Phys.*, 124(044903), 2018.

[144] B. D. O. Richards, A. Boontan, T. Mann, E. Kumi Barimah, C. Russell, D. P. Steenson, and G. Jose. Tm^{3+} tellurite-modified-silica glass thin films fabricated using ultrafast laser plasma doping. *IEEE J. Sel. Top. in Q. Elec.*, 25(8700108), 2019. 95, 122

[145] *Blood glucose sensing through skin by non-invasive finger touch meter*, 2016. Diabetes Technology and Therapeutics. 95

[146] S. Haroche. Nobel lecture: Controlling photons in a box and exploring the quantum to classical boundary. *Rev. Mod. Phys.*, 85:1083, 2013. 109

[147] M. Abramowitz and I. A. Stegun. *Handbook of Mathematical Functions with Formulas, Graphs, and Mathematical Tables.* New York: Dover, 1972. 114

[148] E. S. Kyoseva, A. Beige, and L. C. Kwek. Coherent cavity networks with complete connectivity. *New J. Phys.*, 14:023023, 2012. 118

[149] L. A. Clark, A. Stokes, and A. Beige. Quantum-enhanced metrology with the single-mode coherent states of an optical cavity inside a quantum feedback loop. *Phys. Rev. A*, 94:023840, 2016. 118

[150] H. B. G. Casimir and D. Polder. The influence of retardation on the London-van der Waals forces. *Phys. Rev.*, 73(360), 1948. 123

[151] R. Bennett and C. Eberlain. Quantum electrodynamics of a free particle near dispersive dielectric or conducting boundaries. *Phys. Rev. A*, 86 (062505), 2012. 123

[152] R. Bennett and C. Eberlein. Anomalous magnetic moment of an electron near a dispersive surface. *Phys. Rev. A*, 88(012107), 2013.

[153] S. Fuchs, R. Bennett, and S. Y. Buhmann. Casimir-Polder potential of a driven atom. *Phys. Rev. A*, 98(022514), 2018.

[154] T. Haug, R. Bennett, and S. Y. Buhmann. The Casimir-Polder potential in the presence of a Fock state. *Phys. Rev. A*, 99(012508), 2019.

[155] S. Fuchs, R. Bennett, R. V. Krems, and S. Y. Buhmann. Non-additivity of optical and Casimir-Polder potentials. *Phys. Rev. Lett.*, 121(083603), 2018. 123

[156] H. B. G. Casimir. On the attraction between two perfectly conducting plates. *Proc. K. Ned. Akad. Wet.*, 51(793), 1948. 123

[157] P. W. Milonni and Mei-Li Shih. Source theory of the Casimir force. *Phys. Rev. A*, 45, 1992. 123

[158] P. W. Milonni. *The quantum vacuum*. San Diego, CA: Academic, 1994.

[159] S. K. Lamoreaux. The Casimir force: background, experiments and applications. *Rep. Prog. Phys.*, 68, 2005.

[160] G. L. Klimchitskaya, U. Mohideen, and V. M. Mostepanenko. The Casimir force between real materials: Experiment and theory. *Revs. Mod. Phys.*, 81, 2009. 123

[161] G. L. Klimchitskaya and V. M. Mostepanenko. Casimir free energy of dielectric films: Classical limit, low-temperature behaviour and control. *J. of Phys. Cond. Matt.*, 29, 2017. 123

[162] G. Bressi, G. Carugno, R. Onofrio, and G. Ruoso. Measurement of the Casimir force between parallel metallic surfaces. *Phys. Rev. Lett.*, 88, 2002. 123

[163] R. L. Jaffe. The Casimir effect and the quantum vacuum. *Phys. Rev. D*, 72(021301), 2005. 123